HYDROPOWER POTENTIAL ESTIMATION USING WATERSHED MODELING VIA Q-SWAT ANALYSIS OF WAINIMALA RIVER BASIN, FIJI

By

Sanjay Raj Singh

A minor thesis submitted in partial fulfillment of the requirements for the degree of

Master of

Science in Renewable Energy Management

School of Science and Technology

The University of Fiji

Fiji

July, 2022

Declaration of Originality

I, Sanjay Raj Singh, sincerely declare that this minor thesis is my original work and wherever the work of others has been used, it has been clearly referenced.

Signature _____

Date _____

Name Sanjay Raj Singh

Student ID 20170781

Statement by Principal Supervisor

The research in this minor thesis was performed under my supervision and to the best of my knowledge is the sole work of Mr. Sanjay Raj Singh.

Principal Supervisor

Signature _____

Date _____

Name Dr Ramendra Prasad

Statement by Thesis Advisor

The research in this minor thesis was performed under my supervision and to the best of my knowledge is the sole work of Mr. Sanjay Raj Singh.

Thesis Advisor

Signature _____

Date _____

Name Ms Dhrishna Charan

Dedication

This manuscript is especially dedicated to my family who has given me strength and enthusiasm to carry out the minor thesis. Special thanks to my late parents, grandparents and anyone else who has guided me in any way possible.

Acknowledgements

This minor thesis is the result of a year's work whereby I have been guided, supported and motivated accordingly to successfully complete this report. Hence, it gives me an immense pleasure to express my gratitude and sincerely thank everyone who has helped me in anyway.

First and foremost, I would like to thank almighty for his blessings, mental support and wisdom for successfully completing this minor thesis. I would like to thank my late mum for providing the word of encouragement and moral support for this minor thesis.

Secondly, I express my sincere gratitude and appreciation to my research guide and academic advisors, Professor Anirudh Singh, Former Dean of School of Science and Technology, Dr Ramendra Prasad, Head of Science Department, and Principal Supervisor. Ms. Dhrishna Charan as well for her continuous support, encouragement, patience and guidance. Likewise, I would like to express my sincere gratitude to my colleague, Mr. Lionel Joseph for his guidance and support.

Next, I would like to acknowledge Mr. Anish Maharaj for guiding me on the use of Soil and Water Analysis (QSWAT) model to estimate the theoretical hydropower potential at Wainimala River Basin.

Moreover, my sincere gratitude to Fiji Meteorological Services especially to Mr. Viliame and Mr. Sepesa who has provided the stream flow rate data for Wainimala River.

My special thanks to Mr. Ritesh Dass and Mr. Solomoni from the Ministry of Agriculture for providing the soil data.

Last but not least, my hearty thanks to my wife, Ms. Ashika Singh and my four daughters (Shakshi Alansha Singh, Shreya Shania Singh, Shanvi Vanshika Singh and Shanaya Shyra Singh) for being quite understanding, supportive and cooperative during the research

Abstract

Fiji's energy needs are continually in demand on daily basis and most probably the factors such as impacts of urbanization, rapidly increasing population and strain on conventional energy sources are responsible for that. To meet the required energy demands, it is mostly imported from foreign countries. To prevent vast decrease in fossil fuels and address devastating climate change issues, there is a pressing need for another source of energy termed as green energy which is clean and environment-friendly. Thus, the use and implementation of renewable energy (green energy) sources that include hydropower, solar energy, wind power and geothermal energy over imported oil has proven advantages to curb Greenhouse Gas (GHG) emissions and maintain temperature rise within 1.5°C. This continued effort aims to combat, mitigate and adapt to climate change issues, build resilience and meet nation's renewable energy targets through green growth initiatives eventually leading to sustainable economic growth. Interestingly, Fiji with extensive hilly terrain and rich renewable water resources has greater potential to untap and boost its hydropower electricity to narrow the massive gap between energy and demand. In addition, this effort ensures to meet the country's stipulated energy targets and Sustainable Development Goals (SDGs). A hydrokinetic (HK) potential assessment at the watershed scale was conducted at Wainimala River Basin (WRB) at Naitasiri Province of Central (Eastern) Division in Vitilevu, Fiji. The current study simulated the discharge at Wainimala River utilizing hydrological model; Soil and Water Assessment Tool (QSWAT) coupled with a Quantum Geographic Information System (QGIS). This application is quite crucial and assesses the water resource availability and hydropower potential of rivers and streams and determines the potential hydropower sites for future hydropower developments and calculates avoided emissions. Geospatial data about the topography, soil types, land use/land cover, meteorological inputs (wind speed, maximum and minimum air temperature, precipitation, relative humidity and solar radiation) and digital elevation model were considered in hydrological and hydro-geomorphological characterization of the watershed. Of the delineated 32 sub-basins in the WRB watershed, only 6 were identified as having potential sites with an estimated annual power capacity of 41.17 MW. Interestingly, sub-basins 11 and 21 have very high hydropower capacities. The technical HK potential for 32 sub-basins was estimated to be 53.05 MW which

produced 278831 MWh of energy annually. Moreover, theoretical HK potential was estimated to be 83.07 MW which produced 436616 MWh of energy annually. These estimations were based on an average capacity factor of 60% for hydroelectricity generation in Fiji. Heavy fuel oil (HFO) emitted 1.91 Megatonne (Mt) of CO_2 equivalent emissions whereas 2.10 Mt of CO_2 equivalent emissions were emitted when industrial diesel oil was combusted to generate electricity annually. This means 4.01 Mt of CO_2 equivalent emissions can be saved by replacing the fossil fuel with hydroelectricity. Interestingly, Sequential Uncertainty Fitting (SUFI-2) algorithm within Soil and Water Assessment Tool-Calibration and Uncertainty Programs (SWAT-CUP) is the most appropriate goodness of fit model that can be used in future to evaluate model performance and simulate discharge for calibration and validation periods. Moreover, scenario-based studies based on sedimentation and climate change impacts can be considered for further studies as well. The developed method is very crucial and could be applied to various river systems around Fiji for water resource availability and hydropower potential assessments.

List of Abbreviations, Units and Nomenclature

LIST OF ABBREVIATIONS AND ACRONYMS

ACCO	Adaptive Clustering Covering
ASTER GDEM	Advanced Space borne Thermal Emission and Reflection Radiometer Global-DEM
AGNPS	Agricultural Non-Point Source
AI	Artificial Intelligence
ADB	Asian Development Bank
CO_2	Carbon Dioxide
CMADS	China Meteorological Assimilation Driving Datasets
CDM	Clean Development Mechanism
COP	Conference of the Parties
COVID-19	Coronavirus disease
CSP	Concentrating Solar Thermal
CN	Curve Number
CNCOEF	Curve Number Coefficient
ICN	Daily Curve Number Calculation Method
DM	Data Mining
DoE	Department of Energy
DEM	Digital Elevation Model
DWSM	Dynamic Watershed Simulation Model
EFL	Energy Fiji Limited
SHE	European Hydrologic System
EIB	European Investment Bank
FCCC	Fijian Competition and Consumer Commission
FDoE	Fiji Department of Energy
FEA	Fiji Electricity Authority
FNEP	Fiji's National Energy Policy
RRA	Fiji's Renewables Readiness Assessment
FSC	Fiji Sugar Co-operation
FAO	Food and Agricultural Organization
GA	General Algorithm

GLUE	Generalized Likelihood Uncertainty Estimation
GIS	Geographic Information System
GWP	Global Warming Potential
GOF	Government of Fiji
GGF	Green Growth Framework
GDP	Gross Domestic Product
GHG	Green House Gas
HFO	Heavy fuel oil
H/WQ	Hydrologic and water quality models
HRU	Hydrologic Response Unit
HRU's	Hydrologic Response Units
HSPF	Hydrologic Simulation Program–Fortran
IDO	Industrial diesel oil
IEA	International Energy Agency
INDCs	Intended Nationally Determined Commitments
IPCC	Intergovernmental Panel on Climate Change
IPPs	Independent Power Producers
ISRIC	International Center for Soil Reference and Information
ISSS	International Soil Science Society
iTLTB	iTaukei Land Trust Board
CN2	Initial SCS Runoff Curve Number for Moisture Condition II
FFCB	Initial Soil Water Storage Expressed as a Fraction of Field Capacity Water Content
JOCV	Japanese Overseas Co-operation Volunteers
KGE	Kling-Gupta Efficiency
KOICA	Korean International Cooperation Agency
LULC	Land use/land cover
LH-OAT	Latin Hypercube One-At-A-Time
MCMC	Markov Chain Monte Carlo
MAE	Mean Absolute Error
MSE	Mean Square Error
MoU	Memorandum of Understanding
CH_4	Methane
bR^2	Modified Coefficient of Determination

MNS	Modified Nash-Sutcliffe efficiency
MLR	Multi Linear Regression
NSE	Nash-Sutcliffe efficiency
NDCs	Nationally Determined Contributions
NEP	National Energy Policy
N_2O	Nitrous oxide
OAT	One-At-A-Time
QGIS	Quantum Geographic Information System
PICs	Pacific Island Countries
PSIDS	Pacific Small Island Developing States
PARASOL	Parameter Solution
PSO	Particle Swarm Optimization
PBIAS	Percentage of Bias
PV	Photo Voltaic
PPA	Power Purchase Agreements
PPU	Prediction Uncertainty
RBNN	Radial-Based Neural Network
SSQR	Ranked Sum of Squares
RAM	Random Access Memory
RHAM	Rapid Hydropower Assessment Model
RSR	Ratio of Standard Deviation of Observations to Root Mean Square Error
REDD+	Reducing emissions from deforestation and forest degradation
RE	Renewable Energy
REN 21	Renewables Global Status Report-REN21
RET	Renewable Energy Technology
RETs	Renewable Energy Technologies
RMSE	Root Mean Square Error
ROR	Run-of-river
SA	Sensitivity Analysis
SUFI-2	Sequential Uncertainty Fitting
SHP	Small hydropower projects
SIDS	Small Island Developing States
SID	Small Island Developing State

SRTM	Shuttle Radar Topography Mission
SWRRB	Simulator for Water Resources in Rural Basin
SFTMP	Snowfall temperature (°C)
SC	Soft Computing
SCS	Soil Conservation Service
SOPAC	South Pacific Applied Geoscience Commission
ESCO	Soil Evaporation Compensation Factor
SWAT	Soil and Water Assessment Tool
SWAT-CUP	Soil and Water Assessment Tool-Calibration and Uncertainty Programs
SVM	Support Vector Machines
SURLAG	Surface Runoff Lag Coefficient (days)
SE4All	Sustainable Energy for All
SDGs	Sustainable Development Goals
IRENA	The International Renewable Energy Agency
TVSA	Time Variant Sensitivity Analysis
GWQMN	Threshold Depth of Water in the Shallow Aquifer for Return Flow to Occur
REVAPMN	Threshold Depth of Water in the Shallow Aquifer for Revap
TOPMODEL	Topography Based Hydrological Model
USP	The University of South Pacific
UA	Uncertainty Analysis
UNEEC	Uncertainty Estimation based on Local Error and Clustering
UN	United Nation's
UNDP	United Nations Development Programme
UNESCO	United Nations Educational, Scientific and Cultural Organization
UNFCCC	United Nations Framework Convention on Climate Change
USA	United States of America
USGS	United States Geological Survey
VARS	Variogram Analysis of Response Surfaces
VLIS	Vitilevu Integrated System
WRB	Wainimala River Basin

LIST OF SYMBOLS

SOL_AWC	Available Water Capacity of the soil Layer (mm H_2O mm $soil^{-1}$)
V_SLSUBBSN	Average Slope Length (m)
V_SLP	Average Slope Steepness (m/m)
ALPHA_BF	Baseflow Alpha Factor (days)
BIOMIX	Biological Mixing Efficiency
CI	Computational Intelligence
r_CN2.mgt	Curve Number management
SOIL_Z	Depth of Soil Layer (mm)
CH_K2	Effective Hydraulic Conductivity in Main Channel Alluvium in mm/hr
CH_K2	Global Channel Hydraulic Conductivity
GW_DELAY	Groundwater Delay Time (days)
Gw Revap	Groundwater "Revap" Coefficient
ML	Machine Learning
CH_N2	Manning's *n* Value for the Main Channel
OV_N	Manning's *n* Value for Overland Flow
V_BLAI	Max Leaf Area Index
V_CANMX	Maximum Amount of Water Intercepted by Vegetation (mm)
SOL_BD	Moist Bulk Density (g/cm^3)
SOL_ALB	Moist Soil Albedo
Par_inf.txt	Parameter Information Text
r	Pearson's Correlation Coefficient
V_EPCO	Plant Uptake Compensation Factor
Sol_K	Saturated Hydraulic Conductivity of the Soil (mm h^{-1})
USLE_K	Soil Erodibility (k) Factor
V_GWQMN	Water Limit Level in the Shallow Aquifer for the Occurrence of Base Flow (mm)

LIST OF UNITS

CO_2e	Carbon dioxide equivalent
m^3/s	Cubic meter per second
°C	Degrees Celsius
FJD	Fijian currency (in Dollars)
g/cm^3	Gram per cubic centimeter
GB	Giga Bytes
Gg	Giga gram
GHz	Giga hertz
GW	Gigawatts
GWh	Giga Watt- hour
$ktCO_2$	kilo tonne carbon dioxide
kg/m^3	kilogram per cubic meter
kV	kilo Volts
kWh/day	Kilo Watt- hour per day
MJ/FJD	Mega Joule per Fijian currency (in Dollars)
MW	Megawatt
Mt	Mega tonnes
m	meters
m/s^2	meters per second squared
M	Million
mm	Millimeters
mm/hr	Millimeter per hour
%	Percent
km^2	Square kilometers
TWh	Terawatt-hours
US billion	United States of America currency (Billion dollars)
US M	United States of America currency (Million dollars)
W	Watt
Wh	Watt-hour
'	Minutes
"	Seconds

LIST OF NOMENCLATURE

g	Acceleration Due to Gravity
R^2	Coefficient of Determination
η_g	Efficiency of Generator
η_t	Efficiency of Turbine
Q	Flow Rate (Discharge)
P	Hydropower Potential
h	Hydraulic Head
∞	Infinity
ρ	Mass Density of Water
$\bar{o}$	Mean measured runoff during the simulation period (m^3/s)
s	Mean simulated runoff during the simulation period (m^3/s)
o_i	Measured runoff or discharge (m^3/s)
$-\infty$	Negative Infinity
n	Number of Sub-Basins
n	Number of flow measurements in the analysis
k	Number of independent variables
s_i	Simulated runoff (m^3/s)
i	Sub-basin number
v	Version

Table of Contents

List of Figures

Chapter 1

Chapter 2

Chapter 3

Chapter 4

Chapter 5

List of Tables

Chapter 1

Chapter 3

Chapter 4

Chapter 5

Chapter 1

Introduction

The Small Island Developing States (SIDS) heavily depends on non-renewable energy sources. Similarly, Fiji also heavily relies on fossil fuel and this definitely increases the import bills and releases extensive Greenhouse Gases (GHGs) in the air adding to climate change issue. The ever-increasing fuel prices and inflated cartage costs compounded by the impacts of COVID-19 have pushed the SIDS into a vulnerable state drastically affecting the socio-economic developments. Thus, the utilization of renewable energy technologies (RETs) to meet the increasing energy demands is a prudent green recovery option. In particular, the hydropower as the renewable source of energy is clean and could be used as a solution for future power needs of Fiji. Thus, the effort of this study is to scale-up the percentage renewable energy share leading to sustainable development, building resilience and mitigating climate change issues.

1.1. Global Status of Renewable Energy (RE) – Global Energy Mix

According to REN 21 (2020), the year 2019 has marked the record-breaking year with the largest increase in installed power capacity greater than 200 Gigawatts (GW) particularly for solar Photo Voltaic (PV). However, fossil fuels such as oil and petroleum products largely met the increasing demand in transport sector. Modern bioenergy (biofuels) such as ethanol and biodiesel contributed only 3% to the transport sector whereas for energy sector there had been an increase of 9% biofuels (501 terawatt-hours, TWh) globally in 2019. However, the electricity generation from geothermal totalled around 95 TWh in 2019 with the global capacity of 13.9 GW of which 0.7 GW was added in 2019.

There had been a significant increase of 12% solar PV recording from 115 GW totaling to 627 GW and around 3 Megawatts (MW) of ocean power was contributed to the global electricity generated from ocean power. Interestingly, the wind power has recorded a massive annual increase of 19% globally in 2019 in the global wind power market with 10% new installations in offshore wind energy. This effort has

contributed to the installed capacity of 650 GW wind power globally of which 621 GW is the onshore and the rest offshore (Figures 1.1, and 1.2).

However, there had been a meagre increase of 2.3% hydropower generation with an estimated new capacity totalling 15.6 GW and this effort has increased the global installed hydropower capacity to around 1150 GW. As a result, more studies are required to estimate the hydro-potential in various regions.

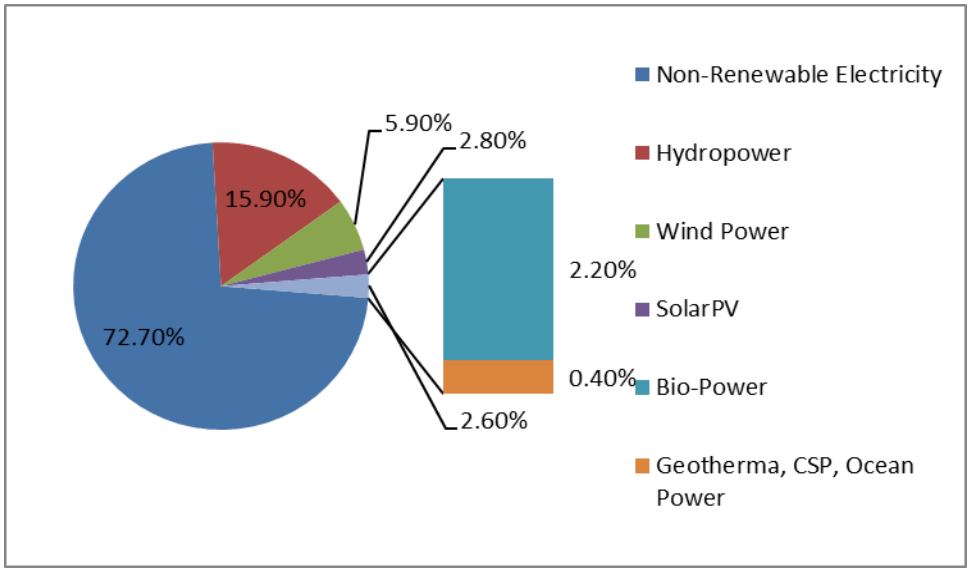

Figure 1.1: Estimated Renewable Energy Share of Global Electricity Production in 2019 (REN 21, 2020).

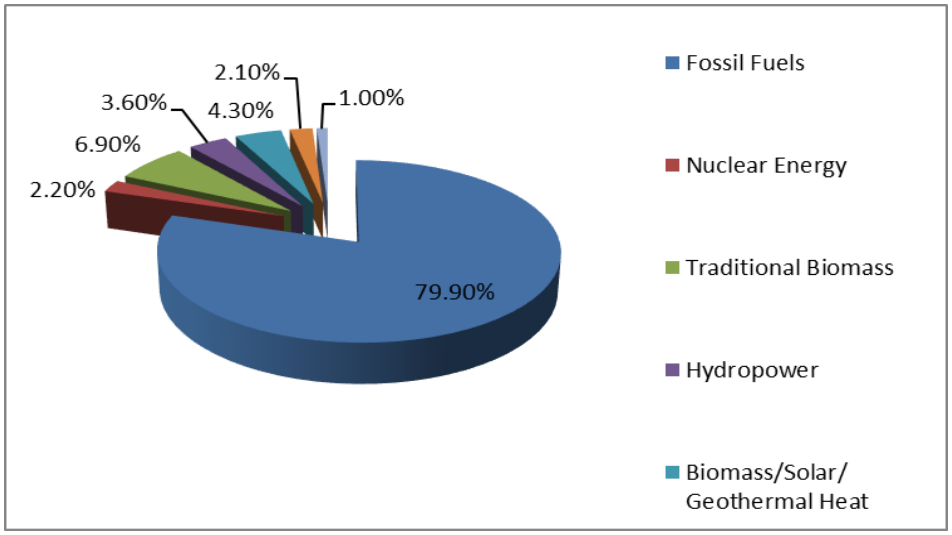

Figure 1.2: Estimated Renewable Share of Total Final Energy Consumption, 2018 (REN 21, 2020).

1.2. Renewable Energy Share in Electricity Generations in PSIDS

Pacific Small Island Developing States (PSIDS) are at high risk to climate change impacts though their contribution is negligible (0.006%) to global emissions (Anantharajah, 2019). In addition, PSIDS confronted the major decline in terms of trade when the oil price spiked which occurred before the global financial crisis causing price inflation (ADB, 2008, 2009; Dornan, 2009; IMF, 2011; Levantis, 2008; Levantis et al., 2006; Sugden, 2009; UNDP, 2007b). In particular, Fiji was hit twice in the 1970s and substantially between 2004-2008 on fuel importation accounting for FJD $744 Million (M) in 2008 (IRENA, 2015).

Thus, PSIDS are taking measures for electricity generations from renewable resources to reduce greenhouse gas emissions whilst keeping the import bills at bay. This also aligns to keep the 1.5°C target instead of agreed 2°C target during United Nations Framework Convention on Climate Change (UNFCCC) Conference of the Parties (COP) negotiations. The PSIDS have set very highly ambitiously Nationally Determined Contributions (NDCs) targets as shown in Table 1.1. This action highly contributes to Clean Development Mechanism (CDM) producing clean energy and meeting SDGs 7 and 13 accordingly (Anantharajah, 2019).

The major driving force for such targets is the energy crisis and high vulnerability to oil prices. These motives will definitely lessen the dependency on fossil fuel importation and improve the Gross Domestic Product (GDP) of the country by reducing high importation bills, increase national economic resilience and definitely increase the percentage share of renewables (Anantharajah, 2019). The Intended Nationally Determined Commitments (INDCs) dictate renewable energy targets that have been collectively presented by countries of SIDS in response to climate mitigation. However, the jointly presented national energy targets by SIDS are not legally binding (IRENA, 2015). Table 1.1 presents the status of renewable energy targets for SIDS with the unique scale of targets which are quite ambiguous. According to IRENA (2015), there has been a gigantic increase from 43 in 2005 to 164 in 2015 in the number of countries trying to achieve their renewable energy targets. Further, Table 1.1 shows that more than half of SIDS obtained the energy targets of 40% and higher.

Fiji is targeting to curb GHG emissions by 30% by 2030 through generating 100% electricity from renewables. Interestingly, Fiji's national energy targets are part of the Green Growth Development (GGF) aligned with Sustainable Energy for All (SE4ALL) initiative of the United Nations (UN) SE4ALL: Rapid Assessment and Gap Analysis. Fiji has greater opportunities for generating electricity from intermittent renewables to feed it to the main grid. Fiji has abundant renewable energy sources and intends to utilize all available renewable energy sources such as hydro, solar, wind and biomass to mitigate GHG emissions to build resilience, adapt and mitigate climate change issues and improve energy security (Lal et al., 2012; Dornan et al., 2016; Anantharajah, 2019). However, the challenges encountered with the inclusion of RETs including lack of exploration, high costs, intermittent and highly weather dependent resulted in Fiji and other SID countries resorting to fossil fuel for energy access or probably use the various combination of technologies (hybrid) such as wind and solar PV or hydro and solar PV to have more reliable electricity supply (Lal et al., 2012).

1.3. Current Status of Hydroelectricity Generations in Fiji

Electricity generation from hydropower has a great impact on the socio-economic status of Fiji. In particular, the Run of River (ROR) continuously for 24 hours a day and operates with low maintenance costs (Raghavan, 2003). Fiji has hilly and mountainous terrain with good rainfall which provides an excellent hydropower resource for the purpose of electricity generation and comparatively the hydropower provides the largest share of electricity supply relative to other renewables. The total installed hydroelectric scheme in Fiji has the generation capacity of 258.9 MW stationed on the island of Vitilevu for its grid power distribution (IRENA, 2015). In terms of grid-connected hydro-electric schemes currently, in Fiji an average of 341-561 GWh of hydroelectricity was generated from 2005 to 2019.

Table 1.1: Adopted renewable energy targets for Small Island Developing States in Pacific Island Countries (Dornan et al. 2016).

Country	**Target ***	**Target Date**	**Current Share of Renewables in Power Generation**
Cook Islands	100%	2020	0
Fiji	81%	2020	45%
Kiribati	45% urban, 60% rural	2025	0
Marshall Islands	20%	2020	0
Federated States of Micronesia	10% urban, 50% rural	2020	28%
Nauru	50%	2020	0
Niue	100%	2020	0
Papua New Guinea	50% GHG emission reduction	2030	Over 40%
Palau	20% **	2020	12%
Samoa	10% **	2016	30%-40%
Solomon Islands	50%	2015	0
Tonga	50%	2020	4%
Tuvalu	100%	2020	5%
Vanuatu	65% **	2020	15%

Notes: * Target is referred to electricity supply; ** Target is referred to primary energy supply.

In 2020, Fiji's average electricity generation mix composed of 57.30% hydro, 35.87% IDO and HFO, 0.12% Butoni wind power and 6.87% Independent Power Producers (IPPs – energy obtained from biomass) (EFL, 2020). Figure 1.3 comparatively displays the percentage share of electricity generation mix from 2007 to 2019. In particular, the electricity generation from hydro shows vast fluctuations between the years 2007 and 2014 and reduced variations between the years 2015 to

2019. Further, Table 1.2 summarises the monthly hydro-based generation in GWh from 2005 to 2019.

These variations in electricity generation are due to unfavourable weather conditions such as El Niño, El Niño Southern Oscillation or severe drought, mechanical and technical problems encountered and natural disasters. Thus, the hydropower plants are unable to work on their full capacity to generate electricity. For instance, in 2019, the electricity generation from hydropower is lower than 2018 due to low rainfall received at Nadarivatu and Wainikasou catchment areas (EFL, 2019). This means that electricity generation from hydropower plants is highly dependent on the amount of precipitation per year. Interestingly, the years 2007, 2008, 2012 and 2013 have shown good rainfall at Monasavu catchment which accounted for increased amounts of electricity generated during that period. Figure 1.4 illustrates the percentage share of electricity produced through hydro from 2005 to 2020.

Comparatively, the Wailoa power station is performing well with continuous increase in annual hydroelectricity generation with respect to Wainikasou and Nadarivatu power stations. Figure 1.5 displays the annual hydro-based generation in million units from 2015 to 2019. Nadarivatu power station has slight increase in hydroelectricity generation but slowly falls in 2018. However, Wainikasou power station has not shown any significant increase or decrease in the hydroelectricity produced over the years.

Electricity generation from wind farm has shown no significant improvements over the years. However, the electricity generation by IPPs has shown slight variations over the years but is slowly increasing from 2016. There are 5 IPPs namely: Tropik Wood Industries Ltd, Nabou Green Energy Ltd, Fiji Sugar Co-operation (FSC)-Ba, FSC-Lautoka and FSC-Labasa responsible for exporting electricity into Energy Fiji Limited (EFLs) energy grid). Despite, Fiji has various means of RETs to produce clean energy; most of the energy is produced by diesel gensets to meet increasing energy demands. Figure 1.3 shows significant variations on electricity production from fossil fuels from 2006 to 2014. As the hydro potential strengthened from 2015, the electricity generation from diesel gensets slowed down.

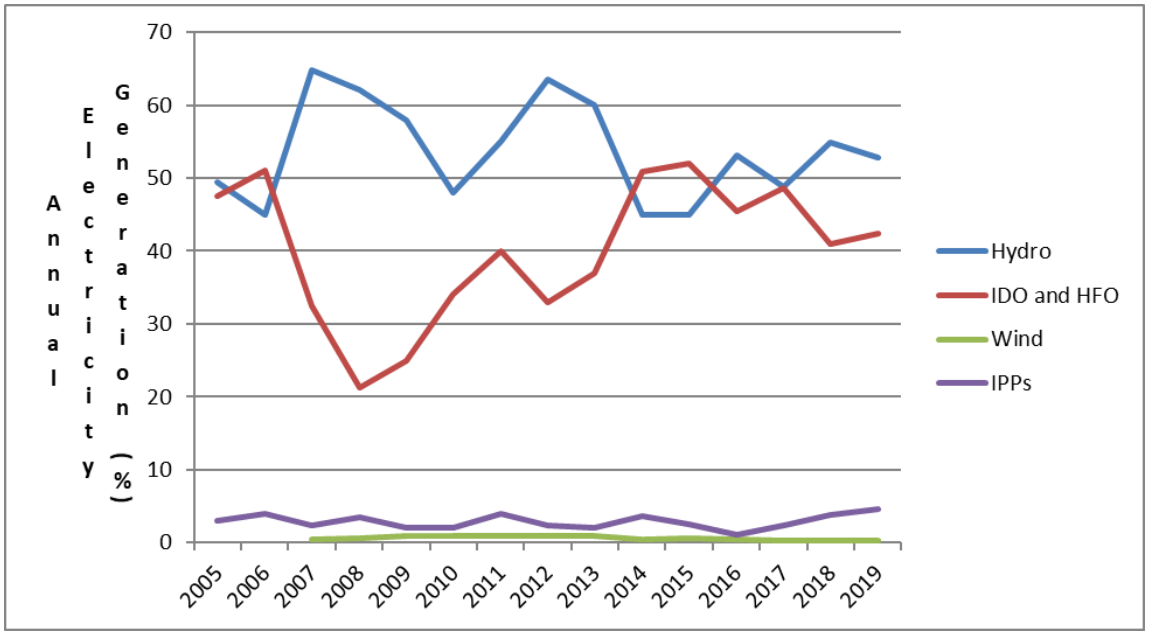

Figure 1.3: EFL's Electricity Generation Mix, 2005-2019 (EFL, 2005 to 2019).

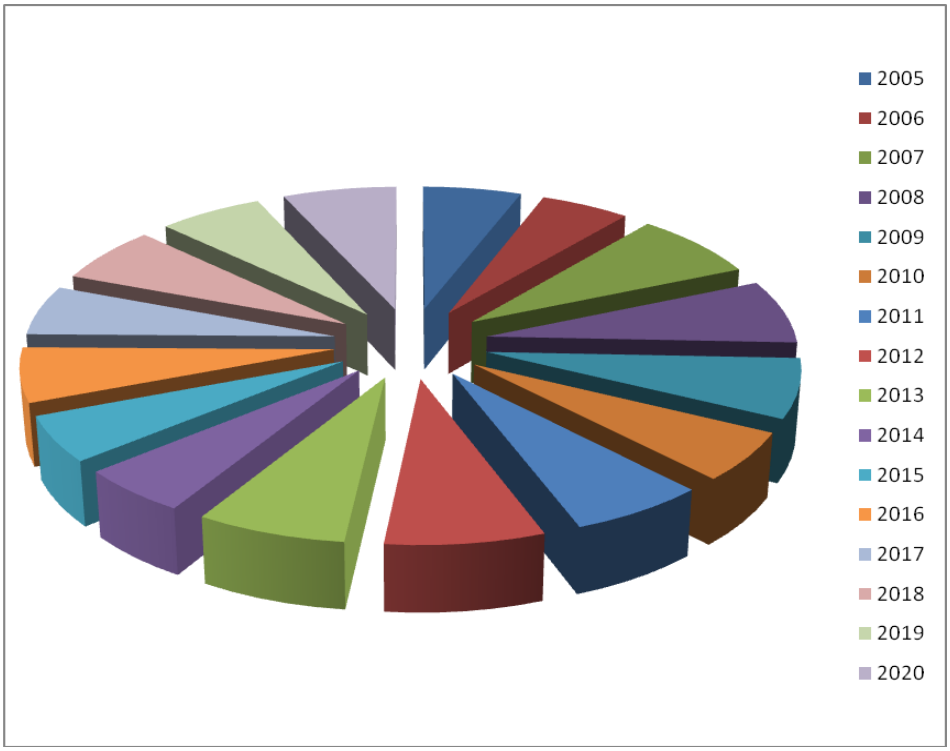

Figure 1.4: Illustrates the percentage share of electricity produced through hydro from 2005-2020 (EFL, 2005 to 2019).

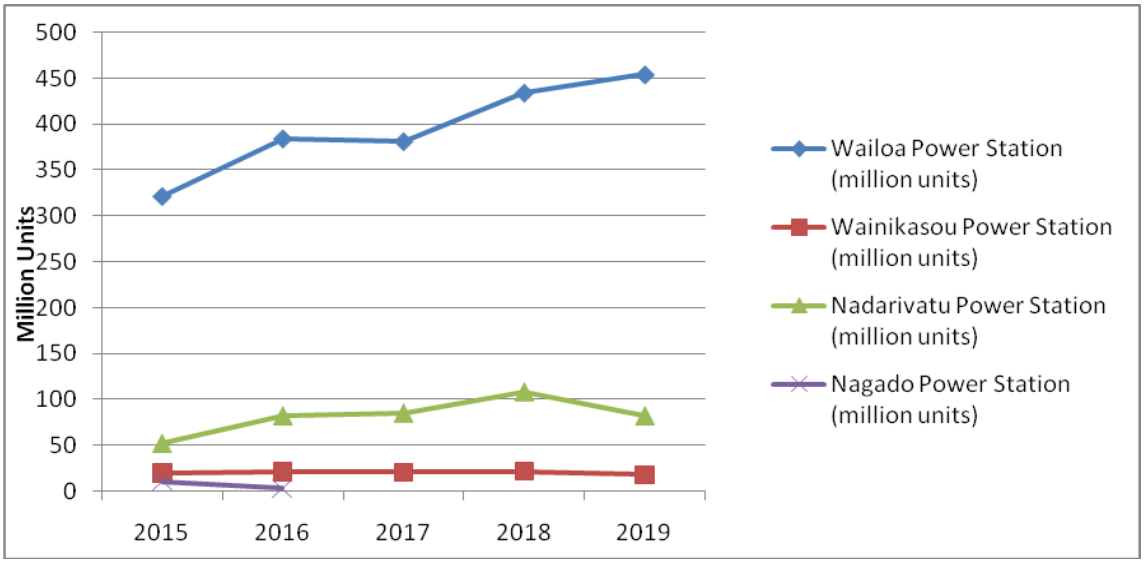

Figure 1.5: Annual Hydro-based Generation, 2015 to 2019 (million units) (EFL, 2015-2019).

Table 1.2: EFL Monthly Hydro-Based Generation, 2005 to 2019 (GWh) (EFL, 2005 to 2019).

Year	Jan	Feb	Mar	Apr	May	Jun	Jul	Aug	Sep	Oct	Nov	Dec	Total
2019	62	57	61	56	57	39	36	37	35	40	40	41	561
2018	64	64	60	55	49	44	38	21	19	41	51	56	562
2017	63	62	62	33	43	33	30	20	19	20	55	50	490
2016	66	48	41	49	50	30	29	34	28	30	40	52	497
2015	47	50	53	39	36	38	25	22	22	25	24	30	411
2014	54	59	50	32	33	26	24	19	20	17	26	46	406
2013	58	51	60	45	40	41	38	39	30	32	44	53	531
2012	52	50	5	45	48	46	44	42	30	42	36	40	526
2011	42	49	51	36	35	30	27	34	30	40	44	50	468
2010	43	37	38	33	35	32	25	23	25	24	48	50	413
2008	47	47	50	45	40	38	36	46	26	35	34	49	495
2007	50	43	50	48	48	39	30	23	31	49	45	50	508
2006	46	37	43	34	30	23	19	16	15	20	25	32	341
2005	22	22	27	26	39	26	20	21	26	27	34	47	338
Ave	51	48	50	41	42	35	30	28	25	32	39	46	468

1.4. Energy Demand

The rising population density, industrialization, urbanization, continued rise in fuel price, increased energy demand and the number of customers being connected to the grid have been increasing over the years. Table 1.3 summarizes the percentage growth in energy consumption with prepaid and post-paid consumers from 2014 to 2019. It is seen that the percentage growth has tripled in 2019 with respect to 2016. Further, Figure 1.6 displays the million units of energy consumed from 2014 to 2019. There has been a vast increase in energy consumption in Fiji from 795 million units in 2014 to 946 million units. This increase was catered for by importing diesel oil since the electricity produced from hydro was at the maximum levels and also depended on weather conditions particularly precipitation (EFL, 2019). As a result of this, Fiji lost most of its Gross Domestic Product (GDP) by spending more on oil imports. For instance, the Fijian government spent around FJD $550 M annually on oil imports from 2008-2011 though there had been a substantial decrease in international oil prices during this period by about a third (IRENA, 2015). According to the Fiji Bureau of Statistics, 64% (land 16%, air 26%, and marine 22%) of total imported fuel has been used by the transport sector. This effort in turn has a negative impact on Fiji's gross national income or economy and is subject to high oil prices, oil price volatility, which raises concerns on the country's energy security (Dornan, 2009).

In response to that, EFL had to further hydro schemes and meet the demands for sustainable development. For instance, Wainikasou hydro electric scheme was commissioned in 2004 with installed capacity of 6.4 MW and anticipated to generate 26 GWh of energy annually. Further, Nagado hydro scheme was commissioned in 2006 with installed capacity of 2.8 MW and expected to yield 12 GWh of energy annually. Afterwards, the commissioning of Nadarivatu Hydro Scheme in September 2012 raised the installed capacity by 40 MW yielding 101 GWh of energy annually (http://efl.com.fj/about-us/renewable-projects/). And finally, the Somosomo hydro electric scheme in Taveuni was commissioned in 2016 with installed capacity of 0.7 MW and expected to yield 2 GWh of energy annually. Additionally, in order to cater for increasing demands of electricity and greater reliability on renewable sources, EFL has expanded its 132 Kilo Volts (kV) development in the transmission network

from Virara settlement to Rarawai, Ba. A 33 kV transmission network was developed from Vuda to Naikabula (outside Lautoka city) (EFL, 2019).

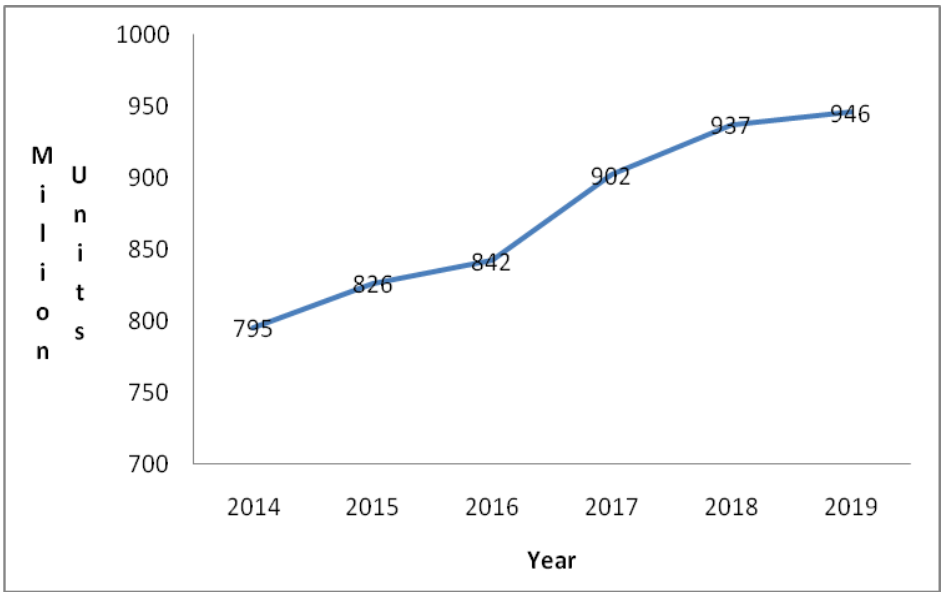

Figure 1.6: Million units of energy consumed from 2014 to 2019 (EFL, 2014 to 2019).

Table 1.3: Percentage growth in energy consumption from 2014 to 2019 (EFL, 2019).

Years	Prepaid Consumers	Postpaid Consumers	Consumer Count	Increase in Consumer Base	% Growth
2014	22,451	144,566	167,017	-	-
2015	23,548	148,391	171,939	4,922	2.95%
2016	24,601	149,929	174,530	2,591	1.51%
2017	26,387	156,026	182,413	7,883	4.52%
2018	28,517	161,887	190,404	7,991	4.38%
2019	37,517	161,503	199,020	8,616	4.53%

1.5. Hydroelectricity and Global Status

Hydropower is relatively an old technique amongst the renewables, and is one of the mature technologies that are cost-effective. In addition, the high efficiency of hydropower plants (about 90% efficient from water to wire) in generating electricity is related to its operational feasibility and economic superiority with greater lifespan and lower operational and maintenance costs (Sharma, 2007; IPCC, 2011). The hydropower or water power is available in the hilly regions where the water falls from higher altitudes to lower elevations deriving power from kinetic and potential energy of moving water (Patil et al., 2013). As a result, the energy from moving water turns turbines connected to the generator generating hydroelectricity. Sharma (2007) and Pandey et al. (2015) stated that electricity generated from hydropower plants are clean, non-polluting (carbon dioxide, (CO_2) free), renewable and independent from international trade. This suggests that electricity generation from hydropower technologies has vast advantages.

The hydropower plant is classified based on the installed capacity. Globally the power output is widely used to classify hydro as micro hydropower plants, mini hydropower plants, small hydropower plants or large hydropower plants. Table 1.4 summarises the category of hydropower based on the installed capacity. This classification varies over the countries and for instance in India the hydropower plants with capacity lower than 15 MW is referred to as “small hydro” (Das et al., 2006).

Table 1.4: Category of hydropower and its installed capacity (Lakshmi et al., 2018).

Hydropower Category	**Installed Capacity**
Micro hydropower plant	0.1 MW
Mini hydropower plant	2 MW
Small hydropower plant	<15 MW
Large hydropower plant	>15 MW

1.6. Research Background

Energy is the crucial component of a country's resource and greatly responsible for the sustainable economic developments. The industrial and residential sectors largely depend on it but in particular, the mechanized agriculture sector heavily depends upon electricity. According to World Bank, Fiji is regarded as a lower-middle-income with the reported per capita of United States (US) $4,397 in 2011 (Systematic Country Diagnostic, 2017).

Interestingly, the energy sector in Fiji is targeting to twofold the renewable energy capacity by 2030 by increasing its hydropower capacity by approximately 150 MW and intends to achieve 100% electrification rate by 2036 (Pacific Energy Update, 2018). Approximately FJD $760 M would be required for these significant investments and as a result of this; the Fijian government has planned to work on the prioritized items in the energy sector. These include: expansion of private sector roles in power generation and privatization of energy utility, increasing the roles and responsibilities of non-EFL renewable energy through small-scale systems and improve transparency and accountability through restructuring regulatory arrangements and an attempt to eliminate manageable conflict of interests (Pacific Energy Update, 2018).

In order to achieve these energy targets, EFL had been working on the following proposed hydro energy projects:

- Qaliwana and upper Wailoa diversion with potential output of 44 MW with generation capacity of 206 GWh has been funded by the European Investment Bank (EIB) (EFL, 2019).
- The lower Ba hydro development scheme with an expected output potential of 49 MW with generation capacity of 216 GWh (EFL, 2019).
- Three hydro power projects in Namosi termed as Namosi hydro scheme at Waivaka, Wainikoroiluva and Wainikovu sites has the combined estimated total power capacity output as 32 MW with energy output of 120 GWh (EFL, 2019).

Apart from developments in hydropower potentials, EFL is engaging with the IPP, Sunergise Limited to develop a 5 MW Qeleloa farm for sustainable development and clean energy source to meet increasing energy demand. Moreover, 1 MW solar farm is expected to be developed at Mua, Taveuni funded by Korean International Cooperation Agency (KOICA). Further, EFL plans to develop waste to energy plant in central Vitilevu (EFL, 2019).

1.7. Research Problem

The rising energy demand for Fiji can not be fulfilled by the current renewable energy supply alone and has to be satisfied by the use and burning of fossil fuels. This inturn poses serious environmental hazards and depletes fossil fuel reserves leading to unsustainable development.

Fiji's highly reliance on imported fossil fuels contributed 30% of the total merchandise (IRENA, 2015). For instance, in 2015, diesel gensets consumed 104,000 tons of fuel oil for grid-connected electricity generation at a cost of US $70 M (EFL, 2016). Furthermore in 2011, the total estimated GHG emissions amounted to approximately 2,700 Giga gram Carbon Dioxide equivalent (Gg CO_2e) of which energy sector contributed 59%; 22% was contributed from agricultural sector; 15% from forestry and; 4% from waste (GOF, 2017).

Thus, in order to reduce import bills, dependency and vulnerability to fluctuating world oil price whilst combating the GHG emissions and mitigating climate change impacts as well as meeting the increasing energy demands and the NDC commitments, Fiji has to opt for sustainable and eco-friendly energy sources such as hydropower. Hydropower is one of the most reliable renewable energy resources today and is dispatchable in nature. Thus, this study intends to scale-up the percentage share of renewable energy in particular hydropower for grid-electricity production to meet increasing energy demands and NDC requirements.

1.8. Aim and Specific Objectives

1.8.1. Aim

The aim of this study is to estimate the ROR hydropower potential capacity of the sub- catchment at Wainimala, Vitilevu, Fiji using SWAT modeling on a QGIS platform.

1.8.2. Research Objectives

There is a large amount of literature available on simulating streamflow of a catchment particularly using SUFI-2 algorithm and surprisingly many other models have been employed elsewhere in the world to achieve this. However, there is a knowledge gap in Fiji and study of this nature is paramount to estimate the streamflow of the catchments in Fiji. Thus, to further this study, hydrological models QGIS based QSWAT will be utilised to achieve this for Wainimala sub-catchment. In addition, other parameters such as the use of elevation, soil type, land use and hydrological variables that includes temperature, precipitation, solar radiation, minimum and maximum temperature data will be utilised to accomplish the project. The specific objectives of the study are:

1. To use QGIS v.31.6 with 30 m x 30 m resolution to delineate the watershed and stream network to create hydrological response units in order to determine the potential head.

2. To estimate discharge and use that to estimate the theoretical and technical ROR hydropower potential at sub catchment in WRB.

3. Provide an insight into the development of micro, small or large hydropower plants using the ROR potentials.

4. Determine the magnitude of carbon abatement potentials.

1.9. Research Motivations

Fiji suffered extensively from high price volatility of fossil fuels during the energy crisis and most of the country's GDP was lost to importation of fossil fuels. In addition, the increasing population, urbanization and rapid industrial developments have certainly led to increased energy demands. To meet these energy demands Fiji heavily resorts to fossil fuels. However, Fiji is slowly

increasing its percentage share of renewable energy and aiming to increase its gross installed capacity to achieve the stipulated energy targets in the near future. Though hydro is the dominant renewable energy source relative to other renewables, there is significantly huge untapped hydro potentials that have not been explored. Thus, this research motivates to use QGIS coupled with QSWAT to model and determine the hydropower potential of Wainimala sub-catchment, calculate the energy potential and determine the amount of carbon dioxide offset.

1.10. Organization of Minor Thesis

The thesis is organized in parts of six chapters:

- Chapter 1- *Introduction* - discusses the global status of renewable energy in the global energy mix stressing on hydropower technology and current status and history of hydropower generation in Fiji. Moreover, the chapter further discusses the research background, aim and specific objectives, research motivations and structure of thesis.

- Chapter 2 – *Literature Review* - discusses the modeling of hydrological cycle, classification and selection of hydrological model. Moreover, the chapter provides an overview of Geographic Information System (GIS) and discusses the processes involved in modeling SWAT-CUP with SUFI-2 and thoroughly discusses the literature on sensitivity analysis.

- Chapter 3 – *Model background and calibration* – discusses on SWAT model framework and Digital Elevation Model (DEM). Moreover, discussions on SWAT-CUP optimization, calibration and uncertainty process, performance indices and valuation are performed using SUFI-2 algorithm. Hydropower assessment and estimation of hydro potential are further outlined.

- Chapter 4 – *Study area and methodology* – describes the watershed area, data acquisition, SWAT model setup and functioning and stresses on the research methodology.

- Chapter 5 – *Results and Discussion* – discusses outcomes of the results such as: stream networks and delineated watersheds, topography, Hydrological Response Units (HRUs), Land Use Land Cover (LULC) of the basin method, slope morphology and soil characteristics. Moreover, differences in elevation led to hydraulic head determination that was involved with estimating the theoretical ROR hydropower potentials. Theoretical and technical hydroelectricity generations at all sub-basins were performed sub-basins with greater potential for hydroelectricity generations were highlighted. Calculations on estimated avoided carbon emissions and the limitations on the use of goodness of fit model are presented.

- Chapter 6 - Finally concludes the outcomes of the specific objectives thus presenting the main findings of the research and suggests further recommendations for the upcoming work.

Chapter 2

Literature Review

This chapter discusses the hydrological cycle (Figure 2.1) and classifies the hydrological models as Black Box Models, Deterministic Models and Conceptual Models (Figure 2.2). Moreover, the criteria on selection of hydrological model are outlined. SWAT model set-up, DEM, watershed delineation and open-source GIS are further discussed. A detailed literature review on hydrological modeling based on SWAT-CUP with SUFI-2 is presented reporting uncertainty analysis and model performance.

2.1. Modeling of Hydrological Cycle

Water is the crucial component of the hydrological cycle and ensures to maintain earth's ecosystem. In addition, the components of hydrological cycle are managed by climate and is responsible for providing the moisture and energy inputs that include maximum and minimum air temperature, daily precipitation, wind speed, relative humidity, solar radiation and relative humidity that ultimately control the water balance (Abbaspour et al., 2015a). The rainfall drives the hydrological cycle and is associated with global socioeconomic activities such as hydro-power potentials, rain-fed agriculture, stream flows and flood control, navigation and various ecological factors (Lofgren et al., 2014). Factors such as the increasing population, land use and climate change impacts has greatly affected the available renewable water that has led to water demand surge (Tamaddun et al, 2016; Kalra et al., 2017; Chen et al., 2017; Kandissounon et al., 2018). Thus, the available water is of great importance and hence coordinated water resource management practices should be prioritized for sustainable development.

The rainfall gauges at different stations continuously record rainfall data unless in extreme conditions such as during high floods, and instrument failure, etc., the hydrologists or engineers' resort to rainfall-runoff simulation models to determine the streamflow (Awasthi, 2021). The simulation model uses hydrologic cycles and incorporate change detection and catchment attributions (Folton et al., 2015; Hassan et al., 2010; Vandenberghe et al., 2006) in simulating hydrologic processes

(Abbaspour et al., 2007a) for stream flow estimations since the hydrologic cycle is climate driven (Arnold et al., 2012). This makes simulation easier and time saving compared to manual collection of data on water quality and quantity from different gauging stations requiring high labor, time and cost (Fekete et al., 2007).

According to Arnold et al. (2012), evapotranspiration, infiltration, surface runoff, return flow, lateral flow, tile drainage, water stored in the soil profile and transmission losses represent the primary elements of the hydrologic processes (see Figure 2.1). Moreover, the environmental problems led by natural and human factors such as LULC changes; soil degradation and climate changes have great impact on ecosystem services affecting water balance elements. Thus, to study these environmental problems there is a need to consider runoff above and below the earth's surface with the use of scientific methods and approaches (Kumar et al., 2017). According to Nguyen et al. (2015), the hydrological studies, impacts of climate change, water resource availability, managing floods and so on are highly important but accurately estimating the surface runoff and evapotranspiration becomes quite challenging.

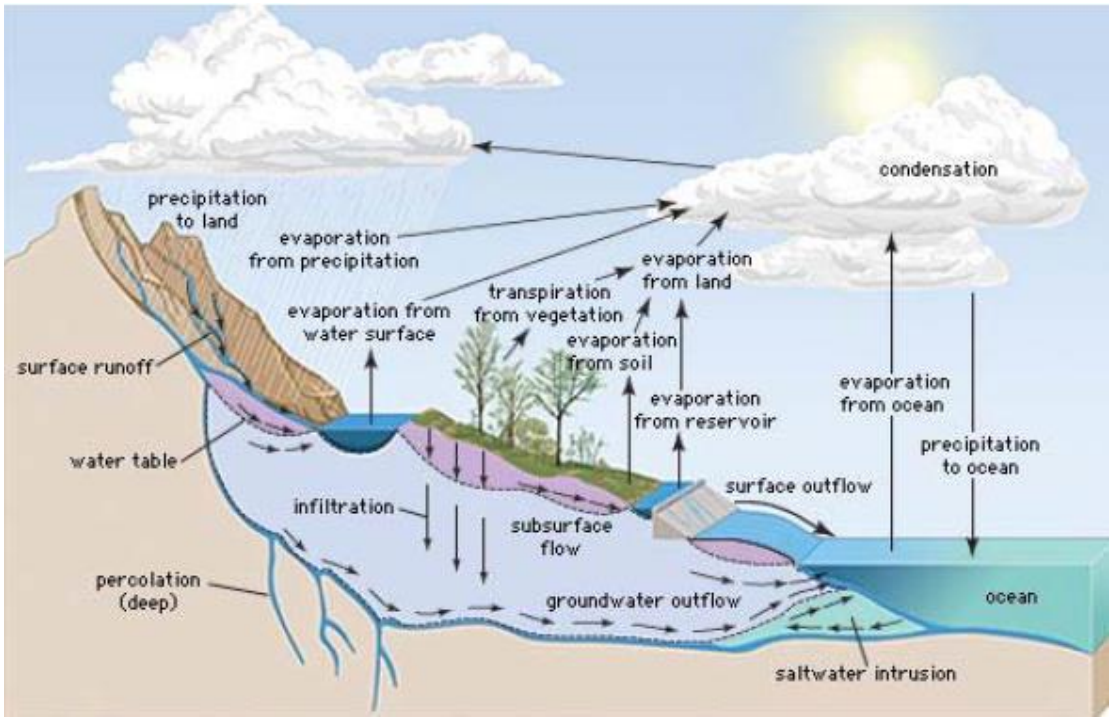

Figure 2.1: Schematic representation of hydrologic cycle (Encyclopedia Britannica).

This suggests that surface runoff being part of the rainfall just flows overland known as overland-flow due to poor soil infiltration that reaches streams and sea. Overland-

flow depends on factors such as amount of precipitation, rainfall intensity and infiltration capacity (Horton, 1993). As such the Hydrologic and Water Quality models (H/WQ) are quite crucial for this purpose to study the impact-based analysis on water resources and its ecosystem services. For instance, H/WQ models are probably becoming more and more widespread and could be possibly used for various purposes. These include: simulation of the hydrological component, sediment transport, chemical yield and consider the impacts of environmental changes on water resources to gauge water quality (Moriasi et al., 2012; Almeida et al., 2018).

It is quite a difficult task to model the basin and its hydrological processes. The task even becomes more complex with the increased size of basin and the number of parameters (Rahaman et al., 2019). Recent developments and access to powerful computers and advancements in computational techniques has prompted the developments in conceptual models (Nyaupane et al., 2018 a&b; Thakali et al., 2016, 2018). In addition, a semi-distributed hydrological watershed model such as SWAT is an effective tool used to assess the impact on topography, land use and climate change on water resources (Patel et al., 2013). In addition, the application of hydrological models is often challenged by different modeling phases such as parameter sensitivity, Uncertainty Analysis (UA) calibration and validation (Zhao et al., 2013; Zhang et al., 2008; Qin et al., 2015; Arnold et al., 2012).

For this purpose, the hydrological phenomena are used that are quantified using water balance equations and are related to factors such as soil type, land use, climate and basin morphology (water balance of a basin) and hydrologic components (Rahaman et al., 2019). However, these conceptual models involve complex processes and are quite tedious (Nyaupane et al., 2018 a&b; Thakali et al., 2018). Thus, computerized models can be employed to estimate the following: streamflow, water quality, flood impacts, sediment and nutrient transport and many more.

Interestingly, these models are quite beneficial and are able to simulate the past, current and future conditions of hydrological processes. The outcome of these simulations allows for sustainable water resource management practices by guiding water resource engineers and managers for the future of hydrological processes

(Rahaman et al., 2019). However, according to Pathak et al. (2016), the extreme events like floods and droughts due to climate change increases uncertainty in the streamflow modeling.

Parameter uncertainties are reduced to achieve the best fit parameters for the hydrological modeling (Singh et al., 2013). For instance, the hydrological cycle can be simulated by utilizing the SWAT model based on water balance which is controlled by climatic inputs such as maximum and minimum air temperatures, daily precipitation and so on (Neitsch et al., 2009).

2.1.1. Classification of Hydrological Models

The classification of hydrological models is based in a number of ways based on the components of the hydrologic cycle. The spatial analysis of the hydrologic cycle and the data quality are strongly linked to the hydrologic modeling and surface water resource planning and management (Mardookhpour et al., 2012). According to Patel et al. (2013 and 2014), the hydrological models are very important, useful and is an effective tool in managing water resources that includes assessing impacts and influence of LULC and the climate change impacts on water resources (Narsimlu et al., 2013; Singh et al., 2016; Srivastava et al., 2008, 2013).

Black Box Models, Deterministic Models and Conceptual Models are the three major categories of hydrological model (Parikh et al., 2019). Figure 2.2 represents the different types of classification of model. Different hydrologists adapt to different modeling approaches for the same hydrological system due to the complex nature of rainfall-runoff processes. For instance, according to Beven (2000), the rainfall-runoff models are classified either as lumped (distributed) or deterministic (stochastic). The distributed hydrologic models are quite simple (the basin is assumed to be a single-homogeneous unit with tiny number of parameters requiring less data). In this case the hydrologic parameters do not differ spatially within the basin and are evaluated only at the outlet leading to satisfactory results predicting discharge (Cunderlik, 2003; Xu, 2002; Boughton, 2004; Croke et al., 2006).
However, the distributed model is not simple and has predictions distributed in space requiring huge quantities of data parameterization in each grid cell (Beven, 2000).

Despite that, the highest degree of accuracy is provided by distributed models (Cunderlik, 2003). On the other hand, the semi-distributed models such as SWAT model (Arnold et al., 1998) have advantages over lumped models since their structure is more physically based and have less demanding input data in comparison to the fully distributed models (Cunderlik, 2003). Moreover, in semi-distributed models, the basins divide further into a number of smaller sub-basins by allowing the parameters to vary partially in space. However, these types of models need huge amounts of parameters to account for the spatial variability (Refsgaard, 1997; Carpenter et al., 2006; Wu et al., 2015). Moreover, the conceptual hydrological models are physically based and produce hydrological output based on limited representation of the physical process (Ward et al., 2000).

The quantification of water quality such as differing range of watershed drainage areas, environmental conditions and pollutants are performed with eco-hydrological models (Abbaspour et al., 2007a; Johnston et al., 2012; Wellen et al., 2015; Brewer et al., 2018) and are classified as either physical, mathematical (that includes lumped conceptual, distributed physically based models) or empirical models (Khoi et al., 2015; Koycegiz et al., 2019). According to Koycegiz et al. (2019) for physically based models, huge quantity of data is required in order to transfer the hydrological process to a computer simulation program. Practically, the distributed physically based hydrological models are preferred over lumped models since the realistic representation of the spatial variability of catchment characteristics are possible with it (Oeurng et al., 2011).

Interestingly, developed distributed hydrological models are frequently used for modeling with successful calibration and uncertainty analysis that include: Agricultural Non-Point Source (AGNPS) (Young et al., 1989), Hydrologic Simulation Program – Fortran (HSPF) (Bicknell et al., 2000), MIKE SHE (Refsgaard and Storm, 1995), Parameter Solution (PARASOL), Adaptive Clustering Covering (ACCO), General Algorithm (GA), Multi-start (M-Simplex), Uncertainty Estimation Based on Local Error and Clustering (UNEEC) (Methan et al., 2017), SWAT (Arnold et al., 1998), Topography based hydrological model (TOPMODEL) (Ambroise et al., 1996) and MOHID Land (Braunschweig et al., 2004), European

hydrologic system (SHE) and Artificial Intelligence (AI) models (Koycegiz et al., 2019).

Conversely, data-driven models that include AI, Computational Intelligence (CI), Soft Computing (SC), Machine Learning (ML) and Data Mining (DM) perform with the lack of knowledge on physical behavior of the system and analyse the system-related data by linking input and output variables (Solomatine et al., 2008).

2.2. Selection of Hydrological Model

There is a range of possible model structures within each class of models. It is quite challenging for a modeler to choose the appropriate model structure for the particular application so that the chosen hydrological model captures the essential information. Hence, Beven (2000) has outlined four criteria listed below for selecting model structures:

1. Opt for readily available models in consideration to worthwhile investments in time and money.
2. Consider that whether the chosen model will be able to meet the objectives and aims of the desired project.
3. Perform a pre-assessment on the assumptions made by the model and identify the assumptions that would be limiting.
4. Prepare a list of input requirements needed by the model and be considerate of time and cost constraints of the project.

The possible maximum theoretical energy stored in the stream is referred to as the gross hydropower potential (Arefiev et al., 2015). However, in reality the gross hydropower potential is not achieved due to factors such as environment flows and restrictions, countries economic, cost benefit analysis and multiple uses of water ways (Palomino Cuya et al., 2013; Shrestha, 2016). Contrary to this, the technical potential is part of hydropower potential which is developed in response to existing site conditions, the available current infrastructure and construction technologies and vast experiences in technical aspects of hydropower developments. Moreover, the part of technical potential that is economically and financially viable is termed as the economic potential (Arefiev et al., 2015). For instance, EFL's annual report presents different figures for the technical and economical hydropower potential of Fiji on yearly basis.

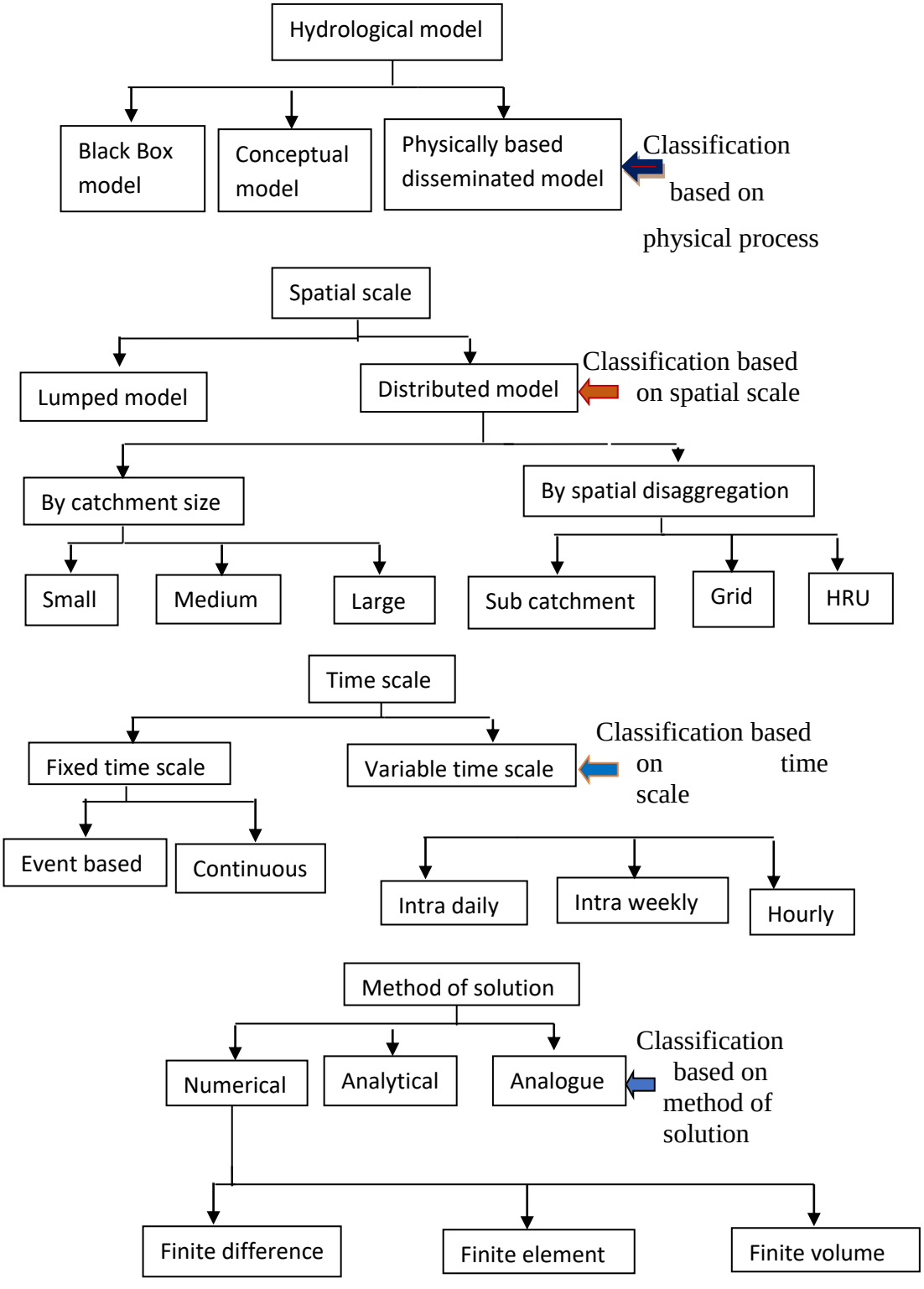

Figure 2.2: Flow chart representing the hydrological model classification (Semu, 2007).

2.3. An Overview of Geographical Information System (GIS)

2.3.1 GIS Model

GIS is a computer-based model and deals with the geographic data or maps to capture and process spatial data of geographic nature. GIS collects, stores, retrieves, transforms and displays spatial data from real world (Patra, 2010) and uses a coordinate system to geo-reference these spatial data. Real world data is organized into different layers such as terrain features, population data, ecological, environmental and demographic information data, land use, flood plains, river drainage, roads and wildlife habitats using GIS Systems. Moreover, GIS manages the large and complex database as part of systematic management (Lakshmi et al., 2018). However, different layers are used for different applications.

Thus, GIS has been used in many applications and is proved to be an efficient tool in the identification of potential hydropower sites for sustainable development. To assess the potential of hydroelectricity, a GIS based hydrological modeling is commonly performed on raster cells with the use of meteorological and topographical datasets. For this, huge amount of input datasets such as Digital Elevation Maps (DEM), LULC, soil map, watershed boundary and weather data are required (Tarife et al., 2017; Lakshmi et al., 2018) to delineate watershed, stream network and number of HRU's. In case of unavailability of potential climatic data, DEM and hydrologic data are used via Rapid Hydropower Assessment Model (RHAM) to calculate the hydroelectric power, and to assess the suitability of hydropower developments in consideration to socio-economic and environmental factors (Lakshmi et al., 2018).

Moreover, the innovative developments such as remote sensing and satellite data in GIS technology is providing new opportunities in evaluating and re-estimating hydropower potentials in many countries around the world (Alterach et al., 2009; Arefiev et al., 2015; Ballance et al., 2000; Feizizadeh et al., 2012; Hall et al., 2004; Punys et al., 2011; Ramachandra et al., 2004). However, GIS based techno-economical assessments are carried out to a lesser extent due to complexities in spotting the ROR hydropower though there are great potentials (Kayastha et al., 2018). On the other hand, ROR hydropower projects schemes at a river basin are

precise and require greater effort and advanced programming skills in order to estimate the flow and elevation difference to calculate power generation capacity (Kayastha et al., 2018). Open-source Cross-Platform Desktop QGIS is largely preferred for this purpose due to free and easy accessibility. In addition, QGIS platform allows viewing and editing spatial data, creating layered maps and performing spatial analysis.

Several semi-distributed (physically based) watershed models have already been introduced in recent years for environment and water resource management simulations (Patel et al., 2013, 2014). Among these models, the SWAT model is well established, successfully and most widely used globally by researchers around the world. SWAT is recognised as the principal spatially distributed hydrological model in addressing the hydrologic and environmental issues (Tan et al., 2019; Khoi et al., 2015; Khalid et al., 2016; Arnold et al., 1990; Narsimlu et al., 2015). This model is also efficient, user-friendly and found to be promising by researchers for assessing and managing water resource in long-term (Rahaman et al., 2019; Guiamel et al., 2020; Epelde et al., 2015). SWAT model is able to perform simulations of climate change impacts on hydrologic processes (Arnold et al., 1993).

According to Parikh et al. (2019), SWAT model is deterministic i.e., the same outputs are produced when each successive model runs using the same inputs and uses non-linear partial differential equations. In addition, the performance of SWAT model was compared with other hydrological models such as Dynamic Watershed Simulation Model (DWSM), HSPF model by Borah et al. (2004) and found that the SWAT model is quite useful for agricultural watersheds monthly predictions. An exception was found during extreme storm events and hydrologic conditions (Bicknell et al., 1997). Moreover, Van Liew et al. (2003) performed a comparative study on streamflow predictions using SWAT and HSPF. It was found that the SWAT model has been more consistent in estimating the streamflow for different climatic conditions and investigating the long-term impacts of climate variability as well.

Further, SWAT model has the capability to perform uninterrupted simulations over a long period of time (Neitsch et al., 2005). However, SWAT model becomes

inefficient and cannot be applied to where the meteorological data are scarce in areas such as glacial and deserts (Meng et al., 2018). In addition, for deterministic SWAT model to work efficiently, a huge amount of data and computational time is required (Parikh et al., 2019). However, this deterministic model presents a more preferable interpretation of the hydrological system.

The determination of potential site(s) for hydropower development requires a thorough examination of historical climatic data. Not only that, an initial pre-feasibility, feasibility, techno-economic analysis and other relevant assessments have to be performed prior to any decisions made on hydropower developments. The use of SWAT modeling on GIS/QGIS platform is highly essential and has been widely used globally in various different studies and researches to identify potential sites for hydropower developments.

The SWAT model has been employed to evaluate impacts of climate change and land management policies on water (Shahoei et al., 2017; Shi et al., 2011). SWAT is being chosen by various researchers for the purpose of varied studies including studies in diverse climate and terrain (Duru et al., 2018; Khatun et al., 2018). Thavhana et al. (2018) adopted the SWAT to simulate streamflow of the Luvuvhu river catchment in South Africa on a monthly timescale. The simulated values have shown good consistency with the observed data except for the P-factor. Utilizing SWAT, Khatun et al. (2018) simulated the streamflow of Satluj Basin (Suni to Kasol) in Himalya region, India. The results showed that the monthly averaged streamflow was satisfactory in the calibration and validation periods.

2.3.2. SWAT-CUP with SUFI-2 (Sensitivity Analysis)

In model optimization, one of the key issues with semidistributed models is the calibration of the sensitive parameters (Jajarmizadeh et al., 2017). According to literature, the input parameters are mostly analysed by SUFI-2 algorithm in SWAT-CUP. For instance, a comparative study on parameter uncertainty analysis to simulate streamflow at Vietnam in Srepok river catchment was performed using Generalized Likelihood Uncertainty Estimation (GLUE), Parameter Solution (Parasol), Particle Swarm Optimization (PSO) and SUFI-2. This study revealed that

SUFI-2 method has the best performance and had advantages in the model calibration and uncertainty analysis. Furthermore, this technique has the ability to perform with smallest simulation runs and obtains good prediction uncertainty bands and model performance (Khoi et al., 2015).

SUFI-2 algorithm has been used by researchers to model calibration and uncertainty analysis of parameters of SWAT model. Spruill et al. (2000) investigated the simulation of daily and monthly stream discharge at central Kentucky watershed by performing sensitivity analysis on 15 parameters using SUFI-2 algorithm. Low correlation coefficient of determination (R^2) values of -0.04 and 0.19 respectively were obtained for measured and simulated daily streamflow during 1995 and 1996 compared with better correlation for monthly discharge between 1995 and 1996 with values of 0.58 and 0.89 respectively. In addition, Guo et al. (2008) simulated the daily streamflow of Xinjiang River Basin, China and reported that (R^2) and Nash-Sutcliffe efficiency (*NSE*) values were higher than those obtained by Yuan et al. (2019). In contrast, Guo et al. (2008) reported the simulated daily streamflow for R^2 and *NSE* values as 0.88 and 0.86 respectively during the calibration and 0.86 and 0.84 respectively during the validation period. Setegn et al. (2008) performed the hydrological modeling in the Lake Tana Basin, Ethiopia using SWAT 2005 model. The authors comparatively used the techniques SUFI-2, GLUE and ParaSol algorithm to model the sub basin to estimate the streamflow and soil erosion of the Gilgel Abay River, Gumera River, Ribb River and Megech River. The sensitive parameters obtained were soil evaporation compensation factor (ESCO), initial Soil Conservation Service (SCS) Initial SCS Runoff Curve Number for Moisture Condition II (CN2), base flow alpha factor (ALPHA_Bf), threshold depth of water in the shallow aquifer for revap (REVAPMN.gw), available water capacity (Sol_Awc), groundwater "revap" coefficient (Gw_Revap), channel effective hydraulic conductivity (Ch_K2) and threshold depth of water in the shallow aquifer for return flow to occur (GWQMN.gw). SUFI-2 and GLUE algorithms have shown good agreement between observed and simulated monthly flows for both calibration and validation phases for all river basins with R^2 and *NSE* values greater than 0.8.

Further, Shi et al. (2011) performed comparative hydrological modeling at the four gauging stations of: Xixian River Basin, Zhuganpu River Basin, Dapoling River

Basin and Changtaiguan River Basin, China to estimate the surface runoff. The authors compared the model performance of SWAT Latin Hypercube One-At-A-Time (LH-OAT) and Xinanjiang (XAJ) model using performance indices and found that both SWAT and XAJ hydrologic models performed equally in simulating daily runoff at four monitoring stations. Both the models produced R^2 and *NSE* values greater than 0.69 and PBIAS values lower than 15% for both calibration and validation phases. XAJ model is easier to work with since it requires minimum input data to work with and is much preferred for forecasting flood and simulating runoff. Conversely, SWAT analysis requires extensive data preparation and is complex, process-based model and has the ability to simultaneously simulate water quantity and quality and evaluate impacts of land use and human activities. Hence, SWAT model is preferred over XAJ since the study area is agricultural based and activities associated are intensive. They evaluated the results for calibration and validation period and reported the R^2, *NSE*, PBIAS and RSR values of 0.74, 0.73, -0.35 and 0.54 respectively during the calibration period and R^2, *NSE*, PBIAS and RSR values of 0.75, 0.69, 18.55 and 0.56 respectively.

Jajarmizadeh et al. (2012) performed the sensitivity analysis using LH-OAT followed by SUFI-2 algorithm in SWAT-CUP to simulate the stream flow at Roodan watershed in Iran. Out of 26 hydrological parameters only 12 parameters were most sensitive where R^2 and *NSE* values for calibration were 0.93 and 0.92, respectively while for validation processes it was 0.83 for both.

Moreover, Salimi et al. (2016) simulated the runoff using SWAT model and SUFI-2 algorithm for Shafaroud, watershed, Guilan Province, Iran. The Soil Bulk Density (SOL_BD) and SCS curve number for moisture condition II (CN2) were the most sensitive parameters. The calibrated and validated SWAT model reported the P-factor, R-factor, R^2 and *NSE* values of 0.51, 0.54, 0.86 and 0.77 respectively during the calibration period and the P-factor, R-factor, R^2 and *NSE* values of 0.63, 0.49, 0.85 and 0.74 respectively. The results of the study have shown a good correlation between the observed and simulated values both during calibration and validation though initially the size of uncertainty band (95 Prediction Uncertainty, PPU) had been very high.

In addition, Narsimlu et al. (2015) performed SWAT model calibration and uncertainty analysis for streamflow at the Kunwari River Basin, India using SUFI-2 algorithm. They calibrated and validated the SWAT model and reported the P-factor, R-factor, R^2 and *NSE* values of 0.82, 0.76, 0.77 and 0.74 respectively during the calibration period and the P-factor, R-factor, R^2 and *NSE* values of 0.71, 0.72, 0.71 and 0.69 respectively. Global sensitivity analysis was used for evaluation and the parameters ALPHA_BNK (Baseflow alpha factor in days), ESCO (soil evaporation compensation factor) reported to be the most sensitive followed by CH_K2 (effective hydraulic conductivity in main channel alluvium in mm/hr) and CN2. The results of the study would benefit the community at large for agricultural water management and soil conservation and assist in mitigating natural hazards such as floods and drought. Moreover, the study conducted by Wu et al. (2015) used GLUE, SUFI-2 and ParaSol analysis methods to evaluate uncertainty estimates for Wenjing River watershed in China. Interestingly, the results indicated that the use of SUFI-2 method provided more reasonable simulated results in comparison to other two methods used. Another similar study performed by Uniyal et al. (2015) in a river basin of eastern India used SUFI-2 and GLUE analysis techniques to evaluate uncertainty estimates in distributed hydrological modeling. The results indicate that both SUFI-2 and GLUE are promising techniques and can be utilised to conduct uncertainty analysis at different catchments having varying agro-climatic conditions.

Further, Mahzari et al. (2016) performed hydrological modeling at 14 different stations to simulate monthly runoff at Gorganrood watershed, Iran using SUFI-2 algorithm. The parameter Curve Number management (r_CN2.mgt) was the most sensitive parameter followed by Threshold Depth of Water in the Shallow Aquifer for Return Flow to Occur (v_GWQMN.gw). Likewise, Khalid et al. (2016) performed sensitivity analysis of Langat River Basin using SUFI-2 algorithm in order to simulate daily streamflow. 21 parameters were analysed for using the local and global sensitivity technique where SCS runoff number (CN2) was the most sensitive parameter when the sensitivity analysis was performed using one-at-a-time (local) technique. In addition, parameters such as Base Flow Alpha Factor (ALPHA_BF), Groundwater Delay Time (GW_DELAY) and Effective Hydraulic Conductivity in the Main Channel Alluvium (CH-K2.rte) were also sensitive when sensitivity analysis was performed using global technique with 2000 iterations.

Gholami et al. (2016) performed hydrological modeling to simulate the daily streamflow at Talar watershed located in the central section of the Alborz Mountains, north of Iran. The authors calibrated and validated the SWAT model for monthly streamflow and reported the R^2 and *NSE* values of 0.02 and -38.28 respectively during the calibration period and the R^2 and *NSE* values of 0.93 each.

Mehan et al. (2017) conducted hydrological modeling in an agricultural watershed of South Dakota to simulate streamflow using SWAT coupled with SUFI-2 algorithm. 24 parameters were selected from the past available literature and global sensitivity function was used within the SWAT-CUP to accomplish this. The results of the study show that Available Water Capacity of the soil Layer (SOL_AWC) was the most sensitive parameter whereas CH_K2 was determined to be the least sensitive. Another study Kumar et al. (2017) conducted hydrological modeling in Tons River Basin, Madhya and Uttar Pradesh in India using SWAT model. They calibrated and validated the SWAT model and reported the P-factor and R-factor values of 0.54 and 0.76 respectively during the calibration period and the P-factor and R-factor values of 0.68 and 0.56 respectively. Likewise, Kouchi et al. (2017) performed hydrological modeling at two watersheds in Iran to simulate monthly streamflow. The authors conducted comparative analysis using the algorithms: SUFI-2, GLUE and PSO and evaluated the model performance using the objective functions (R^2, Modified Coefficient of Determination (bR^2), *NSE*, MNS, RSR, SSQR, KGE and PBIAS). Ayele et al. (2017) performed hydrological modeling and estimated the streamflow and sediment yield of the upper Blue Nile River Basin, Ethiopia. The authors comparatively used SUFI-2, GLUE, ParaSol and PSO algorithms to accomplish this.

Ghadei et al. (2018) performed hydrological modeling of the Ong River Basin, India. They calibrated and validated the SWAT model and reported the P-factor and R-factor values of 0.75 and 0.82 respectively during the calibration period and the P-factor and R-factor values of 0.72 and 0.65 respectively. Their study revealed that the parameter CN was the most sensitive for the sub-basin. Moreover, Dias et al. (2018) performed hydrological modeling of the streamflow of the Furnas HPP reservoir at a monthly scale. The authors used SUFI-2 with SWAT-CUP to evaluate the model performance. They calibrated and validated the SWAT model and reported the *NSE*, R^2 and PBIAS values of 0.86, 0.87 and 1.10 respectively during

the calibration period and *NSE*, R^2 and PBIAS values 0.64, 0.66 and 6.10 respectively. The results of the study reveal that the model performance was better during calibration stage as compared to the validation process. This was due to the observed uncertainty streamflow in 2012.

Another study by Almeida et al. (2018) conducted hydrological modeling of Mucuri River Bain in the Northeast region of the States of Minas Gerais, Brazil. The authors used LH-OAT to perform the sensitivity analysis on 19 parameters to evaluate the model performance with 250 iterations each. In this study calibration was performed at intermediate fluviometric station (Carlos Chagas station) whereas validation was performed at five other locations: three upstream (Diacui Farm, Francisco Sá station, São Pedro do Pampã station) and one downstream (Mucuri station). Based on statistical indices, the stations Francisco Sá, São Pedro do Pampã and Mucuri has shown inferior model performances. Further, Cao et al. (2018) performed hydrological modeling at Lijiang River Basin, China to estimate the daily and monthly streamflow. The authors used SUFI-2 algorithm to evaluate the model performance by measuring Sensitivity Analysis (SA) and UA. They calibrated and validated the SWAT model for monthly streamflow and reported the P-factor, R-factor, R^2, *NSE*, PBIAS and RSR values of 0.79, 0.33, 0.96, 0.96, 7.70 and 0.20 respectively during the calibration period and the P-factor, R-factor, R^2, *NSE*, PBIAS and RSR values 0.63, 0.37, 0.96, 0.95, 7.80 and 0.22 respectively.

Emam et al. (2018) used semi-distributed hydrological modeling to evaluate the best model performance for Thuong Nhat Basin at central Vietnam in the province of Thua Tien Hue. They compared four algorithms: GLUE, SUFI-2, Parameter Solution, Parasol and Particle Swarm Optimization (PSO). SUFI-2 and PSO algorithms are known to show high model performance with P-factor > 0.83, R-factor < 0.56, R^2 > 0.91, *NSE* > 0.89 and 0.18 < PBIAS < 0.32. Similarly, another comparative study by Paul et al. (2018) performed hydrologic modeling for San Joaquin watershed in California using SWAT model to estimate the monthly streamflow. The authors evaluated the model performance using the techniques SUFI-2, GLUE, Parasol and found that SUFI-2 algorithm has performed the best in consideration to the performance indices. Shivhare et al. (2018) at the Ganga River watershed in the state of Uttar Pradesh, India estimated the runoff and sediment

yield. The authors used the SUFI-2, GLUE and Parasol algorithms to analyze the model performance. The results indicate that SUFI-2 algorithm has performed better than other constructed models. They calibrated and validated the SWAT model and reported the R^2 and *NSE* values of 0.78 and 0.76 respectively during the calibration period and the R^2 and *NSE* values 0.71 and 0.756 respectively. Irvem et al. (2018) conducted hydrological modeling at four sites (Uctepe, Himmetli, Korkun and Zamanti) of Seyhan River Basin, Turkey to estimate monthly streamflow. The authors compared SUFI-2, GLUE and ParaSol algorithms to evaluate model performance. The results of the study suggest that SUFI-2 algorithm performed well in consideration to P-factor value > 90%. Likewise, the model also performed better with ParaSol algorithm in consideration to the high values of the objective function, *NSE*.

Tejaswini et al. (2018) used SUFI-2 algorithm in SWAT-CUP package to perform global sensitivity analysis for Kunthipuzha basin using one-at-a-time technique. In this study, 20 parameters were analysed for sensitivity analysis of which ALPHA_BF was the most sensitive followed by CH_K2, CN2, SOIL_Z and Surface Runoff Lag Coefficient (SURLAG). The result of this study has comparable results for the region with other studies previously conducted. Mimich et al. (2018) performed the hydrological modeling at the Kansera dam at Beht River catchment with 1500 iterations to estimate the water runoff. The most sensitive parameter obtained was CN2 followed by ALPHA_BF. Similarly, the authors calibrated and validated the SWAT model for monthly streamflow using SUFI-2 algorithm and reported the P-factor, R-factor, R^2, *NSE*, PBIAS and RSR values of 0.77, 0.96, 0.83, 0.77, -3.9 and 0.48 respectively during the calibration period and the P-factor, R-factor, R^2, *NSE*, PBIAS and RSR values of 0.69, 1.53, 0.78, -10.1 and 0.49, respectively. The results show that monthly simulations during the calibration period are very good while the SWAT model presents good validation results with small uncertainties.

Rahaman et al. (2019) conducted hydrological modeling of Trinity River Basin, Texas, USA to simulate streamflow. The authors used 12 parameters and performed sensitivity analysis using global technique in which CN2 was the most sensitive parameter. The SWAT model was calibrated and validated. During the calibration

period and the P-factor = 0.42, R-factor = 0.52, R^2 = 0.80, *NSE* = 0.87, PBIAS = -28.60 and RSR = 1.12 while the validation period registered P-factor = 0.63, R-factor = 0.61, R^2 = 0.79, *NSE* = 0.76, PBIAS = -12.62 and RSR = 0.87. The monthly simulated streamflow has shown better correlation during validation phase in comparison to observed streamflow during calibration period. The model has been overestimated for the observed scenario during validation period. Mengistu et al. (2019) conducted hydrological modeling in an ungauged catchment in South Africa through regionalization with physical similarity approach (this is to minimize uncertainties in hydrological models) to estimate monthly streamflow using SUFI-2 global sensitivity technique. The authors calibrated and validated the SWAT model and reported the P-factor, R-factor, R^2, *NSE*, PBIAS and RSR values of 0.73, 0.93, 0.83, 0.82, 11.80 and 0.43 respectively during the calibration period and the P-factor, R-factor, R^2, *NSE*, PBIAS and RSR values 0.65, 0.66, 0.72, 0.71, -8.10 and 0.55 respectively.

Yuan et al. (2019) conducted hydrological modeling using SUFI-2 algorithm to simulate both daily and monthly streamflow at Xinjiang River Basin, China. The authors used Global Sensitivity Analysis technique to optimize the model and reported that Baseflow alpha factor (V_ALPHA) as the most sensitive parameter. They calibrated and validated the SWAT model for daily streamflow and reported the P-factor, R-factor, R^2, *NSE*, PBIAS and RSR values of 0.83, 1.31, 0.60, 0.54, -33.1 and 0.68 respectively during the calibration period and the P-factor, R-factor, R^2, *NSE*, PBIAS and RSR values of 0.83, 1.37, 0.43, -27.7 and 0.78 respectively. Similarly, they calibrated and validated the SWAT model for monthly streamflow and reported the P-factor, R-factor, R^2, *NSE*, PBIAS and RSR values of 0.73, 1.37, 0.79, 0.67, -33.6 and 0.57 respectively during the calibration period and the P-factor, R-factor, R^2, *NSE*, PBIAS and RSR values of 0.66, 1.31, 0.60, -26.8 and 0.71 respectively. Ansari et al. (2019) evaluated the hydrological modeling for Keduang sub-watershed to simulate daily and monthly streamflow using SUFI-2 algorithm. The authors calibrated and validated the SWAT model for daily streamflow and reported the *NSE*, R^2, PBIAS and RSR values of 0.57, 0.58, -3.4 and 0.67 respectively during the calibration period and the *NSE*, R^2, PBIAS and RSR values of 0.50, 0.51, -10.7 and 0.65, respectively. While for monthly streamflow the *NSE*, R^2, PBIAS and RSR values were 0.79, 0.81, -6.2 and 0.54 respectively and the

calibration period *NSE*, R^2, PBIAS and RSR values were 0.73, 0.69, -1.9 and 0.71, respectively. They concluded that monthly simulation had better results and the model has performed well both during calibration and validation phases. Parikh et al. (2019) also performed hydrological modeling of Sub-basin of Deo River, Panch Mahal, and Gujarat, India using SUFI-2 algorithm and LHS-OAT technique to perform sensitivity analysis. The authors calibrated and validated the SWAT model for monthly streamflow and reported the R^2, *NSE*, PBIAS and RSR values of 0.89, 0.87, -3.8 and 0.37 respectively during the calibration period and the R^2, *NSE*, PBIAS and RSR values of 0.88, 0.81, -30.6 and 0.43 respectively. They reported that the most sensitive parameter obtained was R_CN2.mgt followed by Available Water Capacity Factor (R_SOL_AWC.sol).

Koycegiz et al. (2019) used SUFI-2 algorithm to calibrate the SWAT model in order to simulate streamflow at the headwater of Carsamba River located at the Konya Closed Basin, Turkey. In this study, the authors performed a comparative analysis of model performance of SUFI-2 algorithm of the SWAT model with data driven models such as radial-based neural network (RBNN) and support vector machines (SVM). The SWAT model performed well and has shown better correlation (R^2 = 0.787 and *NSE* = 0.779) at calibration stage but model's performance decreased at the validation stage (R^2 = 0.508 and *NSE* = 0.502). The SWAT model has shown uneven performance and successfully estimated the low streamflow but high streamflow estimations were relatively unsuccessful. Comparatively, AI models have performed better than SWAT model. Despite this, the SWAT model is considered more than AI models since SWAT model consider the environmental factors while performing spatial analysis in order to simulate streamflow. Secondly, SWAT model has the ability to produce consistent solutions under varying scenarios.

Moreover, Leng et al. (2020) reported the hydrological modeling and simulated the monthly streamflow at Daning hydrological station of Xinshui watershed on the Loess Plateau, China using global sensitivity technique. The authors tested 24 hydrological parameters of which (Moist Bulk Density) R_SOL_BD.sol had been the most sensitive. They calibrated and validated the SWAT model and reported the P-factor, R-factor, R^2, *NSE*, PBIAS and RSR values of 0.77, 0.85, 0.85, 0.83, 0.41and 20.0 respectively during the calibration period and the P-factor, R-factor, R^2,

NSE, PBIAS and RSR values 0.87, 0.90, 0.89, 0.88, 0.34 and 17.6 respectively. The simulated annual average streamflow values during calibration and validation phases are 2.14 m^3/s and 2.68 m^3/s respectively. The authors further reported that the determined streamflow remained within the 95PPU boundary though in some cases especially during winter and flood periods in summer between 1990-1992 streamflow values were underestimated. Gu et al. (2020) initially simulated the hydrological processes (evapotranspiration, filtration, surface runoff, and ground water runoff and sediment erosion) at Manas River Basin, northern China using the China Meteorological Assimilation Driving Datasets (CMADS) version 1.1 for the SWAT model since the study site lacked the potential historical meteorological data. The authors then ultimately estimated the daily and monthly runoff using the global sensitivity analysis (LH-OAT) method of SUFI-2 algorithm through performing sensitivity analysis, calibration and verification processes.

Awasthi (2021) performed hydrological modeling to simulate runoff at Bhagirathi Basin up to Tehri dam using SUFI-2 algorithm. 1000 iterations were performed for 19 parameters and authors found that (Soil Hydraulic Conductivity) SOL_K (1).sol was found to be the most sensitive parameter followed by Snowfall Temperature (SFTMP.bsn). They calibrated and validated the SWAT model for monthly streamflow and reported the R^2 and *NSE* values of 0.78 and 0.74, respectively during the calibration period and the R^2 and *NSE* values of 0.74 and 0.69, respectively. Amin et al. (2020) performed hydrological modeling of Mojo River watershed in Ethiopia using SUFI-2 algorithm to simulate monthly streamflow. From the chosen 13 parameters, the most sensitive parameter obtained was CN2.mgt followed by ALPHA_BNK.rte. The authors used the global sensitivity analysis to evaluate the model performance. They calibrated and validated the SWAT model for monthly streamflow and reported the P-factor, R-factor, R^2, *NSE*, PBIAS and RSR values of 0.82, 0.01, 0.78, 0.75, -10.6 and 0.5 respectively during the calibration period and the P-factor, R-factor, R^2, *NSE*, PBIAS and RSR values of 0.77, 0.01, 0.74, -14.4 and 0.56 respectively.

Literature shows that this method of streamflow estimation has not been performed in Fiji and thus, the use of this robust platform with QGIS/QSWAT approach has numerous advantages. For instance, it is an open-source cross-platform with free

desktop GIS application. This suggests that it is easily accessible for graphical map creation and editing. Additionally, QGIS is quite fast and user-friendly with latest versions available in English and different other languages. QGIS can be easily installed and used on personal computers since it is compatible with windows, Linux, android and macOS.

Chapter 3
Model background and Hydropotential Estimations

This chapter discusses the SWAT Model brief background, with a background of calibration and uncertainty procedures using SWAT-CUP. Then the background of SUFI-2 algorithm incorporated with SWAT-CUP for model optimization via sensitivity analysis is presented. Various performance metrics that have been used and a background is presented. Advanced Space borne Thermal Emission and Reflection Radiometer Global-DEM (ASTER GDEM), watershed delineation and hydropower potential estimation process are discussed finally. The potential of a single basin and all sub-basins are calculated with regression analysis to determine the yield of the catchment area then the power and energy is calculated.

3.1. SWAT Model Framework

The SWAT model is the modification of the Simulator for Water Resources in Rural Basin (SWRRB) model, (Williams et al., 1985; Arnold et al., 1990). The hydrologic SWAT was introduced earlier in 1998 by Arnold et al. (1999) who simulated the river discharges for around 6000 gauging stations in the USA. Essentially, the SWAT model has the ability to simulate a number of hydrologic components such as surface and subsurface flows including streamflow and groundwater flow generation, hydro potential, river basin modeling, water quality modeling, land use management activities on runoff, pollutants, sediment yield modeling, reservoir storage, irrigation, climate and land cover change impacts, nutrient movements associated with hydrological cycle of watershed, agricultural chemical distributions and so on for an hourly or daily time scales (Abeyou et al., 2018; Rahaman et al., 2019; Neitsch et al., 2011; Khalid et al., 2016; Lakshmi et al., 2018). Even the large basins can be simulated by utilising the SWAT (Kurse et al., 2010).

The potent characteristics of SWAT such as being comprehensive, semi-empirical and semi-physically, process-based model, continuous time, semi-distributed river basin model (is a trade-off between fully distributed and lumped models) is a

conceptual mathematical base model. This model approximates the physical behavior of the hydrologic structure using mathematical equations and having a long-term water and sediment tool allows SWAT to work on daily averages by interconnecting contrasting physical processes that happens at the watershed (Bian et al., 1996; Neitsch et al., 2005; Gassman et al., 2007; Arnold et al., 1998, 2012; Andrade et al., 2013; Monteiro et al., 2015; Adu et al., 2018). Another key advantage is that SWAT model minimizes modeling errors due to spatial variability of datasets that results from the assumptions of lumped, stationary and linear systems (Ayele et al., 2017).

The three major components of SWAT model include sub-basin, reservoir routing and channel routing with eight major divisions in the sub-basin component. Additionally, hydrology, weather, sedimentation, soil temperature, crop growth, nutrients, agricultural management and pesticides are the major sub-basin components (Spruill et al., 2000). Amongst the sub-basin components, the hydrology component is composed of surface runoff, percolation, lateral subsurface flow, groundwater flows including snowfall and snow melt, infiltration, evapotranspiration, transmission losses, plant uptake and ponds (Knisel, 1980; Williams et al., 1982; Neitsch et al., 2005). Further, channel inputs are function of channel width, length and flow duration. The components of channel inputs include: length slope, depth, top width, side slope, food plain slope, channel roughness factor and flood plain roughness factor (Spruill et al., 2000). The Modified SCS Curve Number (CN) method is used to estimate the surface runoff volume (Mishra et al., 2003). Kinematic storage model simulates lateral flow whereas the shallow aquifer is created to estimate the return flow (Arnold et al., 1998).

Moreover, in SWAT model the watershed is divided into several sub-watersheds or sub-basins and then further splitted into multiple HRUs (i.e., simulation unit of the model) based on land cover and soil characteristics (Irvem et al., 2018). According to Neitsch et al. (2011), the HRU is defined as an area comprised of a unique land cover and soil type. HRUs incorporate the parameters such as homogeneous soil characteristics, land use and land management (Rahaman et al., 2019; Neitsch et al., 2010; Abbaspour et al., 2015a). A comprehensive review on SWAT model

applications, calibration and validation can be found in Gassman et al. (2007) and Arnold et al. (2012).

SWAT model uses the water balance concept to simulate the hydrology of watersheds at land phase level. From a schematic perspective, several hydrological processes of land including infiltration, surface runoff, base flow, lateral flow, evapotranspiration and canopy storage are used to calculate the water movement in an HRU as presented in Figure 3.1.

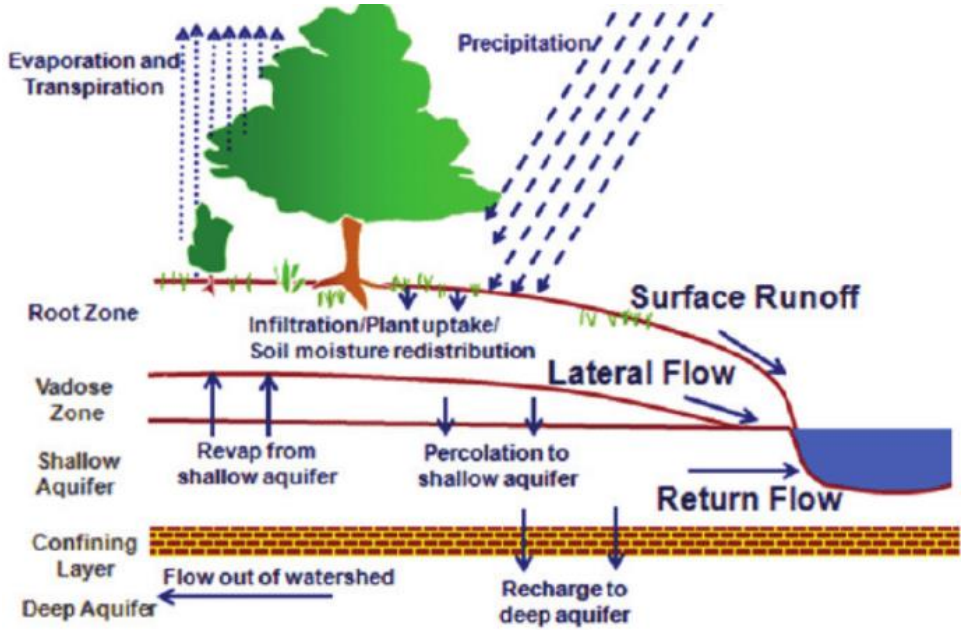

Figure 3.1: Schematic description of the hydrologic cycle in SWAT (Neitsch et al., 2011).

Incorporating these related processes such as precipitation, surface runoff, soil water storage, evapotranspiration and recharge into a mathematical format result in the development of an empirical model. For this purpose, the following equation is used to model the runoff (Neitsch et al., 2011):

$$SW_t = SW_o + \sum_{t=1}^{t} \left(R_{day} - Q_{surf} - E_a - W_{seep} - Q_{gw} \right) \quad \text{(Eq 1)}$$

where

SW_t is the final soil water content (mm H_2O);

SW_o is the initial soil water content on i^{th} day (mm H_2O);

t = time (in days);

R_{day} is the amount of precipitation on i^{th} day (mm H_2O);

Q_{surf} is the amount of surface runoff on i^{th} day (mm H_2O);

E_a is the amount of evapotranspiration on i^{th} day (mm H_2O);

W_{seep} is the amount of water entering the vadose zone from the soil profile on i^{th} day (mm H_2O)

Q_{gw} is the amount of return flow on i^{th} day (mm H_2O)

According to Pinto et al. (2013), the operating sequence of SWAT includes the following steps: heating or warming period, sensitivity analysis, model parameter calibration, validation and simulation. All hydrological models are subjected to various sources of uncertainties regardless of the model design (Emma et al., 2018). Uncertainties arise due to model inputs with measurement errors, assumption and simplification of model structures and approximations of model parameters (Xue et al., 2014; Jin et al., 2010; Setegn et al., 2010). Thus, the calibration of hydrological model becomes a challenging task due to these uncertainties. (Yang et al., 2008). To ensure that the hydrological model works accurately in simulating the hydrological processes, the uncertainties need to be assessed through the careful analysis followed by model calibration and validation. The SWAT model reduces uncertainty through sensitivity analysis of the parameters (Van et al., 2006).

Though these uncertainty parameters are unavoidable but the use of a suitable and promising uncertainty analysis technique known as SA can be employed to control (account for uncertainty) and optimize the model (Wu et al., 2015). It is very essential to estimate the accurate streamflow in order to estimate the occurrence of floods, plan hydraulic structures and devise strategies for agricultural developments (Vilaysane et al., 2015; Dias et al., 2018; Swain et al., 2018). Further, SWAT model is integrated into the GIS platform to manage raster, vector and alphanumeric data. For this, all of the available data gets integrated to build the model so that hydrological and water quality processes can be calculated accordingly (Hallouz et al., 2018).

3.2. Digital Elevation Map (DEM)

DEM is the initial step of the model set up and is the digital topographic dataset employed by the SWAT model for watershed delineation (this generates drainage network), slope gradient, etc. for the topographical model's parameterization (Nguyen et al., 2017) and is represented by geographic/cartographic dataset of elevations in xyz coordinates (United States Geological Survey, USGS), 2012). Moreover, DEM is the geospatial raster data with continuous elevation values with an array of cells or pixels (Thin et al., 2020). According to Sulebak (2000), DEM has been extensively used in numerous applications that include geomorphology and landscape studies, archeology, forestry and educational programs. In addition, DEM plays an important role and guides in understanding the flow behavior, flow directions, flow accumulation and flow pattern suggesting whether the runoff processes are fast or slow (Patel et al., 2013; Wagener et al., 2006; Yadav et al., 2013).

The QSWAT model with DEM processing delineates the watersheds which leads to the creation of watershed properties. These include the following: slope, flow length and stream network density. Additionally, this way of delineating the watershed using DEM is termed as the terrain pre-processing (Merwade, 2012). DEM is publicly available in two important DEM datasets: Shuttle Radar Topography Mission (SRTM) and ASTER GDEM (Sulebak, 2000). Comparatively, ASTER GDEM is preferred over SRTM since it has 30 m resolution in comparison to SRTM which has a resolution of 90 m (Tachikawa et al., 2011; Isioye et al., 2013). Though ASTER GDEM has a better resolution of 30 m x 30 m and preferred for mountainous terrain, SRTM was selected for the present study since SRTM is freely available.

3.3. SWAT Model-Calibration and Uncertainty Procedures (SWAT-CUP)

The SWAT-CUP is a generic interface, a standalone algorithm developed by Abbaspour et al. (2007b) and is able to perform SA, UA, calibration and validation of QSWAT model (Abbaspour et al., 2007b; Schuol et al., 2007). An inversion

modeling method with a huge range of parameters are employed with SUFI-2 algorithm in SWAT-CUP to solve various problems of the SWAT model associated with calibration and validation in order to perform multiple iterations. There are various algorithms used in the SWAT-CUP for this purpose. Thus, SUFI-2 approach with SWAT-CUP is being extensively used globally (Abbaspour et al., 2004, 2007b, 2015b). The SWAT model supports the SWAT-CUP package which then links to the SUFI-2 procedure. For instance, Abbaspour et al. (2004) and Yang et al. (2008) used SUFI-2 technique to evaluate the SWAT model. This package is equipped with parameter SA allowing changes to be done to the input data and considers the most sensitive parameter to give the most output variance (Abbaspour et al., 2007b; Yang et al., 2008). Hence, SUFI-2 technique was applied for evaluating the efficiency of the model performance through SA, model calibration and validation.

3.3.1. Sensitivity Analysis (Model Optimization) Using SUFI-2 Algorithm

Model optimization is the first step of SWAT-CUP analysis known as SA. SA also termed as UA and is performed prior to model calibration to achieve an effective hydrological model for better simulations by reducing the number of parameters in distributed models to prevent over-parameterization (Spear et al., 1980). SA is the fundamental step in hydrological modeling that evaluates and identifies the parameters by ranking them based on the sensitivities. This ensures to obtain the most output variance due to changes in input data (Salteli et al., 2000; Abbaspour et al., 2007) and also recognize the parameters that do not have a remarkable impact on model simulations. Moreover, the evaluation of coefficients: *t-stat* index and *p-value* hypothesis test (Student's test) defines the sensitivity ranking. SA is applied to identify the uncertainties associated with the input variable that affects model performance. The most sensitive or dominant parameters are further calibrated and validated as part of model optimization using inverse optimization algorithms to simulate streamflow (Khalid at al., 2016).

SUFI-2 algorithm is quite convenient and has advantages over other algorithms. It is simpler and preferred with several objective functions since it is a semi-automated

approach and the calibration process is made easier and can be done within the time bounds and quite efficient in terms of localizing an optimum parameter and the number of simulations (Schuol et al., 2008; Sloboda et al., 2011; Khoi et al., 2015; Sao et al., 2020). Moreover, SUFI-2 technique provides a high-quality calibration and uncertainty outcomes can be obtained with a minimum number of model simulations (Yang et al., 2008). It works on Bayesian framework where the uncertainties are determined through sequential fitting process and uses an iterative procedure to account for parameter uncertainty for different sources such as weather, model parameters and model structure and managing water resources (Abbaspour et al., 2004; 2015a; Yang et al., 2008; Tang et al., 2012).

Though being convenient, SUFI-2 algorithm has drawbacks since it is semi-automated and needs a constant interaction with modeler to examine the set of suggested posterior parameters. This means that the modeler needs to be well versed with the knowledge of parameters and their effects on the model output. This type of drawback leads to an additional error called "modeler's uncertainty" (Yang et al., 2008). Further, the incorporation of a large number of parameters makes the computational extensive and hence the calibration process turns to be difficult and complex making it lengthy tedious (Rosso, 1994; Sorooshian et al., 1995; Jajarmizadeh et al., 2012). Therefore, SA is performed in order to reduce the tedious calibration effort (Tejaswini et al., 2018). Despite that, sensitivity and uncertainty analysis need to be carefully performed in order to prevent model overestimation (over-design) or underestimation (insufficient preparation) of hydrologic regimes (Shen et al., 2012; Setegn et al., 2010).

SA is either performed by the technique one-at-a-time (OAT or Local Analysis) or Global Sensitivity Analysis methods. The technique to be employed depends on the chosen parameters that had been applied for SA in the early stages of calibration in SWAT-CUP with the use of default lower and upper limits (Abbaspour et al., 2007a). The OAT analysis is a less reliable technique since this approach recognizes the response from the output by changing each (single) model parameter by a certain fraction while other model parameters are kept at their normal values (meaning that for other constant parameters the information is unknown (Spruill et al., 2000;

Turanyi et al., 2000; Holvoet et al., 2005; Abbaspour et al., 2007a; Tejaswini et al., 2018).

Conversely, the simulation of Global Sensitivity Analysis considers all parameters simultaneously exploring the entire range of model parameter values allowing parameter interaction and its effects on model outputs. Thus, this has an advantage over OAT by capturing the full range of model parameter values and identifies the interactions among parameters as well (Lilburne et al., 2006). Majority of the SA is performed using the technique of Global Sensitivity Analysis.

SUFI-2 algorithm uses the statistics of two bands or indexes; P-factor and R-factor within 95PPU to quantify or map all accounted uncertainties (parameter, conceptual model input, etc.) (Abbaspour et al., 2015b). The percentage measured or actual data (plus its error) bracketed or covered by 95PPU is referred to P-factor while the R-factor is the measure for quantifying the strength of calibration/uncertainty analysis (Khalid et al., 2016; Abbaspour et al., 2004). The R-factor ranges between 0 and infinity and is the mean thickness of 95PPU band divided by the standard deviation of measured data. The width of the uncertainty interval describes the quality of calibration and it is recommended that this value should be as small as possible. In addition, majority of the measured data that is accompanied with the smallest possible uncertainty band is bracketed by SUFI-2 (Abbaspour et al., 2007b; Yang et al., 2008). To calculate 95PPU, 2.5% and 97.5% levels of the cumulative distribution of the output variable obtained through Latin-hypercube sampling are used.

Most often the water modeling uses Latin-hypercube sampling since it is highly effective and robust (Vandenberghe et al., 2001; Abbaspour et al., 2015a, 2015b). However, 5% of very bad simulations are disallowed. Theoretical P-factor values range between 0 and 1. 1 indicates maximum value of 100% that brackets the measured data within the model prediction uncertainty except the outliers. This signifies a perfect or high model simulation and efficiency in consideration to the uncertainty (Abbaspour et al., 2004; 2015b; Ghadei et al., 2018). In addition, the quantity (1-P factor) represents the model error. The P-factor with the highest value of 1 (100%) and R-factor with zero value is a simulation data corresponding exactly to the measured data (Khalid et al., 2016; Abbaspour, 2015a, 2015b) and the low

values of P-factor signifies elevated uncertainties in the output (Setegn et al., 2009). Thus, SUFI-2 algorithm works in such a way and obtains the lowest R-factor and the highest P-factor. This suggests that for stream flow estimation, P-factor value shall be higher than 70% and the R-factor to be around 1 (Abbaspour et al., 2004, 2015b).

Interestingly, both P and R indices are closely related to each other and this suggests that a large P-factor can only be obtained at the expense of a higher R-factor. A number of iterations are performed to accomplish the balance between the P and R factors. Ultimately, in the final iteration the acceptable values of P and R factors shall be achieved between the two. This parameter range is referred to as the calibrated parameters (Abbaspour et al., 2015b; Ghadei et al., 2018). The measured values of these two indices (P and R) determine the strength of calibration and validation process and compare the observed and simulated discharges (Abbaspour et al., 2015b; Ghadei et al., 2018; Arnold et al., 2012). The R-factor is given by Eq. (2) (Yang et al., 2008; Narsimlu et al., 2015) as:

$$r - factor = \frac{\frac{1}{n}\sum_{ti=1}^{n}\left(y^{m}{}_{ti,97.5\%} - y^{m}{}_{ti,2.5\%}\right)}{\sigma_{obs}} \qquad \text{(Eq 2)}$$

where

$y^{m}{}_{ti}$; 97.5% and $y^{m}{}_{ti}$; 2.5% represents the upper and lower boundaries of the 95PPU and σ_{obs} represents the standard deviation of the observed data.

Additionally, the discharge value of P-factor is the function of scale of the project and the appropriate input and calibrated data (Abbaspour et al., 2015b). Certain other factors such as terrain complexities, seasonality and variation in region hydrology also contribute extensively to challenges in hydrological modeling thus complicating the calibration of model parameters (Bajracharya et al., 2020). Thus, to solve these complicating situations, Variogram Analysis of Response Surfaces (VARS) is opted for since seasonality effects contribute to different hydrological processes that dominate at different times of the year. For instance, snowmelt and frozen soil are prominent in cold region and for this TVSA are quite effective. Time variant sensitivity analysis (TVSA) of model parameters uses\

Global Sensitivity Analysis technique known as Variogram Analysis of Response Surfaces (VARS) (Bajracharya et al., 2020).

3.3.2. Model Calibration

The model calibration is the second step of SWAT-CUP analysis after sensitivity analysis where selected input parameters are optimized using the specific algorithm. This is specifically done to parameterize the model. In addition, for calibration to be conducted, it is vital to include the examination of the accuracy of output and process simulation (Sorooshian, 1983) and the model to be calibrated and evaluated through SA and UA (Zheng et al., 2007). In particular, the uncertainties are associated with input, model structure, parameter and output (sources of uncertainty) (Beven 2000; Van Griensven et al., 2008). It is highly important that the hydrologic models used should be very accurately calibrated (Singh et al., 2002; Arnold et al., 2012). In addition, the technique of model calibration and validation could be quite challenging provided the hydrological model chosen is complex with greater number of input parameters (Ghadei et al., 2018) and is rather rigorous with increased number of iterations (Vanrolleghem, 2003). SWAT model can be calibrated by several developed techniques. The SWAT-CUP used in this study utilizes the semi-automated approach (SUFI-2) to calibrate the model both using manual and automated approach. Moreover, users particularly opt for manual calibration and adjust parameters and iterative ranges manually between auto calibration runs. Particularly, for manual calibration the user must possess significant skills and experience in modeling and recognizing parameters.

On the other hand, for automatic calibration the input files have to be filled out once only (Eckhardt et al., 2001). Factors such as parameter sensitivity, number of simulations, number of iterations and the uncertainties associated with the parameters greatly affects the calibration of SWAT model (Methan et al., 2017). The adjustments in parameter values in SUFI-2 are represented using letters. The use of the first letter before the parameter name (R, V and A) represents adjusted parameters. For instance, the use of letter V signifies replacing the existing parameter value whereas letter A represents adding a given value to the existing parameter value and letter R signifies multiplying (1 + a given value) to the existing

parameter value (Brighenti et al., 2019). Before the actual calibration process, the model needs warm-up time since the hydrological model is not aware of the initial conditions of the simulation and the conditions that exert much impact on the simulated process (Li et al., 2015; Ercan et al., 2014; Ajami et al., 2004; Zeckoski et al., 2015). Both the calibrated and validated models will be further evaluated to check the model's accuracy between observed and simulated data.

3.3.3. Model Validation

After the calibration process the model is validated using the calibrated parameters and similarly the applicability of the model is evaluated through several tests to quantify statistical indicators (Pereira et al., 2014; Arnold et al., 2012; Moriasi et al., 2007). During the validation phase, the SWAT results are compared with the observed data without modifying the values of the influencing factors (Shivhare et al., 2018). The validation phase is repeated until the model has achieved satisfactory performance, then the model is tested under different scenarios (Marek et al., 2016).

3.4. Performance Indices and Model Evaluation

Different objective functions such as P-factor, R-factor, R^2, *NSE*, Mean Absolute Error (MAE), Mean Square Error (MSE), Pearson's Correlation Coefficient (r), Percent Bias (PBIAS) and RMSE etc., are used in this study to evaluate the goodness-of-fit i.e., to evaluate the model performances by assessing the closeness of simulated and observed values. This was done for both calibration and validation periods. Table 3.1 presents the ranges and performance grades of different performance objectives. In addition, the statistical indicator *NSE*, which is the normalized dimensionless statistic that quantifies the relative size of the residual variance compared to measured data variance (Nash et al., 1970), was also used. The value of *NSE* varies from -∞ to 1 (Table 3.1) and the high value indicates an accurate model. Hence, *NSE* is calculated using the following equation:

$$NSE = \frac{\sum_{i=1}^{n}(o_i - \bar{o})^2 - \sum_{i=1}^{n}(s_i - o_i)^2}{\sum_{i=1}^{n}(o_i - \bar{o})^2} \quad \text{(Eq 3)}$$

where

o_i is the measured runoff or discharge (m^3/s); s_i is the simulated runoff (m^3/s); $\bar{o}$ is the mean measured runoff during the simulation period (m^3/s); $\bar{s}$ is the mean simulated runoff during the simulation period (m^3/s), n is the number of flow measurements in the analysis and k is the number of independent variables (Gu et al., 2020). In addition, R^2 depicts the degree of collinearity between the simulated and measured streamflow. The R^2 value ranges from 0 to 1 and the higher value signifies better performance (Table 3.1). R^2 can be calculated as follows (Eq. 4):

$$R^2 = \left[\frac{\sum_{i=1}^{n}(o_i - \bar{o})(s_i - s)}{\sqrt{\sum_{i=1}^{n}(o_i - \bar{o})^2}\sqrt{\sum_{i=1}^{n}(s_i - s)^2}} \right]^2 \quad \text{(Eq 4)}$$

Furthermore, PBIAS provides the information about the average trend of the simulated data and indicates whether the trend is greater or less than that of the corresponding observed data (Gupta et al., 1999). PBIAS values with small magnitude are preferred. In particular, PBIAS having the value of zero value (optimum value) indicates better simulation. In addition, the model with positive values indicates underestimation whereas the negative values indicate model over estimation (Gupta et al., 1999). It can be calculated using (Eq. 5):

$$\text{PBIAS} = 100 \times \left[\frac{\sum_{i=1}^{n}(o_i - s_i)}{\sum o_i} \right] \quad \text{(Eq 5)}$$

In addition, RSR, which is the ratio of RMSE to standard deviation of measured data was also used. The values of RSR ranges between optimal values of 0 to ∞ (Table 3.1). In fact, zero RSR indicates zero residual variation or RMSE (Moriasi et al.,

2015) meaning that the model simulates perfectly to a large positive value. Better model simulation performance is obtained with low RSR (Moriasi et al., 2007). Eq. 6 shows mathematical representation of RSR:

$$\mathrm{RSR} = \frac{\sqrt{\sum_{i=1}^{n}\left(Q_m - Q_s\right)_i^2}}{\sqrt{\sum_{i=1}^{n}\left(Q_{m,i} - Q_m\right)^2}} \qquad \text{(Eq 6)}$$

Table 3.1: Classification of statistical indices (Moriasi et al., 2007; Van Liew et al., 2003; Fernandez et al., 2005 and Gu et al., 2020).

Performance grades	R^2	*NSE*	**PBIAS**
Very good	$0.75 < R^2 \leq 1.00$	$0.75 < NSE \leq 1.00$	$\lvert PBIAS \rvert \leq \pm 10$
Good	$0.60 < R^2 \leq 0.75$	$0.60 < NSE \leq 0.75$	$\pm 15 \geq \lvert PBIAS \rvert > \pm 10$
Satisfactory	$0.5 < R^2 \leq 0.60$	$0.36 < NSE \leq 0.60$	$\pm 25 \geq \lvert PBIAS \rvert > \pm 15$
Bad	$0.25 < R^2 \leq 0.50$	$0.00 < NSE \leq 0.36$	$\pm 50 \geq \lvert PBIAS \rvert > \pm 25$
Unsatisfactory	$R^2 \leq 0.25$	$NSE \leq 0.00$	$\lvert PBIAS \rvert \geq \pm 50$

The SWAT performance is reflective of model evaluation. For instance, the SWAT model performs better when *NSE* has values closer to 1 and the simulation is more accurate when PBIAS is close to zero (Gu et al., 2020). After completion of the validation phase and provided the model has achieved the satisfactory performance, then model simulations can be performed according to different scenarios if possible, to gauge the most ideal input parameters with model performance (Marek et al., 2016).

3.5. Hydropower Potential Estimation Process

The transformation of potential energy of falling water from an elevated reservoir into kinetic energy generates hydropower. This electrical energy is produced when the water falls on turbines, driving them and producing mechanical energy which finally operates generators (Kusre et al., 2010). Thus, the theoretical hydropower potential of the ROR of the single sub-basin can be computed using Eq. (7) (Gaiuso, 2017; Jason et al., 2017; Tarife et al., 2017):

$$P = \rho\ \eta_t\ \eta_g\ g\ Q\ h \qquad \text{(Eq 7)}$$

where the theoretical ROR hydropower potential is represented as *P*, mass density of water [1000 kg/m^3] is represented as ρ, the acceleration due to gravity [9.81 m/s^2] is represented as *g*, flow rate (discharge) [m^3/s] is represented as *Q*, and the hydraulic head (elevation difference) [m] is represented as *h* and the efficiency of the turbine is represented as η_t [0.80] and the efficiency of the generator is represented as η_g. Moreover, in order to estimate the hydropower potential of the basin requires prior estimation of the head drop, *h*, and the river discharge, *Q*.

The hydropower potential of the stream can be defined as the maximum amount of hydroelectricity generated (Oliveira et al., 2017), while the hydropower potential depends on numerous factors such as the effective head, discharge, total plant efficiency including turbine and generator efficiencies and other electromechanical components (Setiawan, D, 2015) as shown in Eq. (7). For instance, the large-scale hydropower has turbine efficiency of 90% whereas the micro-scale hydropower has turbine efficiencies between the ranges 60% - 85%. If there are a number of sub-basins then the total power of the basin is calculated by adding the potential of all sub-basins and is calculated according to Eq. (8):

$$P = \sum_{i=1}^{n} \rho \times g \times Q \times H \qquad \text{(Eq 8)}$$

where

i = sub-basin number = i……. n

n = number of sub-basins

The stream discharge can be estimated by either direct or indirect methods. For this study, indirect method of estimating flow at WRB is considered. In particular the runoff is determined as the balance of rainwater which flows or runs over the natural ground surface after losses by evaporation, interception and Hydrograph depicts stage, discharge, velocity or infiltration. Thus, the regression analysis determines the relationship between runoff and precipitation and is calculated according to Eq. (9) (Ramachandra et al., 2004):

$$R = 0.849*P*30.5 \quad \text{(Eq 9)}$$

where

R = runoff

P = rainfall in cm

Equation 9 calculates the runoff based on indirect method of estimating flows at a particular site. The empirical formula; R = 0.849*P*30.5 calculates the surface runoff using the constants 0.849 and 30.5. Regression analysis is used to predict the following variables; peak flow (*Qp*), runoff volume (*Qv*) and runoff coefficient (*C*). This equation is location specific and uses regression analysis to predict flow volumes and flood peaks as a function of rainfall input and antecedent wetness. As a result, the regression of rainfall runoff model cannot be applied to the current study due to unavailability of data or predictor variables such as peak gauge average rainfall (*Rp*), total event rainfall volume (*Rv*), rainfall spatial variability index (Rs), baseflow (*Qb*) as an index of antecedent conditions, and distance of the rainfall centroid from the flow gauge (*Rd*) (McIntyre et al., 2007).

Ramachandra et al. (2004) designed spatial decision support system for assessing micro, mini and small hydel potential in Uttara Kannada District located in the mid-western part of Karnataka, India using Equation 9. It uses the computer-based models including GIS, topographical and hydrometeorological data for analysis. However, this model incorporates other factors such as energy demand, socio-economic costs, bio resource assessment, environment cost assessment, civil construction costs, project life span, construction time, inflation rate, maintenance costs and depreciation to perform hydro energy assessment. Literature shows that the

physically-based rainfall–runoff models still face challenges in predicting the hydrological responses of arid and semi-arid catchments.

The yield of the catchment area is calculated according to Eq. (10)

$$\text{Yield} = C*A*P \quad \text{(Eq 10)}$$

where

C = co-efficient of runoff; A = Catchment area; P = Rainfall

Soil, geology and vegetation determines the value of C. Heavy Forest ranges from 0.1 to 0.2, sandy soil ranges from 0.2 to 0.3, cultivated absorbent soil ranges from 0.3 to 0.4, cultivated or covered with vegetation ranges from 0.4 to 0.6, slightly permeable bare ranges from 0.6 to 0.8 and rocky and impermeable ranges from 0.8 to 1.0.

Power is the function of flow data and average head height given by Eq. (11)

$$P = 9.81*\text{Average (flow data)} *\text{Average head height} \quad \text{(Eq 11)}$$

And energy is determined using (Eq 12)

$$E = P*t*\eta*f \quad \text{(Eq 12)}$$

where

P = Power in KW

t = Operating time in hours

η = Efficiency of the turbine generator assembly

f = co-efficient for seasonal flow variation for river run of river installation.

This study assumes to consider the turbine efficiency (η) of 80% to theoretically calculate the potential power capacity.

3.6. Hydropower Assessment

An assessment of hydropotential at the Wainimala watershed at central Vitilevu, Fiji is conducted at WRB. The method used involves the application of an integrated hydrological model and geospatial analysis, QSWAT coupled with QGIS platform to assess water resource availability, effective head and determine hydropower potential sites for future hydropower development in the watershed. Geospatial information about the topography, soil types, LULC, weather and discharge are considered in hydrological and hydro-geomorphological characterization of the watershed (Kouadio et al., 2022). Studies conducted by Kusre et al., 2010; Pandey et al., 2015; Zarfl et al., 2015; A. M., and Guven, A. (2016) suggested methodology based on hydrological modeling and GIS to assess hydropotential of watersheds for future use. Development of hydropower plants should undergo adequate environmental requirements and needs rigorous planning and management in order to select the site(s) so that ecological impacts of hydropower projects are reduced (Kuriqi et al., 2021). Furthermore, the hydropower potential of a reservoir can be assessed following Bayesian approach and stochastic analysis of its hydrological potential.

Interestingly, hydropower is quite sensitive to climate change especially for precipitation since it has a direct influence on basin runoff that ultimately affects hydropower generation (Berghuijs et al., 2014; Wasko and Sharma, 2017). Thus, the methodology employed and the obtained results could be utilised to create hydroelectric information system with spatial references as decision-making tool in energy matters. This approach could be adopted to support electrification decentralization and thus guarantee energy security (Kouadio et al., 2022).

Chapter 4

Study Area and Methodology

This chapter outlines the study location of the Wainimala catchment area and summarizes the input data required for the study. Then the methodology involved in the estimation of hydropower potential at the sub-basin is presented which comprises of two major parts: i) estimation of streamflow (discharge) along the river system and ii) estimation of potential head drop using DEM. Firstly, discharge along the river sub-basin is estimated by building hydrological model using SWAT tool. In order to accomplish this, specific data such as stream network, LULC map, soil map and the meteorological data (i.e., precipitation, solar radiation, relative humidity, wind velocity, maximum and minimum temperature) are required.

4.1. Description of study watershed

The current study on hydropotential determination was conducted at WRB located in the Naitasiri Province of Central (Eastern) Division in Vitilevu, Fiji (Figures 4.1 and 4.2). According to Fiji Islands Bureau of Statistics (2017), Wainimala covers a total area of 447.24 km^2 with population size of 4,227 inhabitants and population density of 9.518/km^2. Wainimala sub-basin lies between -17° 49' 18" South (Latitude) and 178° 20' 45" East (Longitude) with tropical rainforest climate. The total sub-basin is composed of 444.1 km^2 (Table 5.1). The Wainimala River begins from Monasavu River and diverges at the Laselevu settlement into two major rivers where one major Wainimala River terminates at the Muava Creek while the other merges with Wainibuka River into Rewa River. Wainimala has steep slopes above 500 m with steep land in the uplands of Vitilevu with no flooding. The steep land consists of boulder red brown clay soil with humic latosols.

Figure 4.1: Location map of study site at Wainimala (marked red) (Google map, accessed 28 April 2021).

The landform is hilly, contains massive planar and convex surfaces and has strongly weathered in situ rock. There is no dry season and is subject to continuous rainfall. The annual average rainfall is 3,200-4,800 mm but during dry season there is reduced rainfall with values reaching between 500-800 mm while during wet season there is an increased rainfall and particularly ranges from 2,000-2,800 mm. The elevation range is 500-1500 m and the mean annual temperature is 18°C. The vegetation is entirely covered with dense forest and the land is very occasionally used for subsistence farming (Twyford et al., 1965).

4.2. Data Acquisition

The SWAT model requires meteorological data (temporal input data) to simulate the hydrological conditions of the basin. Furthermore, to run the QSWAT model (rainfall-runoff hydrological modeling), data were compiled from various sources. Table 4.1 summarises the different data types and the sources from where the data was acquired. The following input data were required for this purpose:

i) DEM (topography)

ii) Stream or river network map (sub-catchment)

iii) LULC map

iv) Soil map

v) Hydrometeorological data (precipitation, solar radiation, wind velocity, relative humidity, minimum and maximum air temperatures).

The study incorporates historical weather data of 39 years from period of 1980 to 2018. Unfortunately, there were some missing data for relative humidity and precipitation and Multi Linear Regression analysis was performed using R software to interpolate.

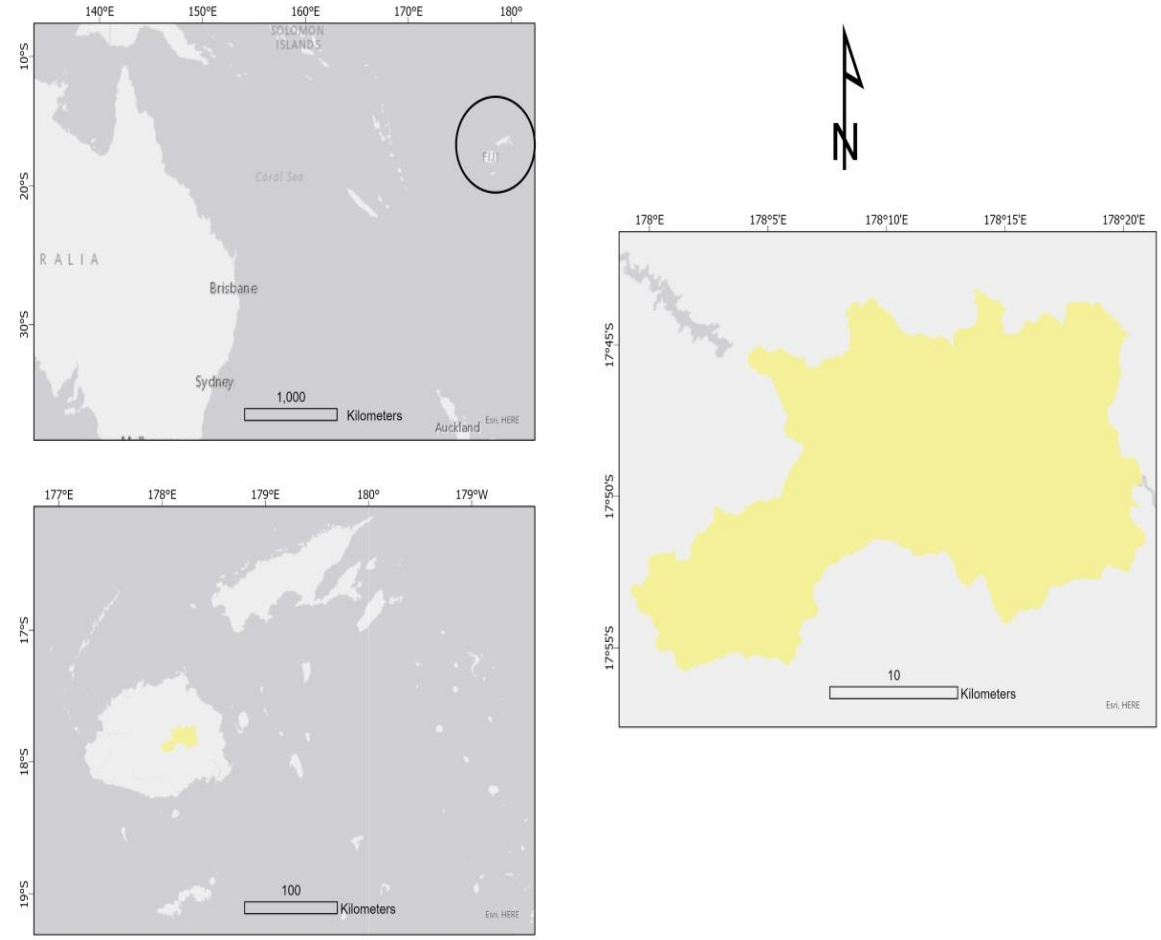

Figure 4.2: Location of WRB.

Table 4.1: Sources of data collection

No.	Data Types	Sources
1	LULC	Global Land Cover [GLC 2000]
2	Soil Data	Ministry of Agriculture Land Use Planning Section, Suva, Fiji and FAO Digital Soil Map
3	Monthly Precipitation Data	Climate Division of Fiji Meteorological Services
4	Monthly Discharge Data	Climate Division of Fiji Meteorological Services
5	Monthly Solar Radiation	Climate Division of Fiji Meteorological Services
6	Wind Velocity	Climate Division of Fiji Meteorological Services
7	Minimum Air Temperature	Climate Division of Fiji Meteorological Services
8	Maximum Air Temperature	Climate Division of Fiji Meteorological Services
9	Relative Humidity	Climate Division of Fiji Meteorological Services
10	DEM (30 m)	USGS (https://earthexplorer.usgs.gov/)

4.3 SWAT Model Setup

In this study, QGIS, SWAT, QSWAT Editor were used to build the hydrological model. All necessary spatial data were made ready prior to starting of the QSWAT modeling work. The QSWAT model uses the physically-based input data including DEM, soil data, LULC, topography and hydrometeorological and climate data in the watershed.

4.3.1. SWAT Model Setup and Functioning

Figure 4.3 illustrates the flowchart of the methodology that is used to estimate ROR hydropower potential of the Wainimala watershed. The study incorporates an agro-hydrological model, i.e., SWAT, integrated with a GIS interface in QGIS software, denoted as QSWAT was applied in the WRB to manage raster and vector data. To do

this, several data points were needed to set up and operate the WRB SWAT model in order to simulate stream flows. A series of stages were required before simulations could be performed using QSWAT model. This process required the use of selected input data to extract the DEM for the selected basin, then the catchment delineation is performed followed by generation of stream network and finally the hydraulic head is determined after identifying the potential points.

- The delineation of the watershed and its associated sub-basins and reaches is the initial step in model construction, i.e., the topographic data in the form of DEM was processed to delineate watershed (Figures 4.3 and 4.4). This study used a 30-m spatial resolution for the entire territory of WRB which was obtained from STRM 1 Arc-Second. The Global Database was sourced freely from the web-site, USGS (https://earthexplorer.usgs.gov/, 23/02/2021). In order to generate DEM, four separate tiles were downloaded for the whole area of Vitilevu, Fiji. Then these tiles were mosaiced and merged into a single DEM using Data management tool for the whole of Vitilevu using QGIS v 1.8.2 and merged DEM were clipped using the administrative boundary map of Wainimala, Fiji (Vitilevu). Thus, the DEM of WRB was obtained with GIS technology.
- The next step involved the coupling of the soil and LULC maps of WRB and soil physio-chemical properties in QSWAT to split the basin into HRUs. HRU constitutes the basic spatial units in hydrological modeling (Kouadio et al., 2022). This suggests that HRUs represent a combination of land use, soil type and slope. Thus, soil and LULC maps are quite vital for model operation. A WRB soil map corresponding to its physio-chemical properties that included soil type, soil layers and texture were obtained from the Ministry of Agriculture Land Use Planning Section, Suva, Fiji and Food and Agriculture Organization (FAO), the International Center for Soil Reference and Information (ISRIC) and International Soil Science Society (ISSS). The LULC map used was secured from the Global Land Cover [GLC, 2000]. Further, once the single mosaiced DEM grid was obtained, the LULC and soil map were overlaid on it to delineate watershed boundaries from DEM (boundary area and drainage network of the watershed, Figure 5.1). Three outlet points were selected within the boundary area and the flow direction

and flow accumulation rasters were used to develop the vector representation of catchments. Moreover, the drainage lines from the selected points in QSWAT gave the number of cells (area) that drained into a particular cell known as the stream (Kayastha et al., 2018). In addition, each level was identified by a parameter set and input data. Interestingly, the incorporation of all data inputs and delineation of watershed process generated total of 32 sub-basins for the study site with 32 HRUs based on land use, slope and soil properties in the study area. In this study, as suggested by Neitsch et al. (2005), a 10% threshold was set while defining HRUs by ignoring the minor LULC, slope and soil types. This was done to avoid unnecessary large number of HRUs which might cause computational issues.

- The final step of the input is the integration of climate data to simulate streamflow. For this, historical monthly climate data from period of 1980 to 2018 (39 years) for Wainimala catchment was obtained from the Climate Division of Fiji Meteorological Services. These meteorological data included precipitation, air temperature (minimum and maximum), solar radiation, wind velocity and relative humidity data.

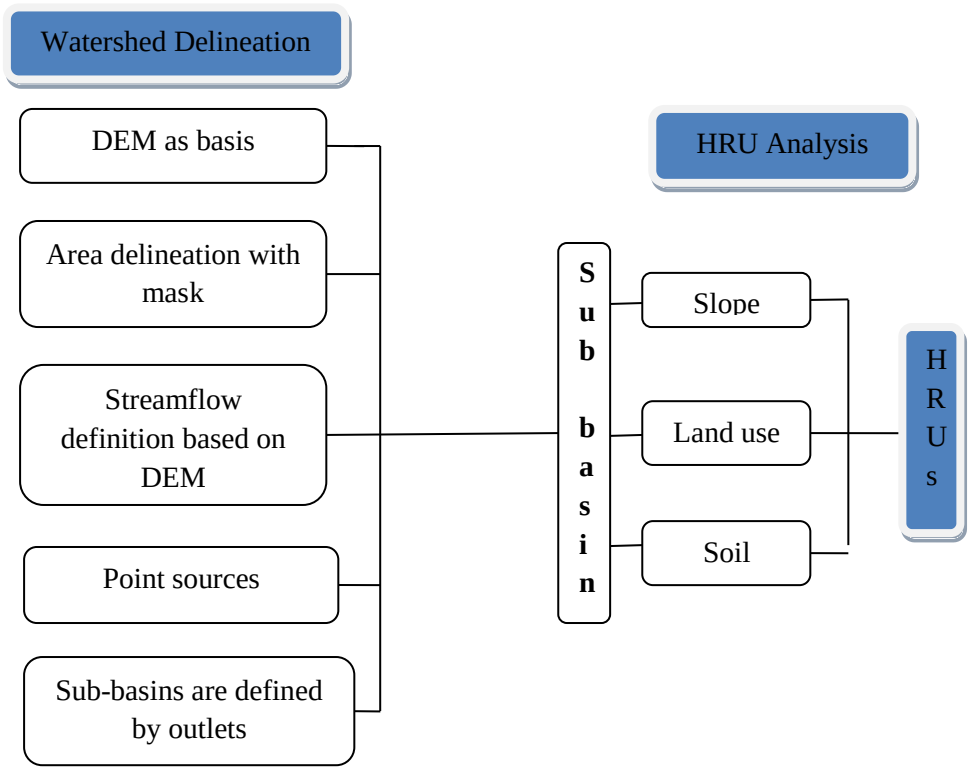

Figure 4.3: A schematic representation of watershed delineation in QSWAT model of the HRU concept (Arnold et al., 2012).

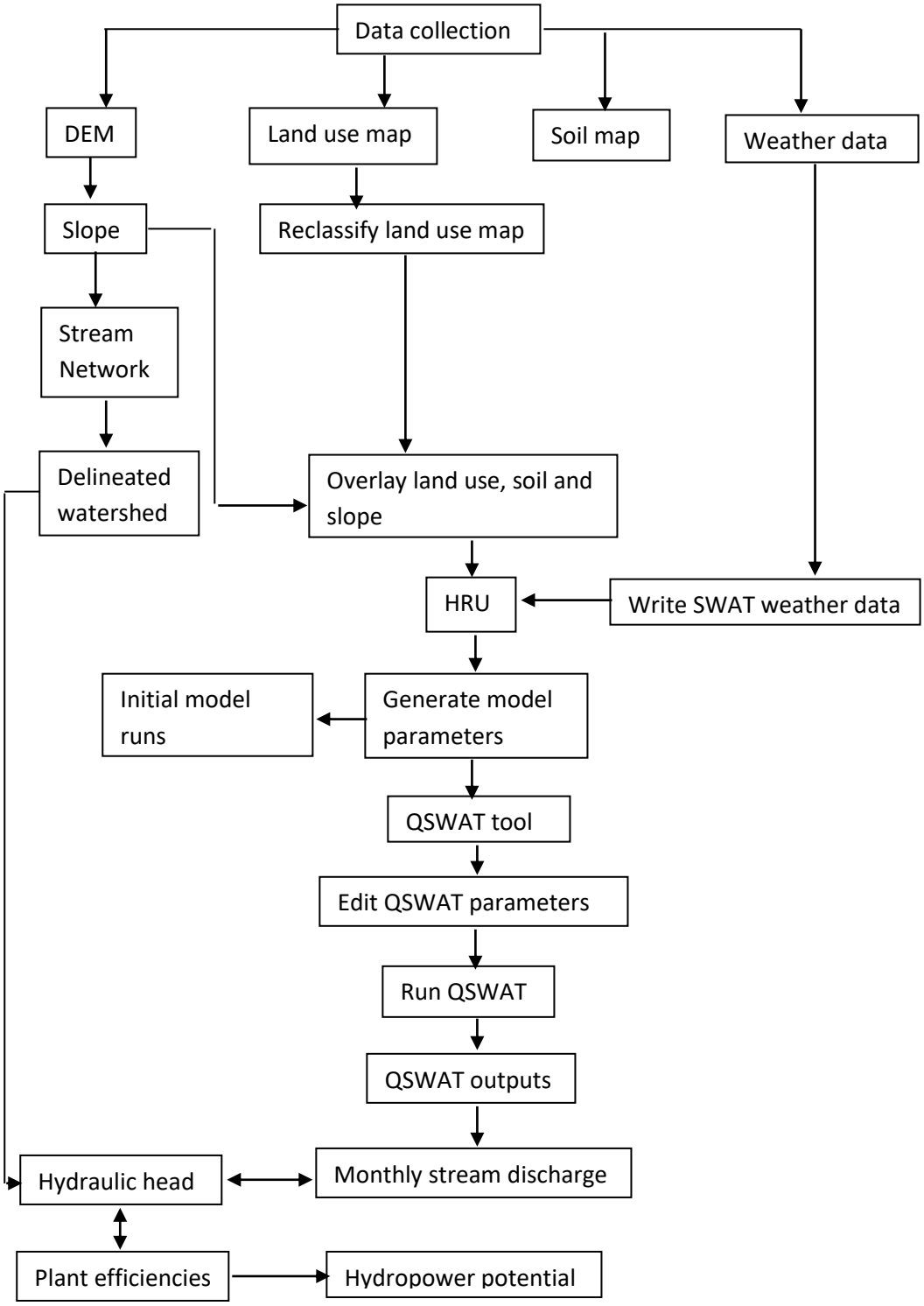

Figure 4.4: QSWAT model development and analysis framework to simulate runoff (Ghadei et al., 2018).

4.3.2. Estimation of Potential Head Drop (Hydraulic Head)

The assessment of hydropower potential of the sub-basin requires potential head drop to be determined along the basin. The simplest method to measure the head difference was by overlaying the DEM of the basin, sub-basin and the river network shape file to obtain the raster value of the upstream and downstream end point of the river sub-basin. Hence, the estimated potential head drop of the river sub-basins was computed as the difference between upstream (maximum elevation) and downstream (minimum elevation) end points of the river. The determined head difference is the amount of energy that can be transformed into electricity by the turbines and generators.

In this study, an effective head is not considered for calculating the hydro potential of sub-basins. Effective head accounts for friction losses in pipes thus reducing head losses. Since dam construction is not part of the current work, hydraulic head is considered for hydro potential calculations.

4.4. Estimation of Capacity Factor (CF) for Hydroelectricity Generation

The determination of theoretical and technical HK requires CF of known value. The literature including EFL annual reports does not report the CF value for hydroelectricity generation for any hydropower stations in Fiji. As a result, the average CF was calculated to determine energy produced. For instance, Wailoa Hydro Station was taken as one of the hydropower sites with installed generation capacity of 80 MW. Eq. (13) was used to calculate the CF for each year from 2016-2020 for a period of 5 years. Individual CF values were used to determine the average CF. Hence, the average CF of 60% was used to calculate the amount of energy produced in KWh for technical HK.

Capacity Factor = Energy Generated (MWh) / Power (MW) x 24 hrs x 365 days

(Eq 13)

4.5. Estimation of Carbon Dioxide Equivalent (CO_2e) for technical HK

For estimating the GHG abatement considering three important GHG's ("Kyoto gases") namely CO_2, methane (CH_4) and nitrous oxide (N_2O). GHG present in the atmosphere ensures to retain the planet's atmosphere warmer than it would be otherwise by reabsorbing and re-emitting the heat. The Intergovernmental Panel on Climate Change (IPCC, 2006) guidelines on National GHG inventories and emission factors were used for this study to determine the emissions of CO_2, CH_4 and N_2O from stationary combustion of HFO and IDO using tier 1 approach (IPCC, 2006). According to IPCC fifth assessment report, the "global warming potential" (GWP) values of CO_2, CH_4 and N_2O are 1, 28 and 265 respectively. GWP is an indicator of the amount of warming a gas has caused over a given period of time (normally 100 years). This suggests that GWP acts as a guide with CO_2 having an index value of 1. Conversely, the GWP for all other GHGs is the number of times more warming they can cause in comparison to CO_2. For e.g. methane has a GWP value of 28 whereas CO_2 has a value of 1. This indicates that 1kg of methane has the capability to cause 28 times more warming over a 100-year period compared to 1kg of CO_2. CO_2 equivalent (CO_2e) describes different GHGs in a common unit and signifies the amount of CO_2 which would have the equivalent global warming impact. Hence, the total GHG emissions are calculated and estimated on the basis of fuel consumption required for the generation of electricity using Eq. (14).

Emissions (t) = Fuel consumption (kt) x Net calorific value of fuel (TJ kt^{-1}) x Emission factor (t TJ^{-1}) (Eq 14)

To estimate CO_2e for technical HK using an average CF of 60% hydroelectricity generation in Fiji, the following steps were considered:

- The first step was to determine the energy generated in KWh using eq (13). EFL uses the fuel types HFO and IDO in 1:1 to produce energy through combustion. Hence, energy generated from HFO and IDO (KWh) are the same. Mass (kg) of HFO produced was estimated at 4.63 KWh/kg and the mass (kg) of IDO produced was estimated at 4.68 KWh/kg. The obtained masses (kg) were converted to kilotonnes (kt).

- The second step involved estimating tonnes of GHGs per year for technical HK. Table 4.2 presents the net calorific value (NCV), CO_2, CH_4 and N_2O emission factors of different fuel types used in calculating the avoided emissions in tonnes for the present study. Hence, the total GHG emissions are calculated and estimated on the basis of fuel consumption required for the generation of electricity using Eq. (13).

Table 4.2: Net calorific value (NCV), CO_2, CH_4 and N_2O emission factors of fuel (Ramachandra et al., 2015).

Fuel	**NCV (TJ kt^{-1})**	**CO_2 EF (t TJ^{-1})**	**CH_4 EF (t TJ^{-1})**	**N_2O EF (t TJ^{-1})**
Coal	19.63	95.81	0.001	0.0015
Natural gas	48	56.1	0.001	0.0001
Naphtha	44.5	73.3	0.003	0.0006
Diesel oil	43.33	74.1	0.003	0.0006
Natural gas	48.632	64.2	0.003	0.0006
LSHS	40.19	73.3	0.003	0.0006
RFO	40.4	77.4	0.003	0.0006
LSFO	41	73.3	0.003	0.0006
HFO	40.2	73.3	0.003	0.0006

Note: NCV-Net Calorific Value, EF-Emission factor, LSHS-Low Sulphur Heavy Stock, RFO-Residual Fuel Oil, LSFO-Low Sulphur Fuel Oil, HFO-Heavy Fuel Oil.

- The third step involved estimating megatonnes of CO_2e for HFO and IDO per year for technical HK. For instance, this was done by adding tonnes of emissions released as CO_2, CH_4 and N_2O from combustion of HFO.

In estimating the emissions, the following assumptions were used:

- The degradation of biogenic carbon in hydropower reservoirs produces emissions of methane and carbon dioxide and is considered to be zero.
- The use of HFO and IDO fuels by EFL is considered to be in 1:1 for electricity generation in thermal power plants.

- Though hydropower is a clean source of energy it does produces emissions during the various stages involved in construction and commissioning. For this study, these emissions are considered to be zero.

Chapter 5

Results and Discussion

This chapter presents the results and discussion of the hydro potential capacity of Wainimala catchment and estimates the avoided GHG emissions as part of sustainable development. The following sections begin by discussing the locations and sub-basins with hydro potential capabilities. It includes the following: drainage network (topography) and projected DEM with delineated watershed defined HRUs and digital LULC map, slope and digital soil map of Wainimala catchment. This is followed by a discussion on estimating the hydropower potential of selected sub-basins and calculating avoided GHG emissions.

5.1. Stream Networks and Delineated watersheds

Figure 5.1 shows the basin boundary of Wainimala catchment with projected stream networks. The basin boundary has a total area of approximately 416, 260 ha (4162 km^2). There are four main river channels in the area with the largest drainage located at the South East of the catchment area. These four streams were used to estimate the natural hydropower potentials at the catchment area. The watersheds were delineated using 30-m resolution SRTM-derived DEM as the main input data in the study area. Moreover, Figure 5.2 shows the delineated watersheds projected along the Wainimala catchment area. The projected elevation at different height levels can be corresponded to the different colors on the map. It is visible from the Figure 5.2 that majority of the projection is elevated in the range 8.62-167.75 m corresponding to the major river channel. Conversely, at a higher elevation the projection is less distributed and is concentrated towards the boundaries of Southwestern region of the catchment area.

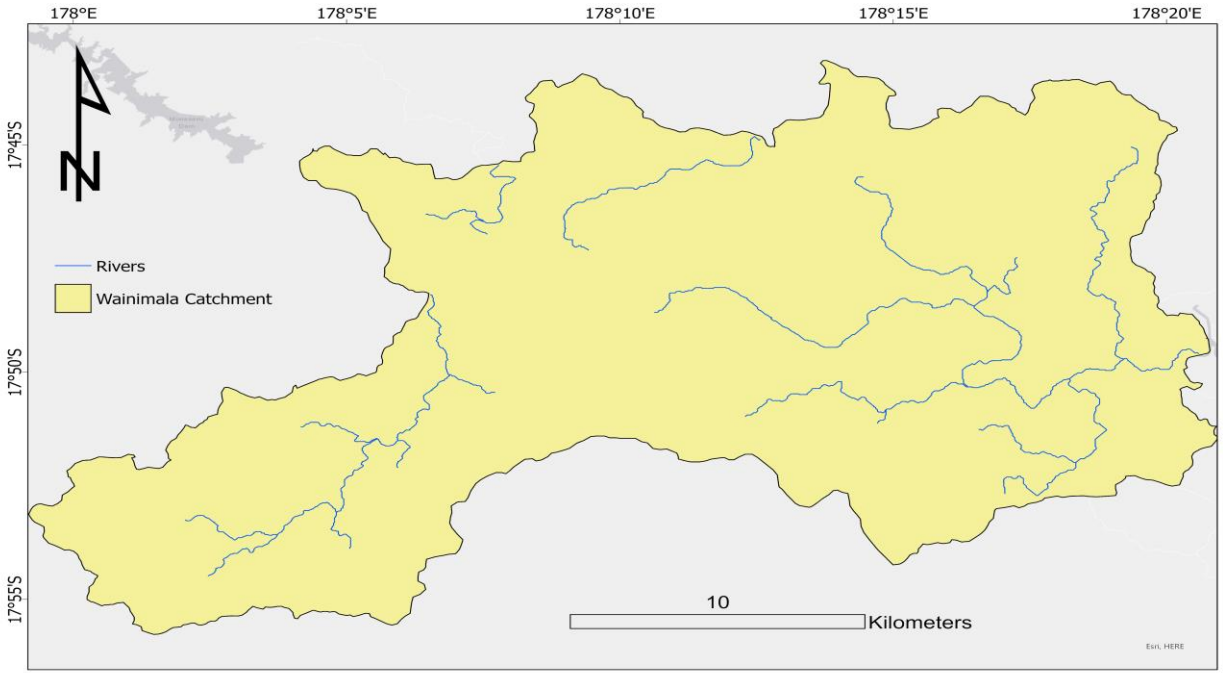

Figure 5.1: Topography (drainage) of Wainimala watershed.

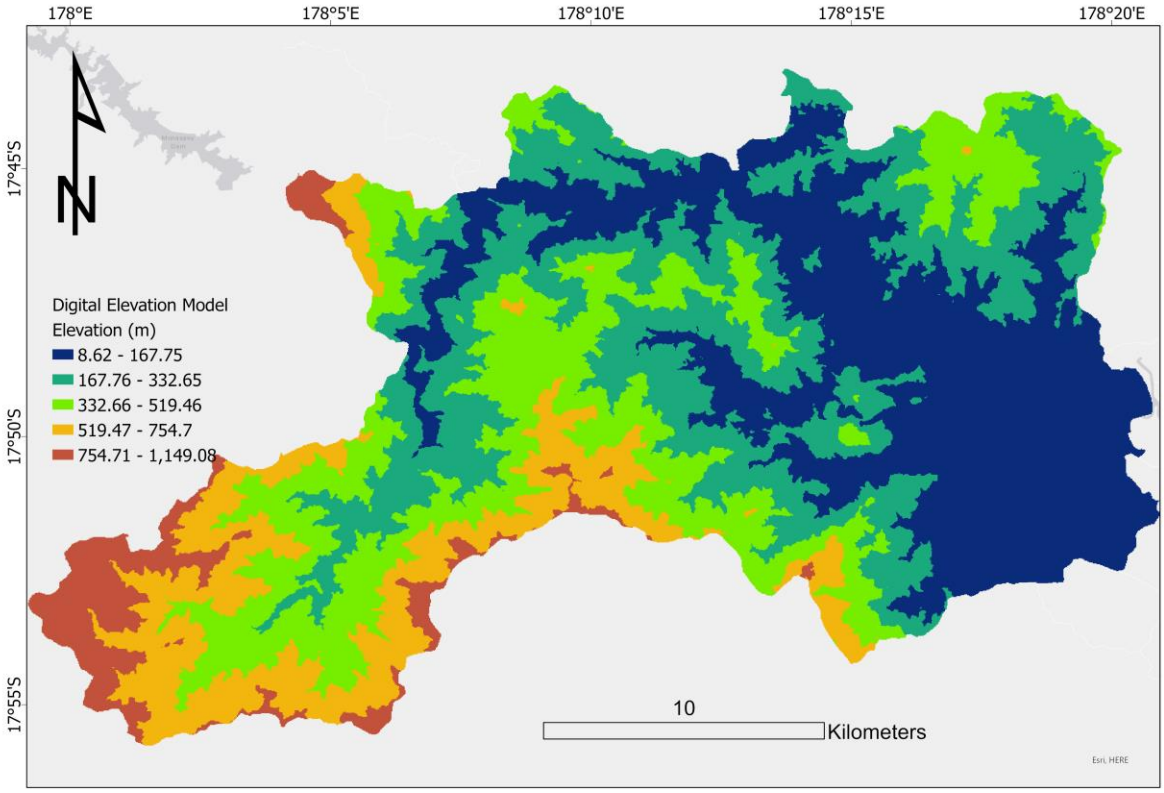

Figure 5.2: Projected DEM (SRTM) with delineated watershed in the Wainimala Basin.

5.2. Hydrological Response Units of the Sub-Basins

The GIS interface for SWAT on soil attributes, land use, projected DEM and stream network resulted in HRU delineation with a total of 32 sub-basins. Each sub-basin with 32 HRUs is characterized by a specific area occupied by each HRU in a sub-basin. Hence, the unique intersections of land use soils within each sub-basin determine HRUs. Figure 5.3 shows the distribution of 32 sub-basins at Wainimala catchment. The boundary area of each sub-basin corresponds to the magnitude of sub-basins. The area in hectares and percentage watershed for each sub-basin is presented in Table 5.1. For greater visibility, each sub-basin in Figure 5.3 is shaded with different colors. Approximately 40.6% of the delineated sub-basins have boundary areas less than 1000 hectares of which sub-basin 10 has the least occupied area of 26.61 hectares. Sub-basin 3 has the largest boundary area of 5465.52 hectares. The total boundary area of 32 sub-basins is 416, 260.32 hectares. Additionally, the parameters such as minimum, maximum and mean elevations measured in meters and standard deviation of each sub-basin is presented in Table 5.2. Sub-basins 2, 7, 13, 17, 18 and 25 have mean elevations greater than 500 m.

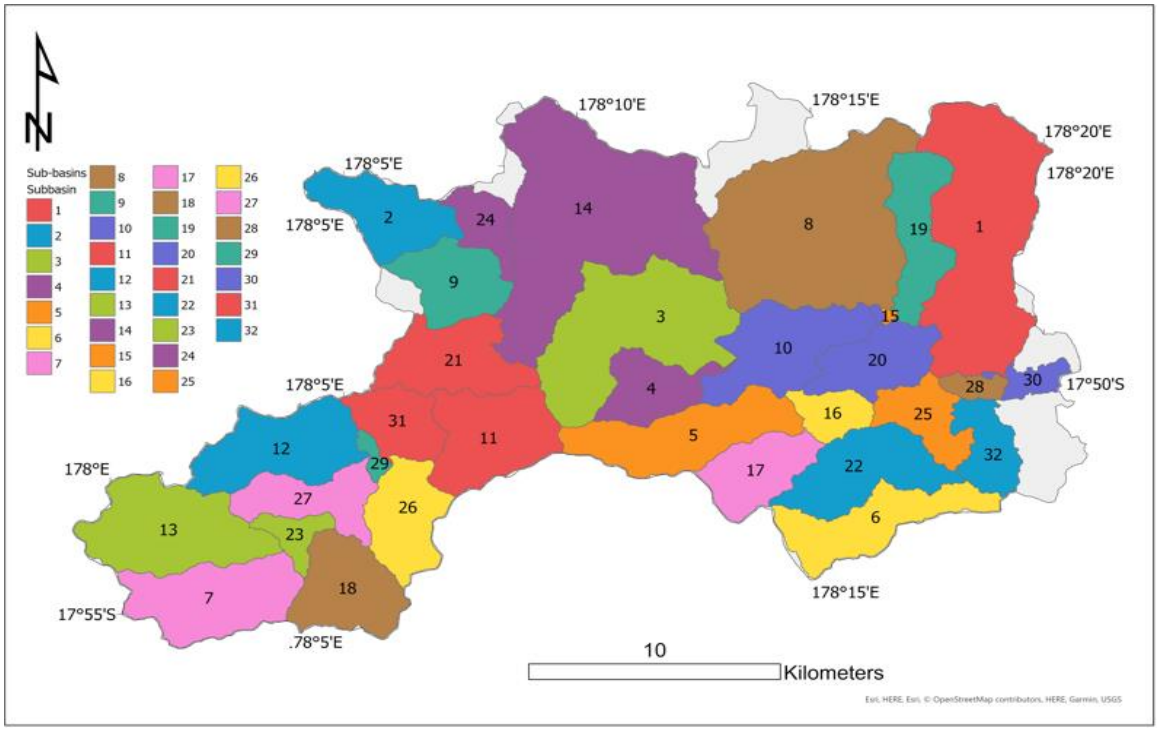

Figure 5.3: Definition of HRUs with sub-basins at Wainimala catchment.

Table 5.1: The areas in hectares and percentage watershed for 32 sub-basins at Wainimala catchment.

Sub-basin	Area (hectares)	% Watershed	Sub-basin	Area (hectares)	% Watershed
1	3784.70	8.46	17	1632.37	3.65
2	1197.66	2.68	18	1308.15	2.92
3	5465.52	12.22	19	1152.33	2.58
4	1588.41	3.55	20	778.93	1.74
5	1735.70	3.88	21	1484.99	3.32
6	1379.18	3.08	22	356.79	0.80
7	1706.70	3.82	23	562.35	1.26
8	4389.45	9.81	24	217.67	0.49
9	1085.52	2.43	25	1131.13	2.53
10	26.61	0.06	26	978.25	2.19
11	488.02	1.09	27	272.92	0.61
12	1012.75	2.26	28	129.39	0.29
13	2047.34	4.58	29	829.22	1.85
14	4832.13	10.80	30	707.44	1.58
15	1063.32	2.38	31	829.0	1.71
16	1379.36	3.08	32	707.0	1.58

Total Area of sub-basins = 416,260.32 ha (4162.6 km ^{2})

Table 5.2: The elevation details for 32 sub-basins at Wainimala catchment.

Sub-basin	Minimum Elevation (m)	Maximum Elevation (m)	Mean Elevation (m)	Standard Deviation	Sub-basin	Minimum Elevation (m)	Maximum Elevation (m)	Mean Elevation (m)	Standard Deviation
1	8	551	195.70	117.72	17	216	1007	546.04	160.25
2	92	1080	514.39	240.21	18	276	1092	573.38	140.43
3	25	819	282.16	147.86	19	24	547	265.34	127.57
4	158	898	494.36	173.62	20	10	232	48.88	39.01
5	48	899	384.37	189.83	21	18	784	215.96	166.69
6	17	785	254.22	206.08	22	275	707	426.22	104.94
7	321	1062	640.25	143.56	23	73	585	207.78	103.31
8	22	554	173.41	111.41	24	8	108	30.87	19.62
9	86	651	263.78	122.03	25	206	1020	583.62	155.27
10	23	116	52.89	25.79	26	220	917	463.84	147.42
11	13	463	141.20	91.88	27	4	72	19.79	7.61
12	47	783	344.67	133.19	28	205	474	314.28	64.51
13	322	1147	776.64	205.65	29	157	633	329.29	104.26
14	41	614	254.53	118.91	30	15	98	33.07	16.57
15	6	452	102.89	91.40	31	16	324	134.21	58.94
16	122	663	295.78	105.53	32	15	453	101.34	84.46

5.3. Land Use/Land Cover of the Basin

The LULC map provides the spatial information on the physical and biological coverage of the Earth's surface. Figure 5.4 presents the classified land use map of Wainimala watershed. There are five classes of vegetation obtained at the study area including Forest Deciduous (FRSD), Pasture (PAST), Range (RNGE), Water (WATR), Forest (Fore) and human settlements. The definitions of these vegetation classes are given in Table 5.3 while Figure 5.4 illustrates the legends used. The SWAT analysis generated a spread sheet with well-defined vegetation classes.

LULC map was classified based on the following: accessibility of roads for transportation, water bodies such as rivers, settlements and forest areas. The total vegetation cover of the study area is 44, 724.32 hectares. Interestingly, the vegetation cover for the catchment area is as follows: range land predominates with 68.48%, followed by pasture (30.93%), water bodies (0.42%) and forestland is 0.15% (Table 5.3). The prime source of income generation for the inhabitants of the region is through agriculture. Root crops such as taro, kumala and cassava are grown. It is visible from Figure 5.4 that there are a very few settlements scattered mainly on the west of the catchment area. According to Fiji Islands Bureau of Statistics (2017), the study area has **a** population density of 4227 with 55.1% of the population between 15-64 years.

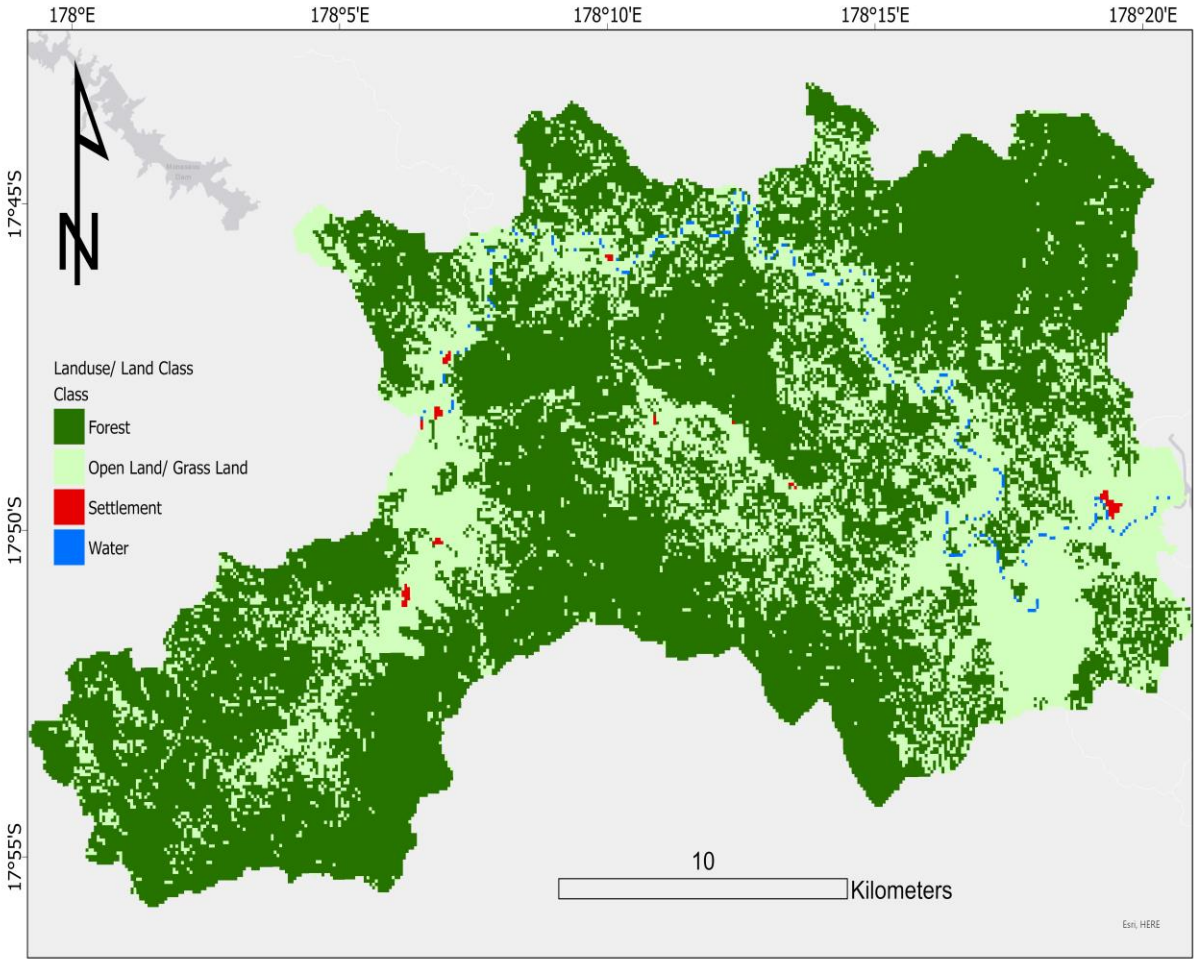

Figure 5.4: Digital LULC map of Wainimala Basin.

Table 5.3: Vegetation Cover at Wainimala Catchment (FAO, 2015).

Vegetation Class	Definition	Area (ha)	% Watershed
Forest Deciduous	Vegetation that is composed primarily of broad-leaved trees that shed all their leaves during one season.	65.89	0.15
Pasture	An area covered with grass or other plants used or suitable for the grazing of livestock	13834.48	30.93
Range	Lands on which the indigenous vegetation is predominantly grasses, grass-like plants, forbs and possibly shrubs or dispersed seeds	30627.93	68.48
Water	Land areas covered under water bodies such as open water, lakes, rivers and dams	186.93	0.42
Forest	Forest area includes both forest land cover (forest land covered by trees) and forest land use (both forest cover and the forest land temporarily without trees)	9.09	0.02

5.4. Soil Characteristics of the Basin

The physical properties of soil are very important since they have a pronounced effect on the hydrological processes within the HRU. The physical properties of soil include: texture, color, structure, porosity, density, consistence, moist bulk density, organic carbon content for different layers of each soil type, permeability, erodibility factor (K), available water capacity in the soil, saturated hydraulic conductivity, length of soil layer from surface to bottom and so on. Table 5.4 presents the soil characteristics for Wainimala catchment.

A digital soil map of the study area was developed with a low resolution at a scale of 1:5000000 based on the Food and FAO and United Nations Educational, Scientific and Cultural Organization (UNESCO) data. It is visible from Figure 5.5 that the basin is composed of two main soil types: Chromic Combisols (Bc39-3c-6219) and Chromic Combisols (Bc42-3c-6222Bc42). Bc42-3c-6222Bc42 soil type is predominant with 69.65%. Table 5.5 reports the soil types present with percentages at the catchment area. Bc42-3c-6222Bc42 being dominant soil type has the following characteristics: moderate permeability, uniform medium-texture profile with organic surface horizons overlying reddish or brownish sub-soils (FAO, 1978). Additionally, it is a moderately well drained soil with high content of clay with perudic moisture regime. Thus, surface run-off is potentially good with low percolation.

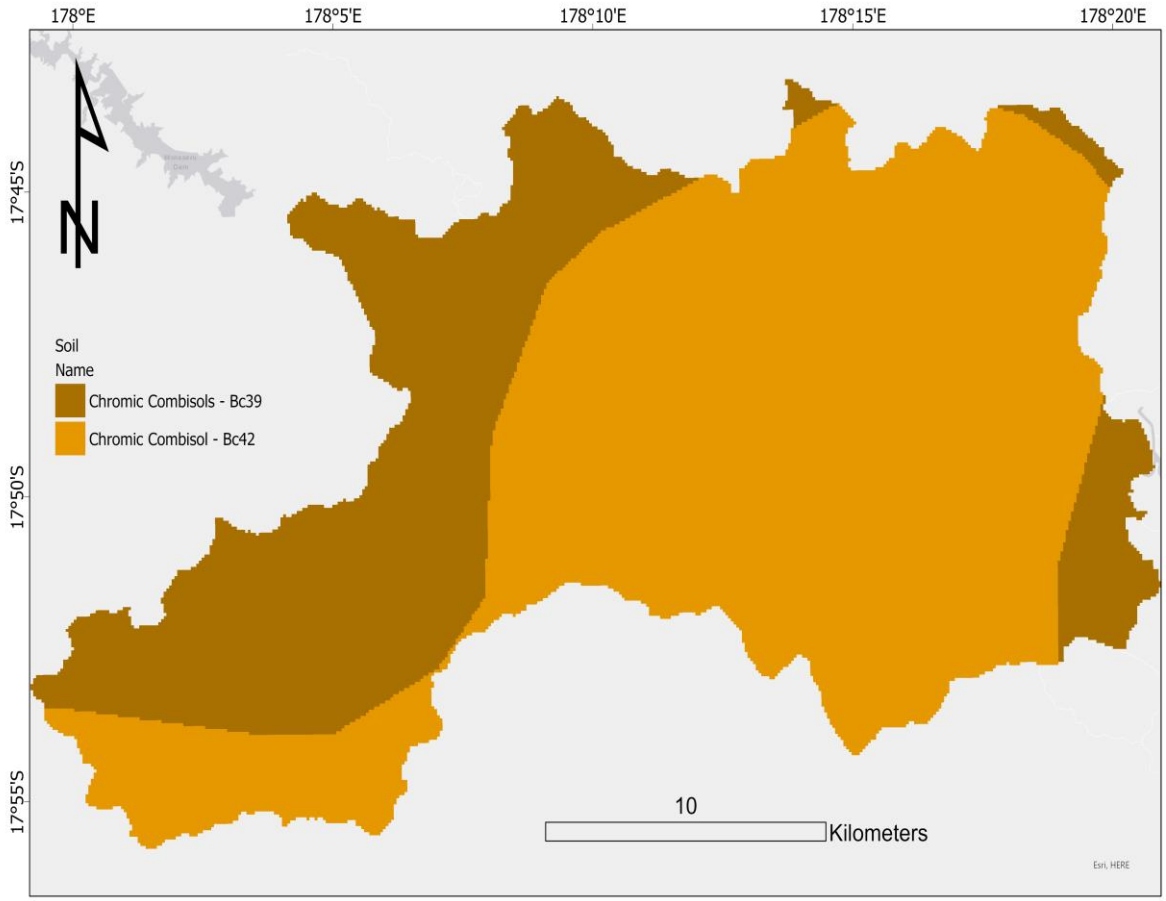

Figure 5.5: Digital soil map of Wainimala Basin.

Table 5.4: Soil characteristics at a sub-basin catchment at Wainimala (Ministry of Agriculture).

Soil Property at Wainimala Catchment	Description
Taxonomy	Oxic Humitropept, fine, kaolinitic, isothermic, upland steepland soil is associated with humic latosols
Soil moisture regime	Perudic
Soil temperature regime	Isothermic
Soil drainage class	Well drained
Soil permeability class	Moderate
Soil erodibility	Massive erosion
Soil pH	Strongly acidic throughout
Organic carbon	Medium values in topsoil (0-25 cm), very low values below it
Organic nitrogen	Medium values in topsoil (0-25 cm), very low values below it
Available phosphorus and nitrogen	Very low
% Base saturation	Low through cation exchange capacity in the mid top soil and low below it
Exchangeable calcium	Low in the top soil and very low in the other horizons
Magnesium	Medium in the top soil and very low in all other horizons (even are below phosphorus and potassium levels)

Table 5.5: Dominant soil type and percentage area at Wainimala catchment.

Soil Type	Area (ha)	% Watershed
Bc39-3c-6219	13570.83	30.34
Bc42-3c-6222Bc42	31148.99	69.65

5.5. Slope Morphology

The slope map in Figure 5.6 provides a colorized representation of the slope and terrain. It also shows the degree of slope steepness for Wainimala catchment depicted by colorization. Flat surfaces (terrain) are purple, shallow slopes are blue, moderate slopes are green and yellow and deep slopes are red. The slope map provides visualization on the possibility of good site to build hydropower plant.

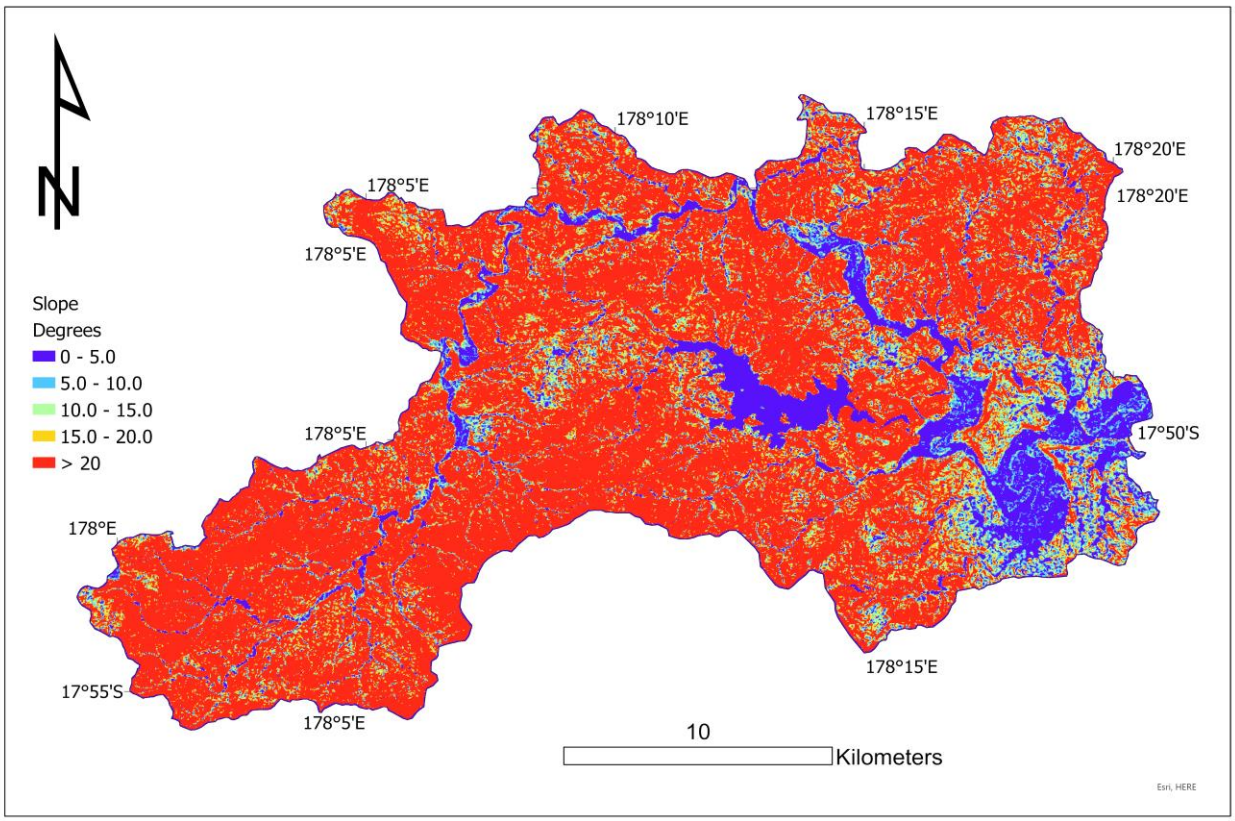

Figure 5.6: Slope map of Wainimala Basin.

Five classes of slope degrees are illustrated in Figure 5.6. Regions marked dark blue with slope heights between 0-5 m is the flat area with least hydro potential capabilities with zero potential since the elevation difference between two adjacent cells is zero with the same elevation statistic. Similarly, the slope degrees between 5.0-10.0 m marked as pale blue also has very low hydro potential capabilities since the elevation difference between two adjacent cells are less. Slope heights between 10.0-15.0 m (marked green) may show some hydro potential capabilities. The slope map with slope degrees between 15.0-20.0 m (marked yellow) and greater than 20.0 m (marked red) is potentially more preferred for development of hydro power plant

with greater elevation difference between cells. Table 5.6 reports the various slope degrees, area in hectares and percentage watershed. It is visible from Table 5.6 that slope degrees between 20.0-9999 m have the greatest watershed percentage (67.92%) covering 30378.23 hectares of the basin. Interestingly, the slope degrees between the ranges 20.0-9999 m has the greatest potential for generation of hydroelectricity since the elevation difference between two adjacent cells is the greatest. However, the actual hydro potential also depends on the discharge rate and the dam retention potential. The theoretical hydropower potential is the product of elevation difference between adjacent cells and discharge.

Table 5.6: Percentage slope degrees for Wainimala catchment.

Slope Degrees (m)	Area (ha)	% Watershed
0-5.0	5056.14	11.31
5.0-10.0	2592.08	5.80
10.0-15.0	2996.87	6.70
15.0-20.0	3701.00	8.28
20.0-9999	30378.23	67.92

5.6. Mean Annual Precipitation

The present study concentrates on historical rainfall data for 39 years from 1980 to 2018 to estimate the discharge and hydro potential of selected sub-basins. The variation in monthly mean precipitation over the 39-year period is illustrated in Figure 5.7. The wet season from November to April received higher precipitation hence has elevated monthly mean precipitation. The month of February received the maximum mean precipitation of 382.64 mm of rainfall. Conversely, minimum monthly mean precipitation was recorded in August with 183.68 mm of rainfall. During the dry spell (May to October), the mean precipitation received was 223.43 mm of rainfall. Interestingly, 50 % of the months received precipitation exceeding 300 mm of rainfall during the study period.

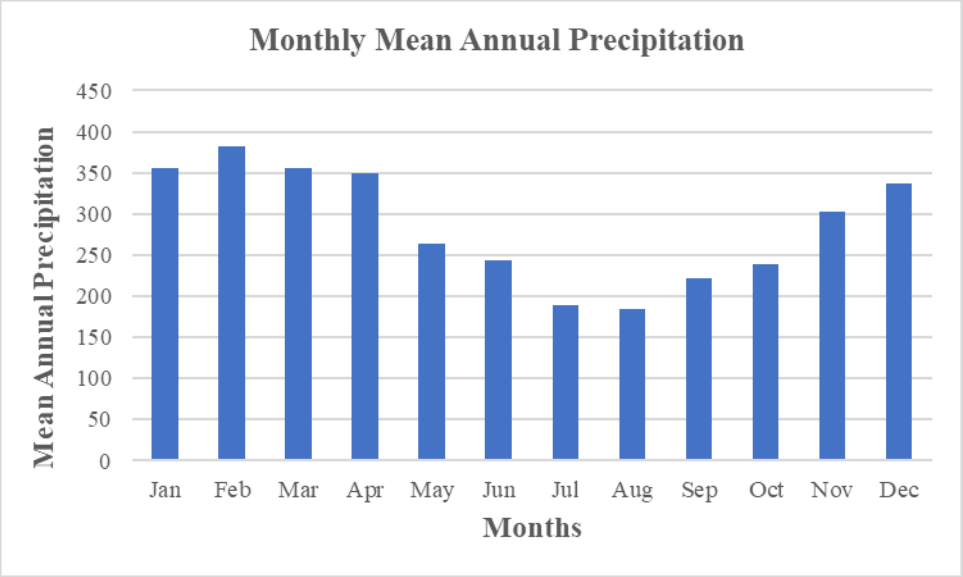

Figure 5.7: Hydrograph representing the monthly mean precipitation for the Wainimala catchment.

Monthly precipitation is an important component of the ROR watershed modeling and the results are presented in the next section.

5.7. Hydraulic Head Estimation

The use of QGIS algorithm on generated DEM determined the minimum, maximum and mean elevations for each sub-basin at Wainimala catchment. The hydraulic head height was obtained by subtracting the maximum elevation from minimum. Table 5.7 summarises the boundary area of each sub-basin (km^2), minimum, maximum and mean elevations and head height. There are greater variations in the obtained hydraulic heads among 32 sub-basins. Head classification is relatively important and is one of the criterions used for classifying hydropower turbines either as high-head, medium-head or low-head. Head heights greater than 50 m are classified as high head, medium heads are between 10-15 m and low heads are less than 10 m (Elbatran et al., 2015). It is visible from Table 5.7 that all sub-basins have head heights greater than 50 m and are therefore classified as high heads. Comparably, sub-basins 15, 28, and 30 have relatively low hydraulic heads amongst 32 sub-basins whereas sub-basin 2 has the maximum mean elevation of 992 m.

Table 5.7: Summary of minimum, maximum and mean elevation to determine head height for 32 sub-basins.

Sub-basin	Area (km^2)	Minimum Elevation	Maximum Elevation	Mean Elevation	Head Height (m)
1	38	9	552	196.78	543
2	12	88	1080	511.68	992
3	9	94	825	324.03	731
4	9	105	788	346.15	683
5	17	47	899	385.43	852
6	14	18	788	254.63	770
7	17	323	1064	641.64	741
8	44	20	555	174.53	535
9	11	87	652	264.76	565
10	55	26	528	172.91	502
11	101	159	902	499.23	743
12	64	216	1006	544.81	790
13	20	321	1143	775.14	822
14	48	31	618	255.96	587
15	56	18	119	60.34	101
16	121	13	456	141.33	443
17	10	52	784	347.60	732
18	13	279	1102	575.64	823
19	12	26	544	266.14	518
20	55	17	465	103.76	448
21	131	124	665	296.54	541
22	15	19	786	215.77	767
23	41	275	707	425.87	432
24	28	72	589	209.97	517
25	161	12	225	50.63	213
26	11	210	1026	586.09	816
27	64	219	920	463.92	701
28	199	11	103	31.56	92
29	82	206	476	318.17	270
30	240	7	73	21.18	66
31	829	275	707	330.28	432
32	707	72	589	34.74	517

5.8. Estimation of Hydropower Potential

Section 3.5 describes the procedures for estimating the hydropower potentials of 32 sub-basins.Total hydro potential of the basin was obtained by adding the potentials of all the sub-basins. Table 5.9 summarises the estimated hydropower potential for 32 sub-basins. Hydroelectricity generation at the basin is calculated as theoretical and technical potentials. Hydropower potential is the function of discharge and hydraulic head producing variations in hydroelectricity generation. This means that generation of lower hydroelectricity is due to either low hydraulic head or discharge (see Table 5.7). Calculations on theoretical hydroelectricity potential at sub-basins exclude efficiencies of both turbine and generator. The total theoretical hydroelectricity potential for 32 sub-basins is estimated to be 83.07 MW.

Conversely, calculations based on technical hydroelectricity potential consider the efficiencies of both turbine and generator. The technical potential takes technical limits into consideration such as electro-mechanical losses associated with equipments of the hydropower plant, efficiencies of the turbine and generator and losses from kinetic energy of the water to the grid. In this study the efficiencies of both turbine and generator are assumed to be 80% and gravitational force is taken as 9.81 m/s^2. The amount of hydroelectricity generation is not only limited by the efficiencies of the turbine and generator. It is the natural variability of discharge driven by changes in the weather pattern that accounts for variations in estimating the amount of electricity generation.

Thus, the total technical hydroelectricity generated for 32 sub-basins was found to be 53.05 MW. Table 5.8 reports classification of hydro plant based on capacity, which revealed that the plant could be classified as medium hydro and can, connect to the grid system to meet increasing energy demands. It is seen that sub-basins 11, 12, 16, 21, 27 and 31 have higher electricity generation potential whereas the remaining sub-basins show slight deviations in hydroelectricity generation. Figure 5.10 illustrates the sub-basins with high hydroelectricity generation potential totalling 41.17 MW as theoretical potential. The shadings in Figure 5.10 depict sub-basins with producing significant hydroelectricity.

However, the hydropower plants simply cannot be constructed on every location along the river basin. In particular, the hydropower reservoirs are built on relatively ideal locations in consideration to the stream network, DEM, LULC map, soil and slope map. It is found in this study (see Table 5.6) that there is a substantial capacity to construct hydropower plant on slopes between 20.0-9999 m. This slope provides a relatively ideal location where a natural valley formation forms a "V-shape" for construction of dam.

Table 5.8: Classification of hydro plant based on capacity (Dave et al., 2014).

Type	**Capacity**
Large Hydro	Has the capacity greater than 100 MWand generally feeds into a large electricity grid
Medium Hydro	Capacity ranges between 15-100 MW and generally feeds a grid
Small Hydro	Capacity ranges between 1-15 MW and generally feeds into a grid
Mini Hydro	Has the capacity greater than 100 kW, but below 1 MW; suitable for either stand alone schemes or more often feeds into the grid
Micro Hydro	Capacity ranges from 5 kW up to 100 kW; generally provides power for a small community or rural industry in remote areas away from the grid
Pico Hydro	Hydro capacity with few hundred watts up to 5 kW

Table 5.9: Hydro power potentials for 32 sub-basins (Note: in all the cases the following constants were used: ρ = 1000 kgm^3; η_t = 0.8; η_g = 0.8; g = 9.81 m/s^2).

Sub-basin	Hydraulic Head (m)	Flow_Out (m^3/s)	Theoretical Potential (MW)	Technical Potential (MW)	Energy (MWh)	Energy/day
1	543	0.370	1.97	1.26	0.64	15.4
2	992	0.159	1.55	0.99	0.50	12.1
3	731	0.094	0.67	0.43	0.22	5.3
4	683	0.094	0.63	0.40	0.21	4.9
5	852	0.185	1.55	0.99	0.51	12.1
6	770	0.142	1.11	0.69	0.35	8.4
7	741	0.182	1.32	0.85	0.43	10.4
8	535	0.455	2.39	1.53	0.78	18.7
9	565	0.142	0.79	0.50	0.26	6.15
10	502	0.558	2.75	1.76	0.90	21.50
11	743	1.290	9.40	6.01	3.07	73.60
12	790	0.785	6.08	3.89	1.98	47.62
13	822	0.287	2.31	1.48	0.75	18.11
14	587	0.502	2.89	1.85	0.94	22.65
15	101	0.578	0.57	0.37	0.19	4.48
16	443	1.235	5.41	3.43	1.75	42.02
17	732	0.110	0.79	0.50	0.26	6.17
18	823	0.140	1.13	0.72	0.37	8.86
19	518	0.120	0.61	0.39	0.20	4.78
20	448	0.558	2.45	1.57	0.80	19.19
21	541	1.663	8.83	5.64	2.88	69.08
22	767	0.146	1.11	0.70	0.36	8.59
23	432	0.515	2.18	1.39	0.71	17.07
24	517	0.372	1.89	1.21	0.62	14.78
25	213	1.673	3.51	2.23	1.14	27.35
26	816	0.156	1.25	0.80	0.41	9.78
27	701	0.785	5.41	3.45	1.76	42.26
28	92	2.060	1.86	1.19	0.61	14.55
29	270	1.028	2.72	1.74	0.89	21.32
30	66	2.461	1.59	1.02	0.52	12.47
31	477	1.290	6.04	3.86	1.97	47.25
32	85	0.366	0.31	0.19	0.10	2.39

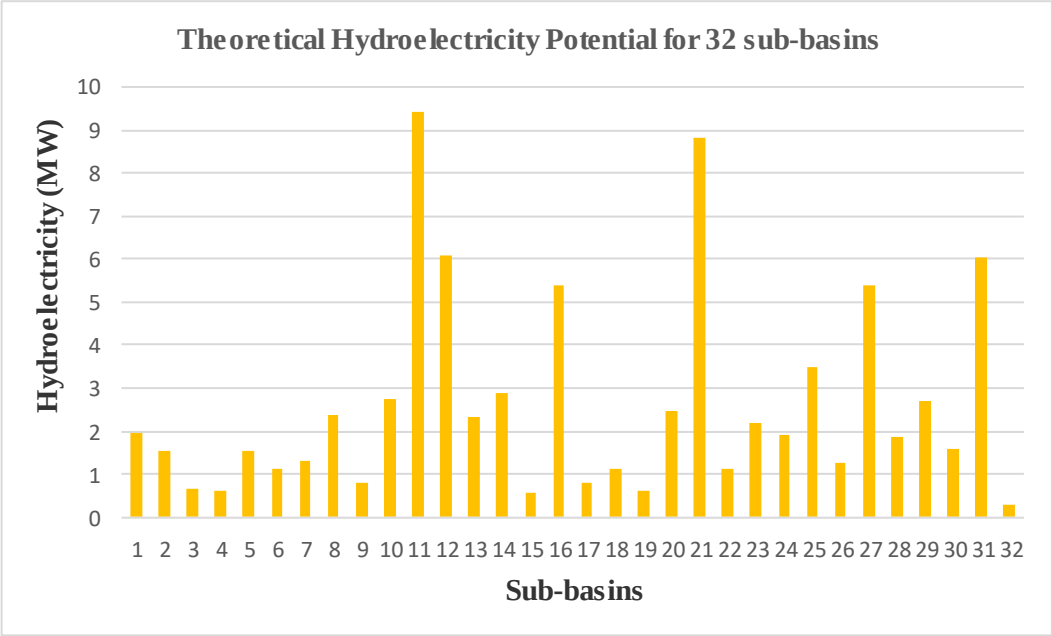

Figure 5.8: Theoretical hydro potential of 32 sub-basins at Wainimala catchment.

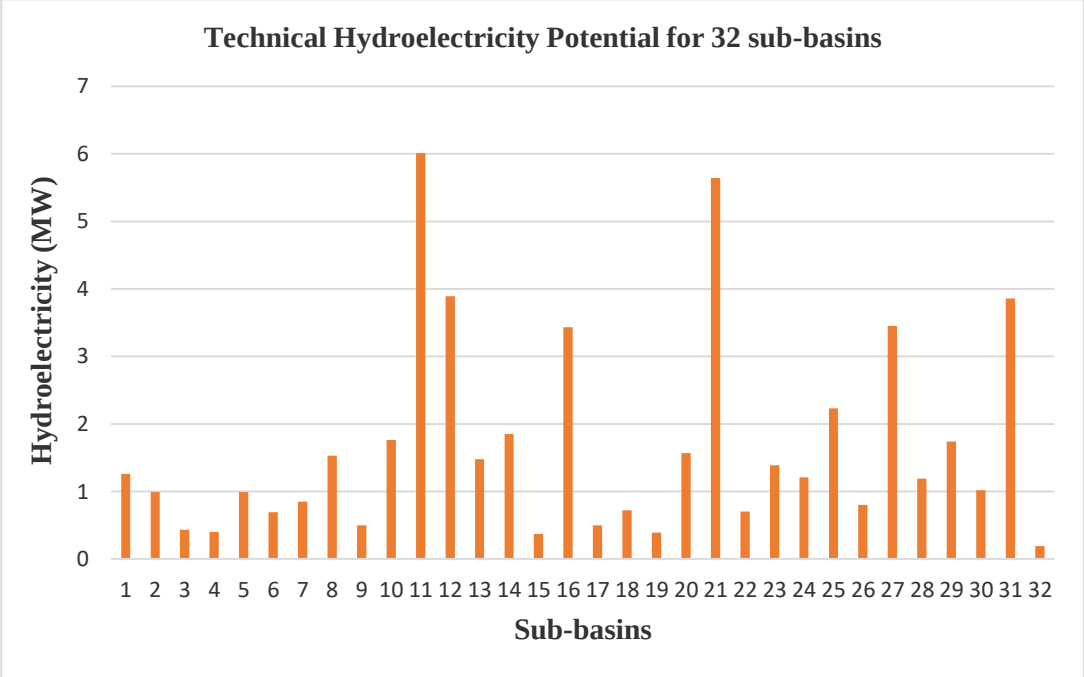

Figure 5.9: Technical hydro potential of 32 sub-basins at Wainimala catchment.

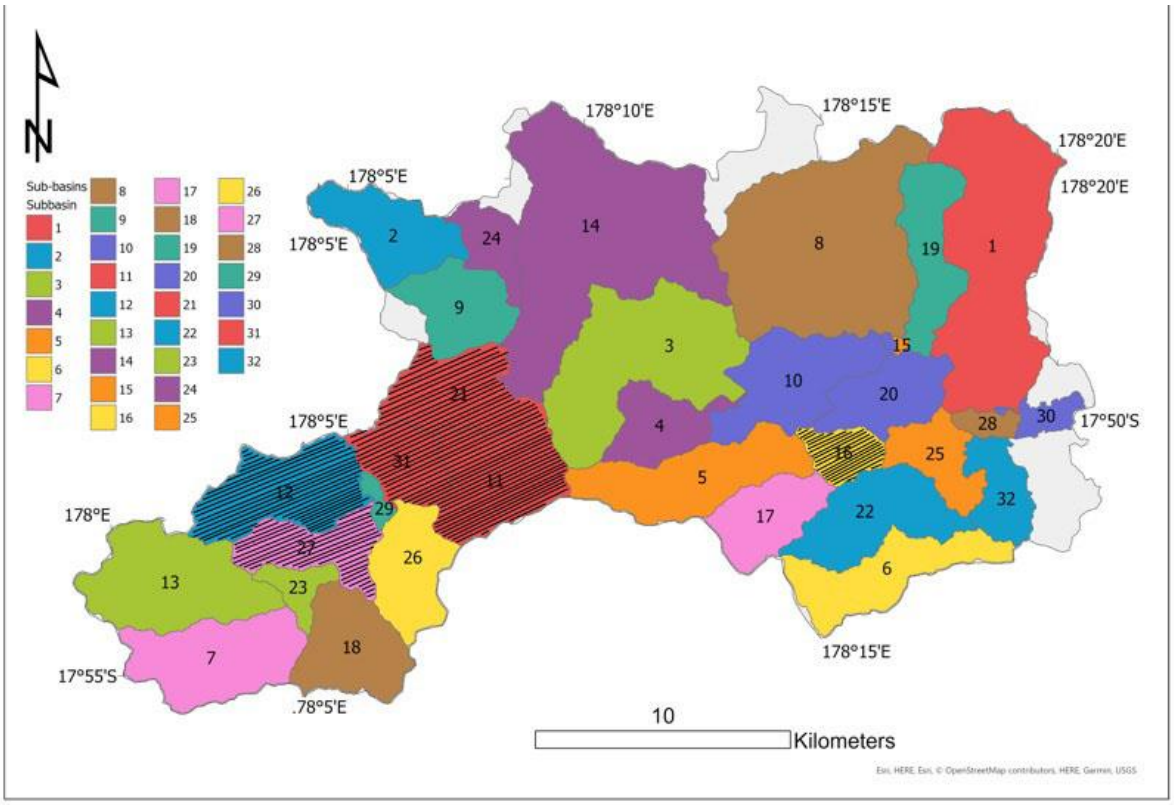

Figure 5.10: Illustrates the sub-basins with significant hydroelectricity generation potentials via shadings. (Basins 11, 12, 16, 21, 27 and 31).

5.9. Estimated Avoided Carbon Emissions

In Fiji, EFL uses thermal power stations (diesel gensets) to produce electricity to meet the increasing energy demands. For this purpose, HFO and IDO have been combusted at Kinoya, Vuda, Ovalau and Labasa thermal power stations to generate electricity that results in GHG emissions such as CO_2, oxides of sulphur (SO_x), nitrogen oxides (NO_x), other trace gases and air borne inorganic particulates that include fly ash and suspended particulate matter (SPM) (Ramachandra et al., 2012; 2016; Teddy 2006; 2011). For instance, thermal power stations generated 349.93 million units in 2020 as compared to 449.62 million units in 2019. Thus, the contribution of thermal generation was 35.85% in 2020 as compared to 42.4% in 2019. It can be noticed that there is a drop in the demand for thermal generation as a

result of Covid-19 impact across the Vitilevu Interconnected System (VLIS) (EFL, 2020).

A comparative analysis is performed to estimate the annual power capacity and hydrokinetic potentials for 32 sub-basins for both theoretical and technical approach and determine the Megatonne (Mt) of GHG emissions avoided annually. EFL uses the fuel types HFO and IDO to produce energy and in order to do this, electricity generated (kWh) from combustion of 1 kg of HFO and IDO has to be determined first. Additionally, the combustion of 1 kg of HFO generated 4.63 kWh of electricity whereas 1 kg of IDO combusts to generate 4.68 kWh of electricity. The variance in electricity generated by 1 kg HFO and IDO is significantly small. The Table 4.10 presents the net calorific value (NCV), CO_2, CH_4 and N_2O emission factors of different fuel types used in calculating the avoided emissions in tonnes for this study. Since, the CO_2 emission factor of IDO is slightly higher than that of HFO, more CO_2 is released per year from HFO. Conversely, CH_4 and N_2O emission factors are relatively less in comparison to CO_2 emission factor. For instance, the emission factors of CH_4 and N_2O are 0.003 (t TJ^{-1}) and 0.006 (t TJ^{-1}), respectively (see Table 4.10) and produced significantly less emissions compared to CO_2 released per year. Of the delineated 32 sub-basins in the WRB watershed, only 6 sub-basins were identified as having potential sites with an estimated annual power capacity of 41.17 MW. Interestingly, sub-basins 11 and 21 have very high hydropower capacities. The technical HK potential for 32 sub-basins was estimated to be 53.05 MW which is expected to produce 278831 MWh of energy annually. Moreover, theoretical HK potential was estimated to be 83.07 MW which would produce 436616 MWh of energy annually. These estimations were based on an average capacity factor of 60% for hydroelectricity generation in Fiji for technical approach (see Table 5.10). From the analysis done on total GHG emissions for technical HK, 1.91 Megatonne (Mt) of CO_2 equivalent emissions were emitted from HFO combustion and 2.10 Mt of CO_2 equivalent emissions were emitted when IDO was combusted to generate electricity annually. This means 4.01 Mt of CO_2 equivalent emissions can be saved by replacing the fossil fuel with hydroelectricity generation from technical HK (see Table 5.11).

Hence, the replacement of imported fossil fuels with indigenous renewables is considered to be one of the crucial factors in accomplishing the national energy policy objectives (IRENA, 2015). Fiji has total installed power generation capacity of 269 MW out of which an estimated 220 MW is generated on the main islands (IRENA, 2015). According to Fiji's Nationally Determined Contributions (NDCs) roadmap, the energy sector in Fiji focusing to escalate the percentage share of renewable energy to 100% by 2030 with respect to the 2013 as reference year whereby RE generation mix hovered around 60%.

Table 5.10: The average capacity factor calculation for Wailoa Station with installed capacity of 80 MW.

Year	**2016**	**2017**	**2018**	**2019**	**2020**
Generation (MWh)	384451	381527	433970	454262	451608
Capacity Factor (CF)	0.548589	0.544416	0.619249	0.648205	0.644418
Average CF			0.600975		

Thus, the amount of hydroelectricity generated from this study would certainly scale up nations hydropower capacity and save substantial GHG emissions. Additionally, this green growth initiative would significantly contribute to the development of sustainable, reliable and affordable energy. These key actions would support nation's economic growth and enhance energy security. Prior to any renewable energy developments, a comprehensive renewable energy resource assessment is essential with pre-feasibility, feasibility and economic analysis. According to IRENA (2015), the costs for RET's are continually decreasing and Fiji can take better advantage of it with its full range of available renewable energy resources.

Though hydropower is one of the mature technologies in Fiji its operations are challenged and obstructed by the following: technical problems such as equipment break downs, sedimentation, difficulty in accessing site, lack of technical expertise amongst the communities responsible for plant operation, extreme weather events

such as severe drought that includes El Niño, El Niño Southern Oscillation, vulnerability to seasonable dissimilarity in annual hydrological cycles and prospective financial schemes (IRENA, 2015). Despite the key barriers, the energy sector in Fiji is progressing well with developments in hydropower technology.

Table 5.11: Mt of CO_2 equivalent emissions from combustion of HFO and IDO for technical HK per year.

Fuel Type	Energy Used (KWh)	t (CO_2)	t (CH_4)	t (N_2O)	t (CO_2 e)	Mt (CO_2 e)
HFO	139415500	1902050.65	1946.16	4639.65	1908636.46	1.91
IDO	139415500	2094902.47	2120.34	5054.90	2102077.71	2.10

5.10. Limitations of the Study

The worldwide impacts of Covid-19 had greater effects on the socio-economic status of the nation, led to poverty and extensive health problems, hindrance to research work, extensive job losses and loss of human lives. Likewise, the impacts of Covid-19 have greatly affected this research work. For this study one of the very important limitations was the use of monthly hydrometeorological data to simulate the streamflow of WRB. Unfortunately, the daily or weekly hydrological data was not available and as a result, there was no other option but to use the available data. In particular, the use of daily data is much preferred over monthly data since it is more realistic with fewer errors. Further independent studies are recommended at daily timescale.

In addition, the discharge at WRB was determined using the integrated QGIS and QSWAT platforms which is freely available. Evaluation of the performance indexes requires the use of SUFI-2 (Sequential Uncertainty Fitting) algorithm, which requires paid licenses. Unfortunately, this was not budgeted and here is also no freely available alternative hence, the model performance has not evaluated and is another limitation of the study.

5.11. Summary

The main driver for implementing renewable energy sources is to mitigate climate change issues by lowering GHG emissions in the atmosphere. There are several broad methods being employed in mitigating CO_2 emissions globally. These include: the use of more efficient conversion of fossil fuels, switching to low-carbon fossil fuels and suppressing emissions, decarbonisation of fuels and flue gases and carbon dioxide sequestration, increasing the use of nuclear power and increasing the use of renewable sources of energy (Sims et al., 2003).

In Fiji, the electricity sector particularly EFL mitigates carbon dioxide emissions by increasing its percentage share of renewable energy through developments in hydroelectricity. Additionally, other means such as extensive afforestation, mangrove restoration and protection programs significantly contribute to decarbonization and sustainable development. In accordance to Fiji's generation mix, nearly half of the power generation is obtained from fossil fuel combustion and these results in GHG emissions. Hence, the installation of more hydroelectricity power plants is the best way to mitigate GHG emissions and this will certainly reduce import bills and effects of climate change.

Chapter 6

Conclusion, Recommendations and Future Prospects

6.1. Conclusion

SWAT and GIS models are quite reliable, effective and useful tools that can be employed or implemented at the study site (watershed) in order to evaluate different hydrological parameters. Moreover, on the basis of literature, SWAT model is pretty useful and has advantages with respect to other hydrological models in estimating various water balance components with relatively good precision. SWAT-CUP equipped with various models is an efficient calibration program. These models have the ability to identify the most sensitive hydrological parameter(s), report uncertainty errors, analyze watershed hydrology and can assist in managing the water balance components. Hence, the SWAT-CUP calibration program has been extensively used in correspondence to water management practices and is therefore relatively much more effective than statistical methods.

The watershed modeling with QSWAT was conducted to estimate the river discharge for 32 sub-basins at Wainimala catchment. First, the physical parameters were used to determine the topography of the basin where four streams were identified with the largest drainage located at the South East of the catchment area. A 30-m resolution SRTM delineated watersheds with 32 sub-basins where the majority of the projection were elevated at the largest drainage in the range 8.62-167.75 m. The distribution of sub-basins was characterized by the standard deviation, minimum, maximum and mean elevations measured in meters. Range land was the predominant vegetation cover with 68.48% and Bc42-3c-6222Bc42 was the predominant soil type that exhibited potentially good soil characteristics with low percolation ideal for hydropower development. 67.92% of the basin area covering 30378.23 hectares fall with slope degrees between 20.0-9999 m had greater potential for hydroelectricity generation. The estimated river flow and effective hydraulic head were used to calculate the theoretical and technical hydroelectricity generation for 32 sub-basins based on precipitation data set.

Wainimala catchment was delineated into 32 sub-basins of which 6 of them had the greater potential for the development of hydroelectricity. Both theoretical and technical approach was considered for the potential capacities of each sub-basin for generating power within the Wainimala watershed. Amongst the 6 sub-basins at the Wainimala watershed, sub-basins 11 and 21 had the greatest hydropower potential capability. According to hydropower classification (see Table 5.9), a medium-scale hydropower with a capacity between 15 MW and 100 MW is most suitable for WRB. The technical HK potential for 32 sub-basins was estimated to be 53.05 MW which produced 278831 MWh of energy annually. Conversely, the theoretical HK potential was estimated to be 83.07 MW which produced 436616 MWh of energy annually. These estimations were based on an average capacity factor of 60% for hydroelectricity generation in Fiji. HFO emitted 1.91 Megatonne (Mt) of CO_2 equivalent emissions whereas 2.10 Mt of CO_2 equivalent emissions were emitted when IDO was combusted to generate electricity annually. This means 4.01 Mt of CO_2 equivalent emissions can be saved by replacing the fossil fuel with hydroelectricity.

6.2. SWAT Recommendations

The hydrological models are to be appropriately used so that model simulations are performed realistically and eventually lead to good policy recommendation. Season-based evaluation that considers the wet and dry periods is recommended as model refinement in order to increase model performance. In addition, potentially more exploitable future hydropower sites can be selected with a geospatial tool in GIS software in consideration to topographical, environmental and hydrological parameters.

6.3. Future Prospects

Goodness of fit model can be performed on the current study later once pandemic ceases. To accomplish this, sensitivity analysis, calibration and validation of the WRB can be performed in SWAT-CUP software through the SUFI-2 version 2 algorithm. This comparatively analyses the obtained observed and simulated streamflow through model calibration and validation. Prior to this, sensitivity

analysis needs to be performed through model operation while varying a particular value of a given model parameter within a specified range. Further, the most sensitive parameter(s) would optimize the model. Various objective functions or performance indexes such as *NSE*, R^2, P-factor, R-factor, MAE, MSE, PBIAS and RMSE can be employed for calibration and evaluate model performance between observed and simulated streamflow bracketed within 95PPU (Kouadio et al., 2022). Interestingly, the results of the performed SWAT model are quite helpful and would allow policy makers to plan and formulate the policies and propose strategies in power generation and expansion in order to meet future electricity demands. In addition, further research such as impacts of climate change, land-use change and percentage sedimentation yield can also be performed by creating scenario-based studies. Ultimately, the output of this study would be beneficial to investors, provide opportunities and can be taken as an input plan in implementing new hydropower plant investments and provide sustainable development.

References

Abbaspour, K.C., Johnson, C.A., van Genuchten, M.T. (2004). Estimating uncertain flow and transport parameters using a sequential uncertainty fitting procedure. Vadose Zone Journal, 3, 1340-1352.

Abbaspour, K.C., Yang, J., Maximov, I., Siber, R., Bogner, K. (2007a). Modelling hydrology and water quality in the pre-alpine/alpine Thur watershed using SWAT. Journal of hydrology, 333, 413-430.

Abbaspour, K., Vejdani, M., Haghighat, S. (2007b). SWAT-CUP calibration and uncertainty programs for SWAT. MODSIM 2007 International Congress on Modelling and Simulation, Modelling and Simulation Society of Australia and New Zealand, 1596-1602.

Abbaspour, K.C. (2015a). SWAT-CUP: SWAT Calibration and Uncertainty Programs—A User Manual; Swiss Federal Institute of Aquatic Science and Technology (Eawag): Dübendorf, Switzerland.

Abbaspour, K.C; Rouholahnejad, E; Vaghefi, S; Srinivasan, R; Yang, H; Klove, B. (2015b). A continental-scale hydrology and water quality model for Europe: Calibration and uncertainty of a high-resolution large-scale SWAT model. Journal of Hydrology, 524, 733-752.

Abeyou, W.W., Ayana, E.K., Yen, H., Jeong, J., MacAlister, C., Taylor, R., Gerik, T.J., Steenhuis, T.S. (2018). Evaluating hydrologic responses to soil characteristics using SWAT model in a paired-watersheds in the Upper Blue Nile Basin. Catena, 163, 332–341. https://doi.org/10.1016/j.catena.2017.12.040.

ADB. (2008). Living with High Prices: A Policy Brief. Asian Development Bank, Manila.

ADB. (2009). Taking Control of Oil: Managing Dependence on Petroleum Fuels in the Pacific. Asian Development Bank, Manila.

Adu, J. T., Kumarasamy, M.V. (2018). Assessing nonpoint source pollution models: A review. Pol. J. Environ. Stud, 27(5), 1913–1922.

Ajami, N.K., Gupta, H., Wagener, T., Sorooshian, S. (2004). Calibration of a semi-distributed hydrologic model for streamflow estimation along a river system. Journal of Hydrology, 298(1), 112-135. DOI: http://dx.doi.org/10.1016/j.jhydrol.2004.03.033.

A. M., and Guven, A. (2016). Al-Juboori modeling, gene expression programming and visual basic programming. Water Resources Manage. 30, 2517–2530. doi: 10.1007/s11269-016-1300-3.

Almeida, R.A., Pereira, S.B., Pinto, D.B.F. (2018). Calibration and validation of the SWAT hydrological model for the Mucuri River Basin. Journal of the Brazilian Association of Agricultural Engineering. 38, 55-63. Doi: http://dx.doi.org/10.1590/1809-4430 Eng.Agric, v38n1p55-63/2018.

Alterach, J., Peviani, M., Davitti, A., Vergata, M. (2009). Evaluation of the residual potential hydropower production in Italy. Hydropower and Dams, 5(June).

Ambroise, B., Freer, J., Beven, K. (1996). Application of a generalized TOPMODEL to the small Ringelbach catchment, Vosges, France. Water Resources Research, 32, 2147-2159.

Amin, A., Nuru, N. (2020). Evaluation of the performance of SWAT model to simulate stream flow of Mojo River watershed: in the upper Awash River Basin, in Ethiopia. Hydrology, 8(1), 7-18.

Anantharajah, K. (2019). Governing climate finance in Fiji: Barriers, complexity and interconnectedness. Sustainability, 11(12), 3414. https://doi.org/10.3390/su11123414.

Andrade, M.A., Mello, C.R., Beskow, S. (2013). Simulação hidrológica em uma bacia hidrográfica representativa dos Latossolos na região Alto Rio Grande, MG. Revista brasileira de engenharia agrícola e ambiental, 17(1), 69-76. http://dx.doi.org/10.1590/S1415-43662013000100010.

Ansari, A., Kato, T., Fitriah, A. (2019). Simulating streamflow through the SWAT model in the Keduang sub-watershed, Wonogiri Reency, Indonesia. Agritech, 39(1), 60-9.

Arefiev, N., Badenko, N., Ivanov, T., Kotlyar, S., Nikonova, O., Oleshko, V. (2015). Hydropower Potential Estimations and Small Hydropower Plants Siting: Analysis of World Experience. Applied Mechanics and Materials, 725–726, 285– 292. http://doi.org/10.4028/www.scientific.net/ AMM.725-726.285.

Arnold, J. G., Williams, J. R., Nicks, A. D., Sammons N. B. (1990). SWRRB: A basin scale simulation model for soil and water resources management. College Station, Tex.: Texas A&M University Press.

Arnold, J.G., Allen, P.M., Bernhardt, G. (1993) A comprehensive surface groundwater flow model. Journal of hydrology, 142, 47-69.

Arnold, J. G., Srinivasan, R., Muttiah, R. S., and Williams, J. R. (1998). Large area hydrologic modeling and assessment part I: model development 1. JAWRA Journal of the American Water Resources Association, 34(1), 73-89.

Arnold, J.G., Srinivasan, R., Muttiah, R.S., Allen, P.M. (1999). Continental scale simulation of the hydrologic balance. J. Am. Water Resour. Assoc, 35(5), 1037–1051.

Arnold, J.G., Moriasi, D.N., Gassman, P.W., Abbaspour, K.C., White, M.J., Srinivasan, R., Santhi, C., Harmel, R.D., Van Griensven, A., Van Liew, M.W., Kannan, N., Jha, M.K. (2012). SWAT: model use, calibration, and validation. Transactions of the ASABE, 55(4), 1491-1508.

Awasthi, N. (2021). Hydrological modeling of Bhagirathi River Basin up to Tehri dam using ArcSWAT.

Ayele, G.T., Teshale, E.Z., Yu, B., Rutherfurd, I.D., Jeong, J. (2017). Streamflow and sediment yield prediction for watershed prioritization in the upper Blue Nile River basin, Ethiopia. Water, 9(782), 1-28.

Bajracharya, A., Awoye, H., Stadnyk, T., Asadzadeh, M. (2020). Time Variant Sensitivity Analysis of Hydrological Model Parameters in a Cold Region Using Flow Signatures. Water, 12(961), 1-24.

Ballance, A., Stephenson, D., Chapman, R., Muller, J. (2000). A geographic information systems analysis of hydro power potential in South Africa. Journal of Hydroinformatics, 2, 247–254. Retrieved from http://www.iwaponline.com/jh/002/jh0020247.htm.

Berghuijs, W. R., Woods, R. A., and Hrachowitz, M. (2014). A precipitation shift from snow towards rain leads to a decrease in streamflow. *Nat. Climate Change* 4, 583–586. doi: 10.1038/nclimate 2246.

Beven, K.J. (2000). Rainfall-Runoff Modeling: The Primer, John Wiley & Sons, Ltd., New York, New York.

Bian, L., Sun, H., Blodgett, C., Egbert, S., Li, WP., Ran, LM., Koussis, A. (1996). An integrated interface system to couple the SWAT model and arc/info. Third international conference on integrating GIS and environmental modeling. Santa Fe: New Mexico.

Bicknell, B.R., Imhoff, J.C., Kittle, J.L., Donigian, A.S., Johanson, R.C. (1997). Hydrological simulation program–fortran, user's manual for version 11: USA Environmental Protection Agency, National Exposure Research Laboratory, Athens, EPA/600/R-97/080, 755.

Bicknell, B.R.., Imhpff, J.C., Kittle, J.L., Jobes, T.H., Donigian, A.S. (2000). Hydrological Simulation Program—Fortran (HSPF); User's Manual for Release 12. USEPA, Athens, Ga.

Borah, D.K., Bera, M. (2004). Watershed–scale hydrologic and nonpoint– source pollution models: review of applications. American Society of Agricultural Engineers, ISSN 0001–235 47(3), 789–803.

Boughton, W. C. (2004). The Australian water balance model. Environ Model Softw, 19(10), 943–956.

Braunschweig, F., Leitao, P., Fernandes, L., Pina, P., Neves, R. (2004). The object-oriented design of the integrated water modelling system MOHID. Developments in Water Science, 55, 1079-1090.

Brewer, S.K., Worthington, T.A., Mollenhauer, R., Stewart, D.R., McManamay, R.A., Guertault, L., Moore, D. (2018). Synthesizing models useful for ecohydrology and ecohydraulic approaches: An emphasis on integrating models to address complex research questions. Ecohydrology, 11.

Brighenti, T.M., Bonuma, N.B., Grison, F., Mota, A.d.A., Kobiyama, M., Chaffe, P.L.B. (2019). Two calibration methods for modeling streamflow and suspended sediment with the swat model. Ecological engineering, 127, 103-113.

Cao, Y., Zhang, J., Yang, M., Lei, X., Guo, B., Yang, L., Zeng Z., Qu, J. (2018). Application of SWAT model with CMADS to estimate hydrological elements and parameter uncertainty based on SUFI-2 algorithm in the Lijiang River Basin, China. Water, 10(742), 1-15. Doi: 10.3390/w10060742.

Carpenter, T. M., Georgakakos, K. P. (2006). Intercomparison of lumped versus distributed hydrologic model ensemble simulations on operational forecast scales. J. Hydrol (Amst), 329(1–2), 174–185.

Chen, C., Ahmad, S., Kalra, A., Xu, Z.-x. (2017). "A dynamic model for exploring water-resource management scenarios in an inland arid area: Shanshan County, Northwestern China." Journal of Mountain Science, 14(6), 1039-1057.

Croke, B. F.W., Andrews, F., Jakeman, A. J., Cuddy, S. M., Luddy, A. (2006). IHACRES Classic Plus: a redesign of the IHACRES rainfall-runoff model. Environ Model Softw, 21(3), 426–427.

Cunderlik, M. Juraj. (2003). Hydrologic model selection fort the CFCAS Project: Assessment of Water Resources Risk and Vulnerability to Changing Climatic Conditions, Project Report I, 1-40.

Dave, S.K., Parmar, A. K., Shah, A.P., Vyas, N.M. (2014). Pico hydropower generation: Renewable energy technology for rural electrification. International Journal of Advanced Research in Engineering, Science & Management, ISSN 2394-1766, 1-10.

Das, S., Paul, P. K. (2006). Selection of Site for Small Hydel Using GIS in the Himalayan Region of India. Journal of Spatial Hydrology, 6(1), 18–28. https://doi.org/10.1017/CBO9780511806049.

Dias, V.D., da Luz, M.P., Medero, G.M., Nascimento, D.T.F., de Oliveira, W.N., Merelles, L.R.D. (2018). Historical streamflow series analysis applied to furnas HPP reservoir watershed using the SWAT model. Water, 10(458), 1-13.

Dornan, M. (2009). Methods for assessing the contribution of renewable technologies to energy security: the electricity sector of Fiji. Pac. Econ. Bull, 24(3), 71–91.

Dornan, M., Shah, K. U. (2016). Energy policy, aid, and the development of renewable energy resources in Small Island Developing States. Energy Policy, 98, 759-767.

Duru, U., Arabi, M., and Wohl, E. E. (2018). Modeling stream flow and sediment yield using the SWAT model: a case study of Ankara River basin, Turkey. Physical Geography, 39(3), 264-289.

Eckhardt, K., Arnold, J.G. (2001). Automatic calibration of a distributed catchment model. Journal of Hydrology, 251, 103-109.

EFL. (2005). Energy Fiji Limited Annual Report 2005. [Online] Available at: http://www.efl.com.fj [Accessed 02 October. 2020].

EFL. (2006). Energy Fiji Limited Annual Report 2006. [Online] Available at: http://www.efl.com.fj [Accessed 02 October 2020].

EFL. (2007). Energy Fiji Limited Annual Report 2007. [Online] Available at: http://www.efl.com.fj [Accessed 02 October. 2020].

EFL. (2008). Energy Fiji Limited Annual Report 2008. [Online] Available at: http://www.efl.com.fj [Accessed 02 October 2020].

EFL. (2009). Energy Fiji Limited Annual Report 2009. [Online] Available at: http://www.efl.com.fj [Accessed 02 October 2020].

EFL. (2010). Energy Fiji Limited Annual Report 2010. [Online] Available at: http://www.efl.com.fj [Accessed 02 October 2020].

EFL. (2011). Energy Fiji Limited Annual Report 2011. [Online] Available at: http://www.efl.com.fj [Accessed 02 October. 2020].

EFL. (2012). Energy Fiji Limited Annual Report 2012. [Online] Available at: http://www.efl.com.fj [Accessed 02 October 2020].

EFL. (2013). Energy Fiji Limited Annual Report 2013. [Online] Available at: http://www.efl.com.fj [Accessed 02 October 2020].

EFL. (2014). Energy Fiji Limited Annual Report 2014. [Online] Available at: http://www.efl.com.fj [Accessed 02 October 2020].

EFL. (2015). Energy Fiji Limited Annual Report 2015. [Online] Available at: http://www.efl.com.fj [Accessed 02 October. 2020].

EFL. (2016). Energy Fiji Limited Annual Report 2016. [Online] Available at: http://www.efl.com.fj [Accessed 02 October 2020].

EFL. (2017). Energy Fiji Limited Annual Report 2017. [Online] Available at: http://www.efl.com.fj [Accessed 02 October 2020].

EFL. (2018). Energy Fiji Limited Annual Report 2018. [Online] Available at: http://www.efl.com.fj [Accessed 02 October 2020].

EFL. (2019). Energy Fiji Limited Annual Report 2019. [Online] Available at: http://www.efl.com.fj [Accessed 02 October 2020].

EFL. (2020). Energy Fiji Limited Annual Report 2020. [Online] Available at: http://www.efl.com.fj [Accessed 14 March 2022].

Emam, A.R., Kappas, M., Fassnachi, S., Linh, N.H.K. (2018). Uncertainty analysis of hydrological modeling in a tropical area using different algorithms. Front. Earth Sci, 1-11 https://doi.org/10.1007/s11707-018-0695-y.

Encyclopedia Britannica. Water Cycle. Available: < www.britannica.com/EBchecked/topic/278858/water-cycle >

Epelde, A., Cerro, I., Sánchez-Pérez, J., Sauvage, S., Srinivasan, R. (2015) Application of the SWAT model to assess the impact of changes in agricultural management practices on water quality. Hydrological Sciences Journal (ahead of-print), 1-19.

Ercan, M.B., Goodall, J.L., Castronova, A.M., Humphrey, M., Beekwilder, N. (2014). Calibration of SWAT models using the cloud. Environmental Modelling & Software, 62(1), 188-196. DOI: http://dx.doi.org/10.1016/j.envsoft.2014.09.002.

Feizizadeh, B., Haslauer, E. M. (2012). GIS-based procedures of hydropower potential for Tabriz basin, Iran. In GI_Forum 2012: Geovizualisation, Society and Learning, 495–502.

Fekete, B.M., Vörösmarty, C.J. (2007). The current status of global river discharge monitoring and potential new technologies complementing traditional discharge measurements. Predictions in Ungauged Basins: PUB kick-off (Proceedings of the PUB kick-off meeting held in Brasilia IAHS Publication 309.

Fernandez, G.P., Chescheir, G.M., Skaggs, R.W., Amatya, D.M. (2005). Development and testing of watershed-scale models for poorly drained soils. Transactions of the ASAE, 48(2), 639-652.

Fiji Bureau of Statistics 2017 Population Census [Accessed 21 April 2021] Available at: https://www.citypopulation.de/en/fiji/admin/naitasiri/0905__wainimala/

Fiji Bureau of Statistics-Key Statistics: September 2019 TRANSPORT [Accessed 04 October 2020].

Fiji's Intended Nationally Determined Contribution [Accessed 13 March 2021] Available at: https://www.reinfofiji.com.fj/wp-content/uploads/2017/11/FIJI_Intended-Nationally-Determined-Contribution-051115.pdf.

Fiji NDC Implementation Roadmap 2017-2030 [Accessed 09 October 2020].

Food and Agriculture Organization of the United Nations. (1978). FAO-Unesco soil map of the world, 1: 5,000,000 (Vol. X - Australasia). Paris: Unesco.

Food and Agriculture Organization of the United States. (2015). Global forest resources assessment. Rome.

FNEP. (2006). National Energy Policy. Department of Energy. Ministry of Energy and Mineral Resources. Fiji Islands. November 2006.

FNEP. (2013). Fiji National Energy Policy 2013 – 2020. Final Draft. The Government of Fiji.

Elbatran, A.H., Yaakob, O.B., Ahmed, Y. M., Shabara, H.M. (2015). Operation, performance and economic analysis of low head micro-hydropower turbines for rural and remote areas: A review. Renew. Sustain. Energy Rev, 43, 40–50.

Folton, N., Andréassian, V., Duperray, R. (2015). Hydrological impact of forest-fire from paired-catchment and rainfall–runoff modelling perspectives. Hydrol. Sci. J, 60, 1213–1224. https://doi.org/10.1080/02626667.2015.1035274.

Gassman, P.W., Reyes, M.R., Green, C.H., Arnold, J.G. (2007). The soil and water assessment tool: Historical development, applications, and future directions, Trans. ASABE, 50(4), 1211-1250.

Ghadei, S.C., Singh, P.K., Mishra, S.K. (2018). Hydrological modeling in the Ong River Basin, India using SWAT model. Journal of Spatial Hydrology, 14(2), 1-26.

Gholami, A., Roshan, M.H., Shahedi., K., Vafakhah, M., Solaymani, K. (2016). Hydrological stream flow in the Talar catchment (central section of the Alborz Mountains, north of Iran: Parameterization and uncertainty analysis using SWAT-CUP. Journal of Water and Land Development, 30 (VII-IX), 57-69 DOI: 10.1515/jwld-2016-0022.

GOF. (2017). DRAFT Third National Communication to the UNFCCC. Suva: Government of Fiji.

Gu, X., Yang, G., He*, X., Zhao*, L., Li, X., Li, P., Liu, B., Gao, Y., Xue, L., Long, A. (2020). Hydrological process simulation in Manas River basin using CMADS. Open Geosclences, 12, 946-957.

Guiamel, I. A., Lee, H. S. (2020). Watershed modelling of the Mindanao River Basin in the Philippines using the SWAT for water resource management. Civil Eng. J, 6(4), 626–648.

Guo, H., Hu, Q., Jiang, T. (2008). Annual and seasonal streamflow responses to climate and land-cover changes in the Poyang Lake basin, China. J. Hydrol, 355, 106–122.

Gupta, H.V., Sorooshian, S., Yapo, P.O. (1999). Status of automatic calibration for hydrologic models: comparison with multilevel expert calibration. J Hydrol Eng, 135–43. Doi: 10.1061/ (asce) 1084-0699(1999)4: 2(135).

Hall, D. G., Cherry, S. J., Reeves, K. S., Lee, R. D., Carroll, G. R., Sommers, G. L., Verdin, K. L. (2004). Water Energy Resources of the United States with Emphasis on Low Head/Low Power Resources. http://doi.org/10.1016/j.renene.2009.08.003.

Hallouz, Faiza., Meddi, Mohamed, Mahe, Gil, Alirahmani, Salaheddine, Keddar., Abdelkader. (2018). Modelling of discharge and sediment transport through the swat model in the basin of Harraza (Northwest of Algeria). Water Science, 32(1), 79-88. https://doi.org/10.1016/j.wsj.2017.12.004.

Hassan, M.A., Church, M., Yan, Y., Slaymaker, O. (2010). Spatial and temporal variation of in – reach suspended sediment dynamics along the mainstem of Changjiang (Yangtze River), China. Water Resour. Res, 46, 1–14. https://doi.org/10.1029/ 2010WR009228.

Holvoet, K., van Griensven, A., Seuntjens, P., Vanrolleghem, P. (2005). Sensitivity analysis for hydrology and pesticide supply towards the river in SWAT. Physics and Chemistry of the Earth, Parts A/B/C, 30, 518-526.

Horton, R.E. (1933). The Role of Infiltration in the Hydrologic Cycle. Eos Trans. AGU, 14, 446-460.

https://www.mindat.org/feature-2195171.html [Accessed 21 April 2021].

https://www.ppa.org.fj/wp-content/uploads/2018/08/EFL-Incorporating-our-Targets-Operations-into-the-Performance-Mngt-System-Karunesh-Rao.pdf [Accessed 09 October 2020].

http://efl.com.fj/about-us/renewable-projects/ [Accessed 09 October 2020].

https://www.citypopulation.de/en/fiji/admin/naitasiri/0905__wainimala/ [Accessed 19 March 2022].

IMF. (2011). Regional Economic Outlook: Asia and Pacific, Managing the Next Phase of Growth. International Monetary Fund, Washington D. C.

International Hydropower Association. (2017). Hydropower Status Report. Iha, 1-83.

IPCC. (2011). IPCC Special Report on Renewable Energy Sources and Climate Change Mitigation. Prepared by Working Group III of the Intergovernmental Panel on Climate Change [O. Edenhofer, R. Pichs - Madruga, Y. Sokona, K. Seyboth, P. Matschoss, S. Kadner, T. Zwickel, P. Eickemeier, G. Hansen, S. Schlmer, C. von Stechow (eds)]. Cambridge University Press, Cambridge, United Kingdom and New York, NY, USA, 1075.

IRENA. (2015). Renewable Energy Target Setting. International Renewable Energy Agency, Abu Dhabi.

Irvem, A., El-sadek, A. (2018). Evaluation of streamflow simulation by SWAT model for the Seyhan River Basin. Çukurova J. Agric. Food Sci, 33(2), 99-110.

IPCC. (2006). Guidelines for National Greenhouse Gas Inventories: Volume 2. Energy: Stationary Combustion (Chapter 2). [online] Available at: https://www.ipcc-nggip.iges.or.jp/public/2006gl/vol2.html [Accessed 15 Mar. 2022].”

Isioye, O.A., Yang, I. S. (2013). Comparison and validation of ASTER-GDEM and SRTM elevation models over parts of Kaduna State, Nigeria. SASGI Proceedings 2013-Stream 1.

Jajarmizadeh, M., Harun, S., Abdullah, R., Salarpour, M. (2012). Using soil and water assessment tool for flow simulation and assessment of sensitive parameters applying SUFI-2 algorithm. Caspian Journal of Applied Sciences Research, 2(1), 37-44.

Jajarmizadeh, M., Sidek, L. M., Harun, S., Salarpour, M. (2017). Optimal calibration and uncertainty analysis of SWAT for an arid climate. Air, Soil and Water Research, 10, 1-14. DOI: 10.1177/1178622117731792.

Jason, J. G. S., Marie, A. S. L., Fesalbon, A., Silapan, J. R. (2017). Estimation of hydropower potential energy using gis and swat hydrologic model in Western Visayas, 1–8.

Jin, X., Xu, C.Y., Zhang, Q., Singh, V. P. (2010). Parameter and modelling uncertainty simulated by GLUE and a formal Bayesian method for a conceptual hydrological model. J Hydrol (Amst), 383(3–4), 147–155.

Johnston, R., Kummu, M. (2012). Water resource models in the Mekong basin: A review. Water Resour. Manag, 26, 429–455.

Kalra, A., Sagarika, S., Pathak, P., Ahmad, S. (2017). Hydro-climatological changes in the Colorado River Basin over a century. Hydrological Sciences Journal, 62(14), 2280-2296.

Kandissounon, G. A., Kalra, A., Ahmad, S. (2018). "Integrating System Dynamics and Remote Sensing to Estimate Future Water Usage and Average Surface Runoff in Lagos, Nigeria." Civil Engineering Journal, 4(2), 378-393.

Kayastha, N., Singh, U., Dulal, K. P. (2018). A GIS approach for rapid identification of run-of-river (ROR) hydropower potential site in watershed: a case study of Bhote Koshi watershed, Nepal. Hydro Nepal, 23, 48-55.

Khalid, K., Alib, M.F., Rahmanc, N.F.A., Mispand, M.R., Harone, S.T., Othmana, H.Z., Bachoka, M.F. (2016). Sensitivity analysis in watershed model using SUFI-2 algorithm. Procedia Engineering, 162, 441-447.

Khatun, S., Sahana, M., Jain, S. K., Jain, N. (2018). Simulation of surface runoff using semi distributed hydrological model for a part of Satluj Basin: parameterization and global sensitivity analysis using SWAT CUP. Modeling Earth Systems and Environment, 1-14.

Khoi, D. N., Thom, V. T. (2015). Parameter uncertainty analysis for simulating streamflow in a river catchment of Vietnam. Global ecology and conservation, 4, 538-548.

Knisel, W. G. (1980). CREAMS: A field-scale model for chemicals, runoff, and erosion from agricultural management systems. Conservation Research Report No. 26. Washington, D.C.: USDA-SEA.

Koycegiz, C., Buyukyildiz, M. (2019). Calibration of swat and two data-driven models for a data – scarce mountainous headwater in semi-arid Konya closed basin. Water, 11(147), 2-17.

Kouadio, C. A., Kouassi, K. L., Diedhiou, A., Obahoundje, S., Amoussou, E., Kamagate, B., Paturel, J., Coulibaly, T. J.H., Coulibaly, H. S. J. P., Didi, R. S., Savane, I. (2022). Assessing the hydropower potential using hydrological models and geospatial tools in the White Bandama Watershed (Côte d'Ivoire, West Africa). Front. Water 4:844934, 1-14. doi: 10.3389/frwa.2022.844934.

Kouchi, D.H., Esmaili, K., Faridhosseini, A., Sanaeinejad, S. H., Khalili, D., Abbaspour, K. C. (2017). Sensitivity of calibrated parameters and water resource estimates on different objective functions and optimization algorithms. Water, 9 (6), 384. https://doi.org/10.3390/w9060384.

Kumar, N., Singh, S.K., Srivastava, P.K., Narsimlu, B. (2017). SWAT model calibration and uncertainty analysis for streamflow prediction of the Tons River Basin, India, using sequential uncertainty fitting (SUFI-2) algorithm. Eart Syst. Environ, 3(30), 1-13.

Kuriqi, A., Pinheiro, A. N., Sordo-Ward, A., Bejarano, M. D., and Garrote, L. (2021). Ecological impacts of run-of-river hydropower plants—Current status and future prospects on the brink of energy transition. Renew. Sustain. Energy Rev. 142, 110833. doi: 10.1016/j.rser.2021.110833.

Kusre, B., Baruah, D., Bordoloi, P., and Patra, S. (2010). Assessment of hydropower potential using GIS and hydrological modeling technique in Kopili River basin in Assam (India). Applied Energy, 87(1), 298-309.

Lakshmi, S. V., Sarvani, G. R. (2018). Selection of suitable sites for small hydropower plants using geo-spatial technology. International Journal of Pure and Applied Mathematics, 119(17), 217-240.

Lal, S., Raturi, A. (2012). Techno-economic analysis of a hybrid mini-grid system for Fiji Islands. International Journal of Energy and Environmental Engineering, 3(10), 1-10. http://www.journal-ijeee.com/content/3/1/10.

Leng, M., Yu, Y., Wang, S., Zhang, Z. (2020). Simulating the hydrological process of a meso-scale watershed on the Loess Plateau, China. Water, 12(878), 2-18. Doi: 10.3390/w12030878.

Levantis, T. (2008). Oil price vulnerability in the Pacific. Pac. Econ. Bull, 23(2), 214–225.

Levantis, T., Groeger, C., McNamara, S. (2006). Are Pacific Countries coping with surging oil prices? Pac. Econ. Bull, 21(3), 115–125.

Li, Q., Chen, X., Luo, Y., Lu, Z., Wang, Y. (2015). A new parallel framework of distributed SWAT calibration. Journal of Arid Land, 7(1), 122-131. DOI: http://dx.doi.org 10.1007/s40333-014-0041-5.

Lilburne, L., Gatelli, D., Tarantola, S. (2006). Sensitivity analysis on spatial models: new approach. Proceedings of the 7th international symposium on spatial accuracy assessment in natural resources and environmental sciences: Citeseer.

Lofgren, B., Gronewold, A. (2014). Climate change in the Midwest: a synthesis report for the national climate assessment, chap, 12, 224–237.

Mahzari, S., Kiani. F., Azimi, M., Khormali, F. (2016). Using SWAT model to determine runoff, sediment yield and nitrate loss in Gorganrood watershed, Iran. Ecopersia, 4(2), 1359-1377. DOI: 10.18869/modares.Ecopersia.4.2.1359.

Mardookhpour, A., Ooshaksaraie, L. (2012). Forecasting stream flow in floodplain by utilizing hydrological and statistical relationship in the Sepidroud catchments. Caspian. Journal of Applied Sciences Research, 11, 54-57.

Marek, G.W., Gowda, P.H., Evett, S.R., Baumhardt, L., Brauer, D.K., Howell, T.A., Marek, T.H., Srinivasan, R. (2016). Calibration and validation of SWAT model for predicting daily ET over irrigated crops in Texas high plains using lysimetric data. Transactions of the ASABE, 59(2), 611-622.

Mclntyre, N., Qurashi, A. A., Wheater, H. (2007). Regression analysis of rainfall-runoff data from an arid catchment in Oman. Hydrological Sciences Journal, 52(6), 1103-1118. DOI: 10.1623/hysj.52.6.1103.

Mehan, S., Neupane, R.P., Kumar, S. (2017). Coupling of SUFI 2 and SWAT for improving the simulation of streamflow in an agricultural watershed of South Dakota. Hydrol Current Res, 8(3), 1-11. DOI: 10.4172/2157-7587.1000280.

Meng, X., Long, A., Wu, Y., Yin, G., Wang, H., Ji, X. (2018). Simulation and spatiotemporal pattern of air temperature and precipitation in Eastern Central Asia using RegCM. Sci. Rep, 8, 3639.

Mengistu, A. G., Rensburg, L. D. van., Woyessa, Y. E. (2019). Techniques for calibration and validation of SWAT model in data scarce arid and semi-arid catchments in South Africa. Journal of Hydrology: Regional Studies, 25, 100621. https://doi.org/10.1016/j.ejrh.2019.100621.

Merwade, B. (2012). Watershed and Stream Network Delineation using ArcHydro Tools. School of Civil Engineering, Purdue University. Accessed: March 15, 2021, < http://web.ics.purdue.edu/~vmerwade/education/terrain_processing.pdf >

Methan, S., Neupane, R.P., Kumar, S. (2017). Coupling of SUFI 2 and SWAT for improving the simulation of streamflow in an agricultural watershed of South Dacota. Hydrol Current Res, 8(3), 1-11.

Mimich, K., Ouali, A.E.A.E., Hmaidi, A. (2018). Using SWAT to simulate a Moroccan watershed, including an assessment of the most sensitive modelling parameters with SUFI2. The International Journal of Engineering and Sciences, 7(10), 23, 50-63. DOI:10.9790/1813-0710035063.

Mishra, S. K., Singh, V. P. (2003). Soil conservation service number (SCS-CN) methodology. Water Science and Technology Library, 42. DOI 10.1007/978-94-017-0147-1

Monteiro, J.A.F., Strauch, M., Srinivasan, R., Abbaspour K., Gucker, B. (2015). Accuracy of grid precipitation data for Brazil: application in river discharge modelling of the Tocantins catchment. Hydrological processes, 30(1), 1419-1430. DOI: http://dx.doi.org/10.1002/hyp.10708.

Moriasi, D.N., Arnold, J.G., van Liew, M.W., Bingner, R.L., Harmel, R.D., Veith, T.L. (2007). Model evaluation guidelines for systematic quantification of accuracy in watershed simulations. Trans ASAE, 50, 885–900. Doi: 10.13031/2013.23153.

Moriasi, D.N., Wilson, B.N., Douglas-Mankin, K.R., Arnold, J.G., Gowda, P.H. (2012). Hydrologic and water quality models: use, calibration, and validation. Trans ASABE, 55(4), 1241–1247.

Moriasi, D.N., Gitau, M.W., Pai, N., Daggupati, P. (2015). Hydrologic and water quality models: Performance measures and evaluation criteria. Trans ASABE, 58(6), 1763–1785. Doi:10.13031/trans.58.10715.

Narsimlu, B. Gosain, A.K., Chahar, B.R. (2013). Assessment of future climate change impacts on water resources of upper Sind river basin, India using SWAT model. Water Resour Manag, 27, 3647–3662. Doi:10.1007/s11269-013-0371-7.

Narsimlu, B., Gosain, A.K., Chahar, B.R., Singh, S.K., Srivastava, P.K. (2015). SWAT model calibration and uncertainty analysis for streamflow prediction in the Kunwari river basin, India, using sequential uncertainty fitting. Environmental Processes, 2, 79–95.

Nash, J.E., Sutcliffe, J.V. (1970). River flow forecasting through conceptual models. Part I – A discussion of principles. J Hydrol, 10, 282–90. Doi: 10.1016/0022-1694(70)90255-6.

Neitsch, S.L., Arnold, J.G., Kiniry, J.R., Williams, J.R. (2005). Soil and Water Assessment Tool. Theoretical Documentation. Version 2005. Springer, Berlin.

Neitsch, S.J., Arnold, J.G., Kiniry, J.R., Williams, J.R. (2009). Soil and Water Assessment Tool Theoretical Documentation Version 2009; College of Agriculture and Life Sciences, Texas A&M University System: College Station, TX, USA.

Neitsch, S.L., Arnold, J.G., Kiniry, J.R., Srinvasan, R., Williams, J.R. (2010). Soil and Water Assessment Tool, Input/Output File Documentation, Version 2009. Soil and Water Research Laboratory, Agricultural Research Service, and Blackland Research Center, Texas Agrilife Research. Texas water resources institute technical report No.365: Texas A&M University, USA.

Neitsch, S., Arnold, J., Kiniry, J., Williams, J. (2011). SWAT Theoretical Documentation Version 2009. Texas Water Resources Institute, 1–647.

Nguyen, H.Q., Kappas, M. (2015). Modeling surface runoff and evapotranspiration using SWAT and BEACH for a tropical watershed in North Vietnam, compared to MODIC product. International Journal of Advanced Remote Sensing and GIS, 4(1), 1367-84.

Nguyen, T. H. T., Mouksassi, M-S., Holford. N., Al-Huniti, N., Freedman, I., Hooker, A. C., John, J., Karlsson, M. O., Mould, D. R., Ruixo, J. J. P., Plan, E. L., Savic, R., van Hasselt, J. G. C., Weber, B., Zhou, C., Comets, E., Mentre, F. (2017). Model evaluation of continuous data pharmacometric models: metrics and graphics. Pharmacometrics & Systems Pharmacology, 6(2), 87-109. https://doi.org/10.1002/psp4.12161.

Nyaupane. N. B. S., Rahaman, M., Wagner. K., Kalra, A., Ahmad, S., Gupta, R. (2018a). Flood Frequency Analysis Using Generalized Extreme Value, Distribution and Floodplain Mapping for Hurricane Harvey in Buffalo Bayou. World Environmental and Water Resources Congress Minneapolis, Minnesota.

Nyaupane, N., Thakur, B., Kalra, A., Ahmad, S. (2018b). Evaluating Future Flood Scenarios Using CMIP5 Climate Projections. Water, 10(12), 1866.

Oeurng, C., Sauvage, S., Sanchez-Perez, J.M. (2011). Assessment of hydrology, sediment and particulate organic carbon yield in a large agricultural catchment using the SWAT model. J. Hydrol, 401, 145–153.

Oliveira, V. A. d., Mello, C. R. d., Viola, M. R, Srinivasan. Assessment of climate change impacts on streamflow and hydropower potential in the headwater region of

the Grande River, Southeastern. Brazil. Int. J. Climatol. 37, 5005-5023. DOI: 10.1002/joc.5138.

Pacific Energy Update (2018). Asian Development Bank. Available at https://www.adb.org/sites/default/files/institutional-document/425871/pacific-energy-update-2018.pdf.

Palomino, Cuya. D. G., Brandimarte, L., Popescu, I., Alterach, J., Peviani, M. (2013). A GIS-based assessment of maximum potential hydropower production in La Plata basin under global changes. Renewable Energy, 50, 103–114. http://doi. org/10.1016/j.renene.2012.06.019.

Pandey, A., Lalrempuia, D., and Jain, S. K. (2015). Assessment of hydropower potential using spatial technology and SWAT modelling in the Mat River, southern Mizoram, India. Hydrol. Sci. J. 60, 1651–1665. doi: 10.1080/02626667.2014.943669.

Parikh, M., Parekh, F. (2019). Hydrological modelling of Deo River Sub-Basin using SWAT-CUP. International Journal of Innovative Technology and Exploring Engineering, 8(12), 2890-6.

Patel, D., Srivastava, P. (2013). Flood hazards mitigation analysis using remote sensing and GIS: correspondence with town planning scheme. Water Resour Manag, 27, 2353–2368. Doi: 10.1007/ s11269-013-0291-6.

Patel, D.P., Srivastava, P.K. (2014). Application of geo-spatial technique for flood inundation mapping of low-lying areas. In: Remote Sensing Applications in Environmental Research. Springer, 113–130.

Pathak, P., Kalra, A., Ahmad, S., Bernardez, M. (2016). Wavelet-aided analysis to estimate seasonal variability and dominant periodicities in temperature, precipitation, and streamflow in the Midwestern United States. Water resources management, 30(13), 4649-4665.

Patil, N. S., Shirkol, I. T., Joshi, S. G. (2013). Geospatial Technology for Mapping Suitable Sites for Hydro Power Plant, (3), 156–160.

Patra, P. (2010). Remote Sensing and Geographical Information System (GIS). The Association for Geographical Studies, (1977), 1–28.

Paul, M., Negahban-Azar, M. (2018). Sensitivity and uncertainty analysis for streamflow prediction using multiple optimization algorithms and objective functions: San Joaquin Watershed, California. Modeling Earth Systems and Environment, 4, 1509-1525.

Pereira, D.R., Martinez, M.A, Almeida, A.Q., Pruski, F.F., Silva, D.D., Zonta, J.H. (2014). Hydrological simulation using SWAT model in headwater basin in southeast Brazil. Engenharia Agrícola, 34(4), 789-799. DOI: http://dx.doi.org/10.1590/S0100-69162014000400018.

Pinto, D.B.F., Silva, A.M., Beskow, S., Mell,o C.R., Coelho, G. (2013). Application of the soil and water assessment tool (SWAT) for sediment transport simulation at a headwater watershed in Minas Gerais state, Brazil. Transactions of the ASABE, 56(2), 697-709.

Practical guide for calculating green house gas (GHG) emissions. Version 1 March 2019.
https://canviclimatic.gencat.cat/web/.content/04_ACTUA/Com_calcular_emissions_GEH/guia_de_calcul_demissions_de_co2/190301_Practical-guide-calculating-GHG-emissions_OCCC.pdf [Accessed 17 March 2022].

Punys, P., Dumbrauskas, A., Kvaraciejus, A., Vyciene, G. (2011). Tools for Small Hydropower Plant Resource Planning and Development: A Review of Technology and Applications. Energies, 1258–1277. http://doi.org/10.3390/en4091258.

Qin, N., Wang, J., Chen, X., Yang, G., Liang, H. (2015). Impacts of climate change on regional hydrological regimes of the Wujiang River watershed in the Karst area, Southwest China. Geoenvironmental Disasters, 2, 1–18.

Raghavan, K. (2003). 100% renewable energy islands in Tuvalu, Fiji and Tonga (forum for renewable energy islands), 1-103.

Rahaman, M. M., Lamichhane, G.R., Shrestha, A., Thakur, B., Kalra, A., Ahmad, S. (2019). Using SWAT to simulate streamflow in Trinity River Basin, Texas, USA. World environmental and water resources congress, 421-435.

Ramachandra, T., Kumar Jha, R., Vamsee Krishna, S., & Shruthi, B. (2004). Spatial Decision Support System for Assessing Micro, Mini and Small Hydel Potential. Journal of Applied Sciences, 4(4), 596–604. https://doi.org/10.3923/jas.2004.596.604.

Ramachandra, T.V., Shwetmala. (2012; 16). Decentralised carbon footprint analysis for opting climate change mitigation strategies in India. Renewable Sustainable Energy Rev, 5820-33.

Ramachandra, T.V., Aithal, B.H., Sreejith, K. (2015). GHG footprint of major cities in India. Renewable and Sustainable Energy Reviews. 44, 473-495. http://dx.doi.org/10.1016/j.rser.2015.12.036.

Refsgaard, J.C., Storm, B. (1995). MIKESHE. In: Singh, V.P. (Ed.), Computer Models of Watershed Hydrology. Water Resources Publications, Colorado, USA. 809–846. (Chapter 22).

Refsgaard, J. C. (1997). Parameterization, calibration, and validation of distributed hydrological models. J Hydrol (Amst), 198 (1–4), 69–97.

REN21 2020. Asia and the Pacific Renewable Energy Status Report. Paris: REN21 Secretariat.

Rojanamon, P., Chaisomphob, T., Bureekul, T. (2009). Application of geo-graphical information system to site selection of small run-of-river hydropower project by considering engineering/economic/environmental criteria and social impact. Renewable and Sustainable Energy Reviews, 13(9), 23362348.

Rosso, R. (1994). An introduction to spatially distributed modelling of basin response. Advances in Distributed Hydrology, 3, 30.

Salimi, E.T., Nohegar, A., Malekian, A., Hosseini, M., Holisaz. (2016). Runoff simulation using SWAT model and SUFI-2 algorithm (case study: Shafaroud watershed, Guilan Province, Iran). Caspian J. Environ. Sci, 14(1), 69-80.

Saltelli, A., Chan, K., Marian, S. (2000). Sensitivity Analysis. John Wiley & Sons: Chichester.

Sao, D., Kato, T., Tu, L. H., Thouk, P., Fitriyah, A., Oeurng, C. (2020). Evaluation of Different Objective Functions Used in the SUFI-2 Calibration Process of SWAT-CUP on Water Balance Analysis: A Case Study of the Pursat River Basin, Cambodia. Water, 12(2901), 1-22.

Schuol, J.; Abbaspour, K.C. (2007). Using monthly weather statistics to generate daily data in a SWAT model application to West Africa. Ecol. Model, 201, 301–311.

Schoul, J., Abbaspour, K.C., Srinivasan, R., Yang, H. (2008). Estimation of fresh water availability in the West African sub-continent using the SWAT hydrologic model. Journal of Hydrology, 352, 30-49.

Semu, Ayalew. (2007). Lecture notes on deterministic hydrology. Addis Ababa University, Addis Ababa.

Setegn, S.G., Srinivasan, R., Dargahi, B. (2008). Hydrological modelling in the Lake Tana Basin, Ethiopia using SWAT model. The Open Hydrology Journal, 2, 49-62.

Setegn, G., Srinivasan, R., Melesse, A.M., Dargahi, B. (2009). SWAT model application and prediction uncertainty analysis in the Lake Tana Basin, Ethiopia. Hydrol. Process, 24, 357–367. DOI:10.1002/hyp.7457.

Setegn, S.G., Srinivasan, R., Melesse, A.M., Dargahi, B. (2010). SWAT model application and prediction uncertainty analysis in the Lake Tana Basin, Ethiopia. Hydrol. Process, 24, 357–367.

Setiawan, D. (2015). Potential sites screening for mini hydro power plant development in Kapuas Hulu, West Kalimantan: aa GIS approach. Energy Procedia, 65, 76-82.

Shahoei, S., Porhemmat, J., Sedghi, H., Hosseini, M., and Saremi, A. (2017). Daily Runoff Simulation in Ravansar Sanjabi Basin, Kermanshah, Iran, Using Remote Sensing Through Srm Model and Comparison to Swat Model. Applied Ecology and Environmental Research, 15(3), 1843-1862.

Sharma, M. P. (2007). Environmental Impacts of Small Hydro Power Projects. International Conference on Small Hydropower (October), 1–9.

Shen, Z.Y., Chen, L., Chen, T. (2012). Analysis of parameter uncertainty in hydrological and sediment modeling using GLUE method: A case study of SWAT model applied to Three Gorges Reservoir Region, China. Hydrol. Earth Syst. Sci, 16, 121–132.

Shi, P., Chen, C., Srinivasan, R., Zhang, X., Cai, T., Fang, X., Qu, S., Chen, X., and Li, Q. (2011). Evaluating the SWAT model for hydrological modeling in the Xixian watershed and a comparison with the XAJ model. Water resources management, 25(10), 2595-2612.

Shivhare, N., Dikshit, P.K.S., Dwivedi, S.B. (2018). A comparison of SWAT model calibration techniques for hydrological modeling in the Ganga River watershed. Engineering, 4, 643-652 http://creativecommons.org/licenses/by-nc-nd/4.0/

Shrestha, H. M. (2016). Exploitable Potential, Theoretical Potential, Technical Potential, Storage Potential and Impediments to Development of the Potential: The Nepalese Perspective. Hydro Nepal: Journal of Water, Energy and Environment, (19), 1–5. http://doi.org/10.3126/hn.v19i0.15340 55.

Sims, R.E.H., Rogner, H-H., Gregory, K. (2003). Carbon emission and mitigation cost comparisons between fossil fuel, nuclear and renewable energy resources for electricity generation. Energy policy 31, 1315-1326.

Singh, V.P., Woolhiser, D.A. (2002). Mathematical modeling of watershed hydrology. Journal of hydrologic engineering, 7, 270-292.

Singh, V., Bankar, N., Salunkhe, S.S., Bera, A.K., Sharma, J.R. (2013). Hydrological stream flow modelling on Tungabhadra catchment: parameterization and uncertainty analysis using SWAT-CUP. Current Science, 104, 1187-1199.

Singh, G., Saraswat, D. (2016). Development and evaluation of targeted marginal land mapping approach in SWAT model for simulating water quality impacts of selected second generation biofeedstock. Environ. Modelling & Software, 81, 26-39. Doi: https://doi.org/10.1016/j.envsoft.2015.12.001.

Sloboda, M., Swayne, D. (2011). Autocalibration of environmental process models using a PAC learning hypothesis. Environmental Software Systems Frameworks of eEnvironment, 528-534.

Solomatine, D., See, L.M., Abrahart, R.J. (2008). Data-Driven Modelling: Concepts, Approaches and Experiences, Practical Hydroinformatics. In Water Science and Technology Library; Springer: Berlin, Germany, 68, 17-30.

SOPAC (n.d.), "Catalogue of Pacific Rivers: Fiji", www.pacificwater.org/_resources/article/.

Sorooshian, S. (1983). Surface water hydrology: Online estimation. Rev Geophys, 21(3), 706–721.

Sorooshian, S., Gupta, V. (1995). Model calibration. Computer Models of Watershed Hydrology, 23-68.

Spear, R.C., Hornberger, G.M. (1980). Eutrophication in Peel Inlet, II, Identification of critical uncertainties via generalised sensitivity analysis. Water Research, 14, 43–49.

Spruill, C., Workman, S., Taraba, J. (2000). Simulation of daily and monthly stream discharge from small watersheds using the SWAT model. Transactions of the ASAE, 43, 1431-1439.

Srivastava, P., Mukherjee, S., Gupta, M. (2008). Groundwater quality assessment and its relation to land use/land cover using remote sensing and GIS. Proceedings of International Groundwater Conference on Groundwater Use - Efficiency and Sustainability: Groundwater and Drinking Water Issues, Jaipur, India, 19–22.

Srivastava, P.K., Han, D., Ramirez, M.R., Islam, T. (2013). Appraisal of SMOS soil moisture at a catchment scale in a temperate maritime climate. J Hydrol, 498, 292–304.

Sugden, C. (2009). Responding to high commodity prices. Asian-Pac. Econ. Lit, 23(1), 79–105.

Sulebak, J.R., (2000). Application of Digital Elevation Models. DYNAMAP "White Paper", 2000. SINTEF Institute of Applied Mathematics, Department of Geographic Information Technology. Accessed: March 15 2021, < http://gisknowledge.net/topic/terrain_modelling_and_analysis/sulebak_dem_applications_00.pdf >

Sustainable Energy for All (SE4All): Rapid Assessment and Gap Analysis, 1-56.

Swain, S., Verma, M.K., Verma, M.K. (2018). Streamflow estimation using SWAT model over Seonath River basin, Chhattisgarh, India. Hydrol. Model, 81, 659–665.

Systematic Country Diagnostic. (2017). Report No. 116491-FJ.

Tachikawa, T., Hatol, M., Kabu, M., et al., (2011). Characteristics of ASTER GDEM version 2. Geoscience and Remote Sensing Symposium (IGARSS), 2011 IEEE International.

Tamaddun, K., Kalra, A., Ahmad, S. (2016). Identification of streamflow changes across the continental United States using variable record lengths. Hydrology, 3(2), 24.

Tan, M. L., Gassman, P. W., Srinivasan, R., Arnold, J. G., Yang, X. Y. (2019). A Review of SWAT studies in Southeast Asia: applications, challenges and future directions. Water, 11, 1-25.

Tang, J., Yang, W. Z-y L, J-m B, Liu C. (2012). Simulation on the inflow of agricultural non-point sources pollution, in Dahuofang reservoir catchment of Liao River. J Jilin Univ, 42, 1462–1468.

Tarife, R. P., T, A. P., Gulben, E. J. G., Al Raschid, Haroun, Macalisang, C, P., Teresa, M., Ignacio, T. (2017). Application of geographic information system (GIS) in hydropower resource assessment: A case study in Misamis Occidental, Philippines. Int. J. Environ. Sci. Dev, 8 (7), 507–511.

Teddy, Teri. (2006; 2011). Energy data directory and year book. The energy and Resource Institute: New Delhi.

Tejaswini, V., Sathian, K.K. (2018). Calibration and validation of SWAT model for Kunthipuzha basin using SUFI-2 algorithm. Int.J. Curr. Microbiol. App. Sci, 7 (1), 2162-2172. http://www.ijcmas.com.

Thakali, R., Kalra, A., Ahmad, S. (2016). Understanding the effects of climate change on urban stormwater infrastructures in the Las Vegas Valley. Hydrology, 3(4), 34.

Thakali, R., Kalra, A., Ahmad, S., Qaiser, K. (2018). "Management of an Urban Stormwater System Using Projected Future Scenarios of Climate Models: A Watershed-Based Modeling Approach." Open Water Journal, 5(2), 1.

Thavhana, M., Savage, M., and Moeletsi, M. (2018). SWAT model uncertainty analysis, calibration and validation for runoff simulation in the Luvuvhu River catchment, South Africa. Physics and Chemistry of the Earth, Parts A/B/C.

Thin, K.K., Zin, W.W., San, Z.M.L.T., Kawasaki, A., Moiz, A., Bhagabati, S.S. (2020). Estimation of run-of-river hydropower potential in the Myitnge River Basin. Journal of Disaster Research, 15(3), 267-276. DOI: 10.20965/jdr.2020. p 0267.

Turanyi, T., Rabit, z H. (2000). Local methods. Sensitivity Analysis, 81-99.

Twyford, C.C., Wright. (2013). A reference manual for utilising and managing the soil resources of Fiji. 1-166. https://issuu.com/uluinayauj/docs/manual_for_utilising_soil.pdftest

USDA (United States Department of Agriculture). (1986). Urban Hydrology for Small Watersheds, Technical Release 55(TR-55), 2nd ed. Natural Resources Conservation Service, Conservation Engineering Division, Washington, DC, USA

UNDP. (2007a). Energy and Poverty in the Pacific Island Countries. United Nations Development Programme, Bangkok

UNDP. (2007b). Fuel to Change: Overcoming Vulnerability to Rising Oil Prices. United Nations Development Program, Bangkok.

United States Geological Survey (USGS). (2012). Digital Elevation Model (DEM). Accessed: April 20 2021. http://tahoe.usgs.gov/DEM.html.

Uniyal, B., Jha, M.K., Verma, A.K. (2015). Parameter identification and uncertainty analysis for simulating streamflow in a river basin of Eastern India. Hydrol. Process, 29 (17), 3744–3766. http://dx.doi.org/10.1002/hyp.10446.

U.S. Energy Information Administration. (2016). Electricity Explained - Basics. (https://www.eia.gov) [Accessed 13 October 2020].

Van Liew, M.W., Arnold, J.G., Garbrecht, J.D. (2003). Hydrologic simulation on agricultural watersheds: Choosing between two models. Trans. ASAE, 46(6), 1539–1551.

Van, Griensven. A., Meixner, T., Grunwald, S., Bishop, T., Diluzio, M. (2006). A global sensitivity analysis tool for the parameters of multi-variable catchment models. Journal of hydrology, 324, 10-23.

Van Griensven, A., Meixner, T., Srinivasan, R., Grunwals, S. (2008). Fitfor-purpose analysis of uncertainty using split-sampling evaluations. Hydrol Sci J, 53(5), 1090–1103.

Vandenberghe, V., Van Griensven, A., Bauwens, W. (2001). Sensitivity analysis and calibration of the parameters of ESWAT: Application to the river Dender. Water Science and Technol, 43(7), 295-301.

Vandenberghe, V., Griensven, A., Van, Bauwens, W., Vanrolleghem, P.A. (2006). Effect of different river water quality model concepts used for river basin management decisions, 277–284. https://doi.org/10.2166/wst.2006.322.

Vanrolleghem, P.A. (2003). A comprehensive model calibration procedure for activated sludge models. Proc Water Environ Fed, 210–237.

Vilaysane, B., Takara, K., Luo, P.P., Akkharath, I., Duan, W.L. (2015). Hydrological stream flow modelling for calibration and uncertainty analysis using SWAT model in the Xedone river basin, Lao PDR. Proc.Environ. Sci, 28, 380–390.

Wagener, T., Wheater, H.S. (2006). Parameter estimation and regionalization for continuous rainfall-runoff models including uncertainty. J Hydrol, 320, 132–15.

Ward and Robinson. (2000). Principles of hydrology. McGraw HILL INTERNATIONAL EDITIONS. New York.

Wasko, C., and Sharma, A. (2017). Global assessment of flood and storm extremes with increased temperatures. *Sci. Rep.* 7:7945.

Wellen, C., Kamran-Disfani., A.-R., Arhonditsis, G.B. (2015). Evaluation of the current state of distributed = nutrient water quality modeling. Environ. Sci. Technol, 49, 3278–3290.

Williams, J. R., Nicks, A. D. (1982). CREAMS hydrology model—Option one. In applied modeling catchment hydrology. Proc. Int. Symp. Rainfall-Runoff Modeling, 69-86, ed. V. P. Singh, 18-21 May 1981, Mississippi State, Miss. Littleton, Colo.: Water Resources Publ.

Williams, J. R., Nicks, A. D., Arnold, J. G. (1985). SWRRB, A simulator for water resources in rural basins. ASCE J. Hydrol. Eng, 111(6), 970-986.

World Energy Council. (2017). Hydropower Development 2017. (https://www.worldenergy.org/) [Accessed 13 October 2020].

Wu, H., Chen, B. (2015). Evaluating uncertainty estimates in distributed hydrological modeling for the Wenjing River watershed in China by GLUE, SUFI-2, and ParaSol methods. Ecol. Eng, 76, 110–121. http://dx.doi.org/10.1016/j.ecoleng.2014.05.014.

Xu, C. Y. (2002). WASMOD—the water and snow balance modelling system. In: Singh V P, Frevert D K, eds. Mathematical Models of Small Watershed Hydrology and Applications (Chapter 17). Chelsea: Water Resources Publications, LLC.

Xue, C., Chen, B., Wu, H. (2014). Parameter uncertainty analysis of surface flow and sediment yield in the Huolin Basin, China. J. Hydrol. Eng, 19 (6), 1224–1236.

Yadav, S.K., Singh, S.K., Gupta, M., Srivastava, P.K. (2013). Morphometric analysis of Upper Tons basin from Northern Foreland of Peninsular India using CARTSAT satellite and GIS. Geocarto Int, 1–38.

Yang, J., Reichert, P., Abbaspour, K.C., Xia, J., Yang, H. (2008). Comparing uncertainty analysis techniques for a SWAT application to the Chaohe Basin in China. J. Hydrol, 358, 1–23.

Young, R.A., Onstad, C.A., Bosch, D.D. (1989). AGNPS: a nonpoint source pollution model for evaluating agricultural watersheds. J. Soil Water Conserv, 44 (2), 168–173.

Yuan, L., Forshay, K.J. (2019). Using SWAT to evaluate streamflow and lake sediment loading in the Xinjiang River Basin with limited data. Water, 12(39), 1-22. Doi: 10.3390/w12010039.

Zarfl, C., Lumsdon, A. E., Tockner, K. (2015). A global boom in hydropower dam construction. Aquatic Sciences, (77), 161–170. http://doi.org/10.1007/ s00027-014-0377-0.

Zeckoski, R.W., Smolen, M.D., Moriasi, D.N., Frankenberger, J.R., Feyereisen, G.W. (2015). Hydrologic and water quality terminology as applied to modeling. Trans ASABE, 58(6), 1619–1635.

Zhao, Q., Ye, B., Ding, Y., Zhang, S., Yi, S., Wang, J., Shangguan, D., Zhao, C., Han, H. (2013). Coupling a glacier melt model to the Variable Infiltration Capacity (VIC) model for hydrological modeling in north-western China. Environ. Earth Sci, 68, 87–101.

Zhang, Z., Wang, S., Sun, G., McNulty, S.G., Zhang, H., Li, J., Zhang, M., Klaghofer, E., Strauss, P. (2008). Evaluation of the MIKE SHE models for application in the Loess Plateau, China. J. Am. Water Resour. Assoc, 44, 1108–1120.

Zheng, Y., Keller, A.A. (2007). Uncertainty assessment in watershed scale water quality modeling and management: 1. Framework and application of generalized likelihood uncertainty estimation (GLUE) approach. Water Resour Res, 43. Doi: 10.1029/2006WR005345.